An Analysis Framework for Distribution Network DER Integration in India: Distributed Solar in Tamil Nadu

Kapil Duwadi, Killian McKenna, Akshay Jain, Kajal Gaur, Adarsh Nagarajan, David Palchak
National Renewable Energy Laboratory

Tamil Nadu Generation and Distribution Company (TANGEDCO)

NREL is a national laboratory of the U.S. Department of Energy
Office of Energy Efficiency & Renewable Energy
Operated by the Alliance for Sustainable Energy, LLC

This report is available at no cost from the National Renewable Energy Laboratory (NREL) at www.nrel.gov/publications.

Contract No. DE-AC36-08GO28308

Technical Report
NREL/TP-6A20-78114
March 2021

An Analysis Framework for Distribution Network DER Integration in India: Distributed Solar in Tamil Nadu

Kapil Duwadi, Killian McKenna, Akshay Jain, Kajal Gaur, Adarsh Nagarajan, David Palchak
National Renewable Energy Laboratory

Tamil Nadu Generation and Distribution Company (TANGEDCO)

NREL is a national laboratory of the U.S. Department of Energy
Office of Energy Efficiency & Renewable Energy
Operated by the Alliance for Sustainable Energy, LLC

This report is available at no cost from the National Renewable Energy Laboratory (NREL) at www.nrel.gov/publications.

Contract No. DE-AC36-08GO28308

Technical Report
NREL/TP-6A20-78114
March 2021

National Renewable Energy Laboratory
15013 Denver West Parkway
Golden, CO 80401
303-275-3000 • www.nrel.gov

NOTICE

This work was authored in part by the National Renewable Energy Laboratory (NREL), operated by Alliance for Sustainable Energy, LLC, for the U.S. Department of Energy (DOE) under Contract No. DE-AC36-08GO28308. Funding provided by the Children's Investment Fund Foundation (CIFF) under Contract No. ACT-18-42. The views expressed herein do not necessarily represent the views of the DOE, U.S. Government, or CIFF. The methodology, formula, and analysis used and presented in this report and the views herein do not necessarily represent the views of or are endorsed by the Tamil Nadu Generation and Distribution Corporation (TANGEDCO). TANGEDCO has not evaluated the accuracy or validity of the findings in this report.

Perspective

This report is part of a two-part series that represents a yearlong collaboration with the Tamil Nadu Generation and Distribution Corporation Limited (TANGEDCO) on power sector planning. The first report in this series, the *Pathways for Tamil Nadu's Electric Power Sector 2017-2030* report, outlines the National Renewable Energy Laboratory's (NREL) work with TANGEDCO's electricity sector planning department to develop a model of the state's power system and evaluate multiple scenarios of system growth given resource constraints, costs of technologies, and power sector policies. This second report focuses on the rapidly transforming distribution network in the state. The report outlines a framework developed by NREL with TANGEDCO's distribution utility to quickly and accurately analyze the impacts of integrating renewable energy, specifically rooftop solar photovoltaic (PV), onto Tamil Nadu's distribution system. Together these studies help to prepare Tamil Nadu for a rapidly transforming power system.

NREL's partnership with TANGEDCO is the first of several collaborations with India's states to enhance their ability to plan for and effectively manage the transformation of India's power system to higher levels of renewable energy. A better understanding of the impacts of this transition allows for better practices, more effective policies, and increased capacity to absorb new technologies. The results of these collaborations are forthcoming and are available *online*. This work is supported by the Children's Investment Fund Foundation (CIFF).

Acknowledgments

The authors are hugely thankful for the collaboration from our partner utility in this report, the Tamil Nadu Generation and Distribution Company (TANGEDCO). TANGEDCO's team, specifically their distribution and geographical information system (GIS) teams, were invaluable throughout this effort in providing data, input and feedback throughout this study. We are grateful to those who provided comments and support throughout the study, including Julieta Giraldez, Jeremy Keen and Jaquelin Cochran at the National Renewable Energy Laboratory (NREL), Martin Scherfler and Reshma Suresh of Auroville Consulting and Deepak Krishnan of the World Resources Institute. We are also thankful for the early inputs from Vishnu Rao of the Citizen consumer and civic action Group (CAG). Any errors and omissions are solely the responsibility of the authors. This work was funded by the Children's Investment Fund Foundation (CIFF).

List of Acronyms

CIFF	Children's Investment Fund Foundation
CRI	customer risk index
DER	distributed energy resource
EEI	Energy Efficiency Index
EMeRGE	Emerging technologies Management and Risk Evaluation on distribution Grids Evolution
GIS	Geographical Information Systems
GSF	grid support function
LEI	line efficiency index
LLRI	line loading risk index
NREL	National Renewable Energy Laboratory
NVRI	nodal voltage risk index
PCC	point of common coupling
PV	photovoltaic
QGIS	quantum geographical information system
QSTS	quasi-static time series
SARDI	system average risk duration index
SCADA	supervisory control and data acquisition
SNE	system net export
TANGEDCO	Tamil Nadu Generation and Distribution Company
TEI	transformer efficiency index
TLRI	transformer loading risk index
TNE	transformer net export

Executive Summary

Tamil Nadu is one of India's pioneering States in the growth and development of renewable energy and continues to be a leader as wind and solar energy grow around the country [1]. The Tamil Nadu Generation and Distribution Company (TANGEDCO), a vertically integrated utility responsible for power generation, transmission, and distribution for the state of Tamil Nadu, has managed this transformation, which has largely taken place on the bulk power system. A major challenge for TANGEDCO and other state utilities going forward will be the increasing adoption of distributed energy resources (DERs) on their medium- and low-voltage (high- and low-tension) distribution networks, driven by ambitious renewable energy targets for India, with a target of 175 GW of renewable capacity from wind and solar by 2022 [2], and 450 GW by 2030 [3]. The National Renewable Energy Laboratory (NREL) collaborated with TANGEDCO to establish a framework for holistic distribution system analysis considering the potential risks and/or benefits of the anticipated integration of high levels of rooftop solar photovoltaic (PV) systems. Overall, high penetration PV deployment is shown to decrease asset loading and reduce under-voltages (these are described by a new metric, the system average risk duration index [SARDI]) relating to system voltages and line and transformer overloading (Figure ES- 1).

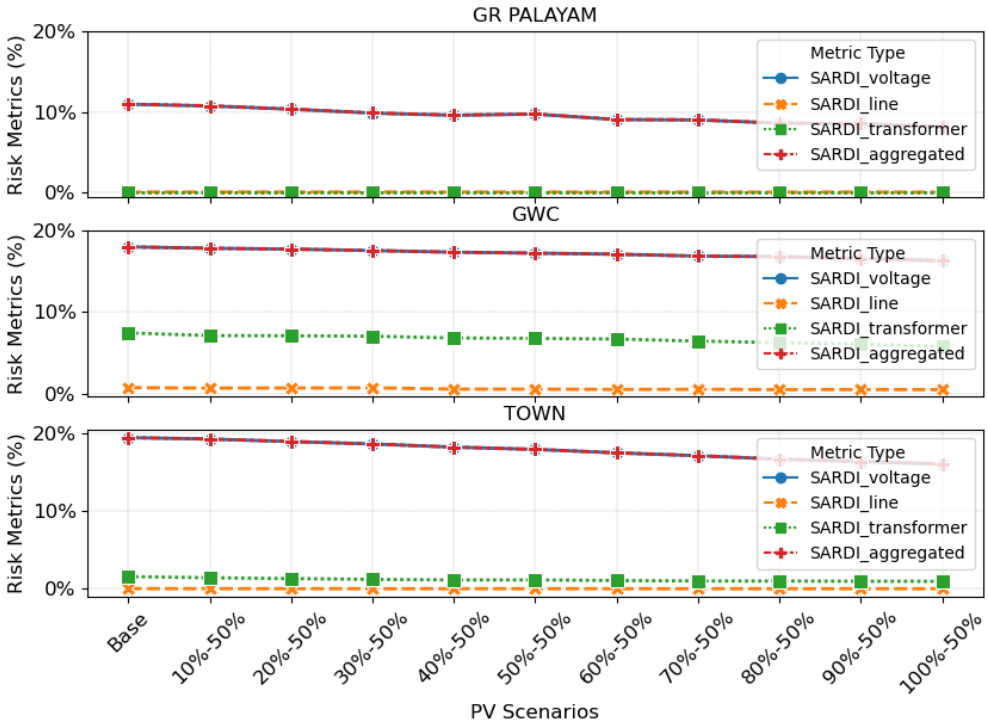

Figure ES- 1. SARDI for three TANGEDCO feeders (baseline year 2018) under increasing penetration levels looking at the number of customers and % of annual energy customer to annual PV production (shown as %-% on the x-axis)

Note: In scenarios where annual PV energy production is equal to customer annual energy consumption, customers only have PV panel capacities of 1–2-kW.

NREL has performed detailed analyses of solar rooftop PV integration for three TANGEDCO distribution feeders and ran scenario analysis of increasing penetration of customers with rooftop PV. Figure ES- 1 shows a scenario where PV capacities area sized to have an annual energy

production equal to annual energy consumption at a customer site. This case produces PV capacities in the range 1–2 kW. The analysis in this report contains the following findings:

- **Impact of Rooftop Solar PV:** Increasing solar PV adoption levels for the modeled TANGEDCO feeders improves overall power quality by increasing low voltages originally observed on the network. Negative impacts occurred only at very high PV penetration levels, with a small number of distribution assets experiencing overloading.

- **Potential of PV Inverter Volt-VAR Support:** Volt-VAR support has traditionally been used to lower potential over-voltages that can be caused by large deployments of PV. On TANGEDCO feeders, it can serve to mitigate under-voltages, bringing low voltages up toward nominal. NREL also examined continuous volt-VAR support (i.e., inverter providing constant support rather than just during PV production hours), and this provided additional support in increasing nighttime low voltages. Overall, high voltages were not of concern.

NREL developed a custom approach to distribution network analysis for TANGEDCO, defining risk by assessing the magnitude of power quality violations, the number of customers impacted, and the duration of violations. This allowed NREL to compare the original operating risk without PV to the scenarios with solar PV. The novelty of the work allows defining the hosting capacity levels with associated *risk* to the network (either improved or worsened) of different PV penetration levels (i.e., location adoption and capacity levels) rather than defining hosting capacity solely based on the first network violation. *This has been developed into an open-source publicly available analysis framework called Emerging technologies Management and Risk evaluation on distribution Grids Evolution (EMeRGE).*

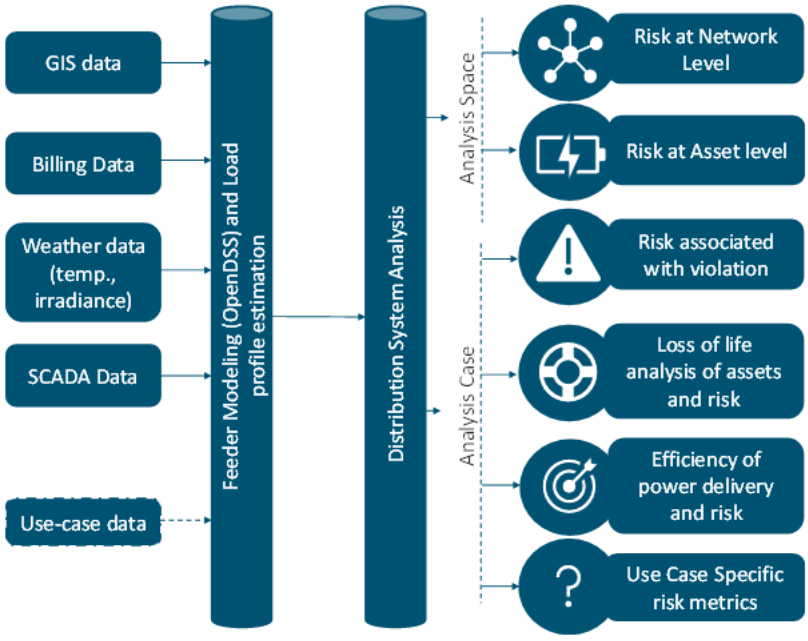

Figure ES- 2. NREL framework for TANGEDCO distribution feeder modeling and distribution system analysis

NREL developed a tool that used TANGEDCO GIS data to model distribution feeders and billing and supervisory control and data acquisition (SCADA) data to develop customer class load profiles (e.g., residential, industrial, commercial, and agricultural), given that no customer-level time-series load profiles were available. The approach also examined overall network efficiency and the impact of changing power flow on transformer loss of life. The overall framework detailing feeder modeling and risk analysis is presented in Figure ES- 2.

Table of Contents

List of Figures

List of Tables

1 Introduction

Tamil Nadu, a state in southeastern India, is at the forefront of achieving India's ambitious renewable energy targets: to have installed 175 GW of renewable capacity from wind and solar by 2022. When including large hydro in this target, it brings the total to 225 GW [2]. For context, in 2018, the peak load of the country was 189.95 GW [4]. India has added to these plans with a target of 500 GW of renewable energy capacity by 2030.

Tamil Nadu is a state with both a large amount of installed renewable energy resources, along with great potential for more capacity, both at the bulk system and distributed generation level. As of 2020, Tamil Nadu had the second-highest installed renewable power capacity (14.83 GW) after Karnataka (15.32 GW) [5]. In 2018, Tamil Nadu had 8.59 GW of installed wind power and 2.22 GW of installed solar power capacity.

The work in this report details research performed by the National Renewable Energy Laboratory (NREL) for the Tamil Nadu Generation Distribution Company (TANGEDCO) to support distributed energy resource (DER) integration, specifically solar photovoltaic (PV), on their distribution network. This research was supported by the U.S. Department of Energy, the Hewlett Foundation, and the Children's Investment Fund Foundation (CIFF). The overall aim of this research was to build distribution planning and analysis tools to help TANGEDCO integrate distributed solar rooftop PV.

TANGEDCO is a vertically integrated utility responsible for power generation, transmission, and distribution for the state of Tamil Nadu. The utility supplies 28.8 million customers and has an installed generation capacity of 32.97 GW (as of May 2018) [6]. A major challenge for TANGEDCO will be the increasing adoption of DERs on their medium- and low-voltage (high- and low-tension) distribution networks. NREL collaborated with TANGEDCO to establish a framework for holistic distribution system analysis considering the potential risks and/or benefits of the introduction of emerging DER. NREL has assisted TANGEDCO with the following contributions:

- Developed an automated distribution network feeder creation tool from TANGEDCO geographical information system (GIS) data
- Developed a methodology for TANGEDCO to create load shapes for the key different load sectors (e.g., industrial, commercial, agricultural, residential) based on their available data (bimonthly billing data and distribution network feeder head supervisory control and data acquisition [SCADA] data)
- Developed a tool for the assessment of new distributed PV interconnection requests and assess the risk of such systems to network power quality
- Developed a holistic distribution analysis framework (see Figure 1) to assess the existing risk of the network based on power quality from quasi-static time-series (QSTS) power flow
- Assessed the risk to three TANGEDCO distribution feeders under high penetration of distributed solar PV

- Analyzed the potential benefits of using advanced inverter functions, such as volt-VAR, to improve power quality at high penetration of distributed solar PV.

NREL has deployed the analysis tools and associated dashboards at TANGEDCO utility company. The utility has been actively converting network feeders and running the analysis tools and aims to integrate the developed capabilities into their planning processes.

1.1 Background: TANGEDCO Distribution Advances

TANGEDCO is developing visibility capabilities of their high and low-tension (also referred to as medium and low-voltage) networks through investing in their GIS. TANGEDCO is undertaking the task of mapping the assets of the distribution system from the medium-voltage down to the low-voltage network, herein referred to as the high-tension and low-tension networks. Building out the GIS mapping will allow TANGEDCO to create models to capture the technical behavior and power flow for these networks, which is one of the principal tasks of this research. The visibility of load behavior remains a challenge for TANGEDCO, as SCADA data is only available for their primary distribution substations, meaning there is little visibility of downstream and load class characteristics. Tamil Nadu also has ambitious renewable energy targets with the Ministry of New and Renewable Power (MNRE) sanctioning 5 MW in residential sector to Tamil Nadu Energy Development Agency (TEDA) for implementation of Phase–II Grid Connected Rooftop Solar (GCRTS) Scheme, with a rooftop solar target of 3,600 MW by 2023 [7]. Tamil Nadu also has a target to install solar pumps for over 20,000 agricultural sites at the grid-edge [8]. High tension customers in Tamil Nadu can currently install rooftop solar under a net feed-in mechanism. The following are the key distribution challenges facing TANGEDCO:

- **Utilizing GIS Mapping:** To arrive at an accurate power flow study, TANGEDCO is using its available GIS-based asset information to compute the length of the feeders (the system will automatically calculate feeder length), connected transformer capacity, and connected consumers. TANGEDCO is ambitious in geotagging all assets and consumers, which can be used in visualizing distribution assets, real-time network status, network planning, and as part of technical analysis.

- **Visibility of Load Characteristics:** The real-time load characteristics obtained from SCADA systems is currently available only in major towns for monitoring the real-time distribution system parameters. TANGEDCO may also use the same for distribution planning purposes.

- **Integration and Interconnection of Solar PV:** As mandated by TNERC Order No. 03 dt. 25.03.2019 under Tamil Nadu Solar Energy Policy 2019, solar rooftop services are affected in all low-tension categories (except Huts and Agriculture) up to the sanctioned demand [9]. Grid connectivity for rooftop solar systems is restricted to 90% of the distribution transformer capacity subject to the technical feasibility. Up till now, the impacts of integration of solar PV with respect to existing system parameters of the grid had not been studied; however, a technical feasibility study may be done on the existing system parameters with the analysis tools provided by NREL, which will be helpful to TANGEDCO for the operation and maintenance teams during the interconnection of PV. The analysis tool dashboards developed by NREL may be used to showcase the results.

1.2 Technical Approach: Framework for Distribution Analysis

NREL has developed a comprehensive distribution network analysis framework for TANGEDCO utilizing their GIS, SCADA, billing, and local weather data to create a comprehensive model of their distribution network operation. These data are used to build up a detailed model of the current system operation (also referred to as "base case" scenario), and, from there, the model is taken into a risk assessment and decision-making framework (Figure 1). Risk is established by assessing the impact of emerging DERs, such as solar PV, on network voltages and thermal loading. This report focuses on solar PV, but the framework has been designed such that it can easily be repurposed for other emerging DERs.

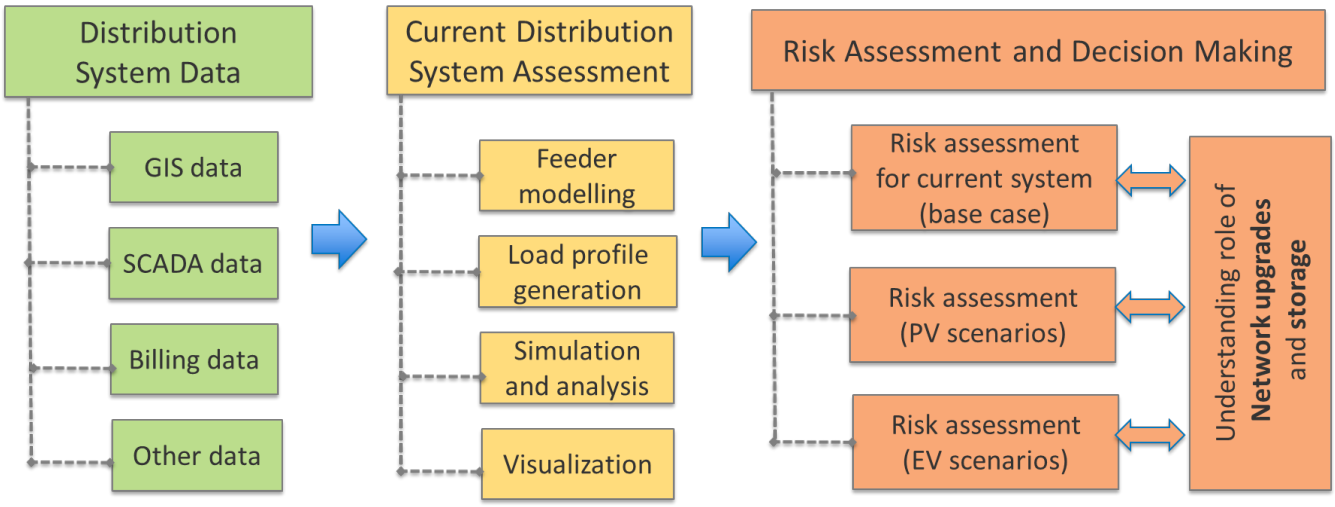

Figure 1. NREL framework for TANGEDCO distribution system analysis

A traditional problem with many power-flow analyses, particularly when it comes to the integration of solar PV, is a fundamentally flawed concept of hosting capacity and its relation to network violations. Hosting capacity itself has numerous definitions, but generally refers to the capacity of DER that a network can accommodate before violating a constraint. There is a large variation in hosting capacity definitions and constraints, from the number of network constraint violations, the depth and duration of violations, and the stochasticity (i.e., randomness) of where the PV capacity is allocated among other metrics. The variation in the definition of these variables and the thresholds of network constraints will produce different hosting capacity results. The novelty of the work here is to move away from defining the hosting capacity of the network as a single value but look at the associated *risk* to the network (either improved or worsened) of different PV penetration levels (i.e., location adoption and capacity levels) of solar rooftop PV. This is important, particularly when distribution networks already operate with a tolerated level of risk (i.e., with power quality excursions). *This work has been developed into an open-source publicly available analysis framework called Emerging technologies Management and Risk evaluation on distribution Grids Evolution (EMeRGE).*

1.3 Report Assumptions

The analysis in this report has some limitations based on assumptions and availability of data required for modeling distribution network feeders at TANGEDCO. To produce the results, the following assumptions were made:

- **Load profiles:** Direct load profiles for customers on the feeder were not available. As a result, NREL used regression models on TANGEDCO SCADA data and customer bimonthly billing data to produce representative load profiles for residential, commercial, industrial, and agricultural sectors.

- **Network modeling and GIS data**: TANGEDCO is in the process of mapping all its assets and consumers in GIS, and this process is being actively updated. The GIS data used in the report represents a snapshot in that process that is still being improved upon. As a result of limited data, the load-flow results have yet to be validated against field measurements downstream of the distribution substation.

2 Distribution Network Feeder Modeling

A major benefit of this collaboration with TANGEDCO is being able to now model distribution network feeders. Modeling distribution feeders enables TANGEDCO to do load-flow analysis to assess both the current health of the network and power quality, but also to aid in running scenario analysis for distribution planning and operation. Network modeling involves using GIS data on asset characteristics, location, and connectivity, and building an electrical network from these data. This can be a time-consuming and intensive process, so NREL has taken TANGEDCO data and scripted automated processes to create network models from GIS data.

NREL has developed an open-source tool, scripted in Python,[1] for converting GIS data (.shp files) into the OpenDSS distribution model format, along with other capabilities, called Emerging technologies Management and Risk evaluation on distribution Grids Evolution (EMeRGE) [10], [11]. EMeRGE leverages OpenDSS, a popular open-source distribution system simulator developed by the Electric Power Research Institute, as the platform to perform network load-flow [12]. OpenDSS is used for its ability to solve three-phase unbalanced power flow and easy interface to Python. Additional scripts and dashboards are developed in Python for analyzing multiple scenarios, handling large data sets from time-series power flow, and for visualizing the results.

A further important step in the analysis is the development of time-series load consumption and PV production profiles to enable time-series analysis. NREL has developed a tool, scripted in R,[2] an open-source programming language popular for statistical analysis and model development, to estimate load profiles for four types of consumer classes from the data obtained, explained in Section 3 [13]. The rest of this section describes the data obtained from TANGEDCO and the distribution network conversion tool.

2.1 Description of Available Data

NREL was provided with SCADA, GIS, and bimonthly billing data from TANGEDCO for three distribution feeders, herein referred to as GR PALAYAM, GWC, and TOWN. SCADA data contained approximately minute resolution power and voltage data at the feeder-head level, GIS data contained distribution system assets information in a .shp file format, and bimonthly billing data was provided in .xlsx file format and contained bimonthly energy consumption for all customers for 2018. SCADA data and bimonthly billing, along with various other information about customers, were used to estimate time-series load profiles using statistical models and is explained in detail in Section 3. Table 1 summarizes data for all three feeders.

[1] Python Software Foundation. Python Language Reference, version 2.7. Available at http://www.python.org.
[2] R Core Team (2020). R: A language and environment for statistical computing. R Foundation for Statistical Computing, Vienna, Austria. URL https://www.R-project.org/.

Table 1. All Data Received From TANGEDCO for the Three Feeders

Parameters	GR PALAYAM	GWC	TOWN
Total Low-Tension Customers (0.44 kV line-to-line voltage)	1,708	1,943	6,243
Total High-Tension Customers (11 kV line-to-line voltage)	3	0	0
Peak Load (MW)	3.0	1.2	4.0
Number of Distribution Transformers (11/0.44 kV)	16	12	27
Number of High-Tension Lines	209	205	215
Number of Low-Tension Lines*	2,959	594	4,154
% Residential Customers Count	81.76%	88.06%	75.63%
% Commercial Customers Count	14.0%	11.01%	23.06%
% Industrial Customers Count	2.22%	0.8%	1.0%
% Agricultural Customers Count	2.02%	0.13%	0.31%

* Does not include service wires from low-tension poles to customers. Customers were connected to the nearest low-tension or high-tension pole, using a service conductor depending on customer.

2.1.1 Assumptions

The following assumptions were made in modeling TANGEDCO distribution feeders:

- **Service conductors:** All low-tension consumers are connected to the nearest low-tension pole all aluminum alloy conductors of size 4.0. The conductor length is assumed to be equal to the shortest distance between the nearest pole and the customers. RABBIT conductors of size 7/3.35 are used to connect high-tension consumers to the nearest high-tension pole. The feeders are modeled with this conductor from the substation transformer to the distribution transformers.

- **Conductor clearance and conductor spacing:** Based on discussion with TANGEDCO, vertical conductor spacing is assumed for both high-tension and low-tension lines (including both single and three-phase); the height of the top conductor to the ground is assumed to be 9 meters for high-tension lines and 8 meters for low-tension lines, and the spacing between two conductors is assumed to be 1 meter for high-tension and 0.47 meters for low-tension lines.

- **Load type:** No information was provided for type of customer load. We assumed all low-tension loads to be star-connected and high-tension loads to be delta-connected, and all loads were also assumed to have a constant power consumption with respect to the voltage supply.

- **Multiple three-phase tapping:** It is a common practice in India to have multiple three-phase taps from the distribution transformer. Based on discussions with the distribution utility, three-phase conductors are tapped from all distribution transformers.

2.2 Conversion Process

NREL extracted data on distribution assets (conductors, transformers, customers, and so on) from .shp files in a CSV file format with the help of QGIS, a free open-source cross-platform desktop tool that allows viewing, editing, and analyzing of geospatial data [14]. During this process, coordinate fields for distribution components were added if they were missing in the original attribute table using QGIS. A special plugin MMQGIS was used to extract coordinates for line elements within QGIS.

In a second step, the extracted CSV files were converted into standard format with required fields only. During this process only the columns necessary to develop the OpenDSS input files are kept. A tool was developed using Python, which converted the CSV files in standard format to the .dss files representing the distribution feeder model. Assumptions made for unavailable data are explained in Subsection 2.1. Figure 2 gives a pictorial representation of the conversion process. The conversion process leveraged elements of NREL's distribution transformation tool (DiTTo) [15].

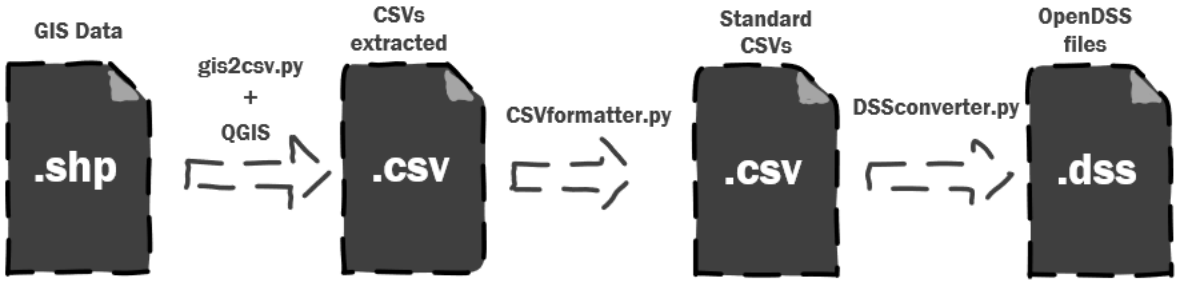

Figure 2. Conversion process from GIS data to OpenDSS model

3 Creation of Load Profile Archetypes

A major challenge in conducting distribution network power-flow analysis for TANGEDCO is the lack of available load shapes and archetypes. As advanced metering infrastructure has not been implemented at TANGEDCO and SCADA system data only covers the feeder head aggregated feeder load (i.e., primary distribution substation), there is a lack of data to produce load shapes for different customer classes (i.e., industrial, commercial, agricultural, and residential). Creating customer class load shapes is of key benefit to TANGEDCO and enables holistic analysis of their distribution system by enabling time-series power-flow and load shape analysis. While distribution operational upgrades recommend rolling out SCADA to more distribution assets (e.g., low-tension distribution transformers, and so on) and to implement a plan to roll out an advanced metering infrastructure, NREL has come up with a method to produce load profile archetypes to make up for the current data scarcity.

TANGEDCO provided NREL with two data sets: feeder head SCADA data for three distribution feeders and customer bimonthly billing data for the customers on those feeders. NREL has performed quality control on the data, removing outliers that were suspected data errors and consolidating all the data into 15-minute resolution timestamped time series data. NREL then established a novel methodology to isolate customer class load shapes by utilizing only the SCADA and customer bimonthly billing data by using a regression analysis technique and exogenous data inputs, such as weather and customer billing classes.

3.1 Input Data and Quality Control

TANGEDCO was able to provide NREL with two data sets: feeder head SCADA data and customer bimonthly billing data. These data were provided for three different TANGEDCO feeders. In addition, NREL obtained TANGEDCO customer class and tariff categories along with historical weather data from Chennai International Airport.

3.1.1 Format of Data

NREL used four different data sets to produce load shapes and archetypes for TANGEDCO. Two data sets were received from TANGEDCO, which were feeder head SCADA data and customer bimonthly billing data (Table 2). In addition, NREL obtained customer class and tariff category data, publicly available from TANGEDCO, to map customers based on their tariff class to different load sectors (e.g., residential, commercial, agricultural, and so on) and obtained Chennai International Airport weather data to use as an exogenous input for the load shape methodology (Table 3) [16].

Table 2. Data Received From TANGEDCO

Data From TANGEDCO	Format of Data	Description of Data
SCADA Data	Approx. 1-minute time-series, Active Power, Reactive Power, Voltage, Current	1 year (2018) of feeder head (primary distribution substation) data for three different feeders
Customer Bimonthly Billing Data	Bimonthly energy consumption data (kWh), customer code, sanctioned load, and tariff class per customer	1 year (2018) of bimonthly billing per customer energy consumption data for three different feeders

Table 3. Additional Data Used for Analysis

Data From TANGEDCO	Format of Data	Description of Data
Customer Class and Tariff Category	Mapping of customer tariff classes to customer load classes (e.g., residential, commercial, and so on)	Tabular mapping from TANGEDCO (publicly available)
Chennai International Weather Data	Hourly resolution weather data including temperature, wind speed, and humidity	1 year (2018) of weather data for Chennai International Airport from METAR aviation routine weather reports.

The mapping from TANGEDCO tariff categories (available in the customer bimonthly billing data) and the different customer classes are shown in Table 4 [17].

Table 4. TANGEDCO Customer Class and Tariff Category

Customer Class	Tariff Category
Industrial	LT III-A(1), LT III-A(2), LT III-B
Residential	LT I-A, LT I-B, LT I-C
Commercial	LT II-A, LT II-B(1), LT II-B(2), LT V
Agricultural	LT IV

3.2 Methodology to Create Load Shapes

The methodology described calculates the proportion that each load class (e.g., residential, commercial, industrial, and agricultural) contributes toward the total feeder head time-series demand. First, the annual peak load of the feeder (from SCADA data) was divided proportionally among all the customers in the GIS file. For that, the proportion for each customer, *i*, was determined as follows:

$$\boldsymbol{proportion_i} = \frac{\sum_{t=1}^{6} \boldsymbol{kWh_{it}}}{\sum_{i=1}^{N}\sum_{t=1}^{6} \boldsymbol{kWh_{it}}}$$

where N is the total number of customers serviced by the feeder, $kWh_{i,t}$ is the energy consumption of the customer, i, during a bimonthly bill period t. The $proportion_i$ was further multiplied by the peak load of each feeder to obtain load multiplier values for each customer. For the GR Palayam feeder, the peak load from SCADA was further divided proportionally between high-tension and low-tension customers. The proportion was determined using corresponding *CLOAD* values provided in the high-tension and low-tension customers' GIS files. No information on high-tension customers for the other two feeders was known.

Based on the tariff class information provided by TANGEDCO, customers were assigned to residential, industrial, commercial, and agricultural load classes, per Table 4. Using a distribution of customers into the four sectors based on the bimonthly energy consumption and the weather data, the following model was created to generate typical load shapes for customers for each of the four sectors. The model can be described with the following formulation:

$$MW_{f,h} = \alpha_b + \sum_{b=1}^{6} \beta_{1b} * h * Com_{f,b} + \sum_{b=1}^{6} \beta_{2b} * h * Res_{f,b} + \sum_{b=1}^{6} \beta_{3b} * h * Ind_{f,b} + \lambda_r * temp_h * Res_{f,b} + \lambda_i * temp_h * Ind_{f,b} + \lambda_c * temp_h * Com_{f,b} + \gamma_t * temp_h + \gamma_h * h + \gamma_w * workingday + \in_{f,h}$$

Where:

$MW_{f,h}$ is the power in MW reported for feeder, f, during hour h in the study period,

α_b is a monthly constant,

$Com_{f,b}$ is the proportion of energy consumption from commercial customers for feeder f during the corresponding bimonthly billing period, b,

$Res_{f,b}$ is the proportion of energy consumption from residential customers for feeder f during the corresponding bimonthly billing period, b,

$Ind_{f,b}$ is the proportion of energy consumption of industrial customers for the feeder f during the corresponding bimonthly billing period, b,

$temp_h$ is the temperature observed in hour, h,

workingday is equal to 1 if the day is not a weekend or a public holiday.

After fitting, the model regression coefficients are created, the output of which indicates the importance of each coefficient as shown below.

Table 5. Variables, Coefficients, Standard Error, and T-Statistics for the Developed Load Model

Independent Variables	Coefficient	Standard Error	t-statistic
workingday	0.03484	0.00369	9.43***
Temp*Res	0.04365	0.00178	24.45***

The coefficients on these two variables are positive (i.e., the load increases with temperature and is also higher on a working day than on a weekend/holiday). The standard error for the model is 0.238 with an R-square of 97%. Because it is an out-of-model-range prediction, the absolute power values have an improbable range. Thus, the predicted power values were further normalized to understand the changing loads relative to one another, instead of an absolute interpretation.

3.3 Customer Class Load Shape Results

The developed methodology enables an approximation to isolate the residential, commercial, industrial, and agricultural load profiles from the aggregate TANGEDCO SCADA feeder head data. The estimated profiles are separated into two broad periods, defined as summer and winter seasonal load profiles. The normalized (i.e., per customer per kW peak) profiles for residential, industrial, commercial, and agricultural are shown in Figure 3, Figure 4, Figure 5, and Figure 6, respectively.

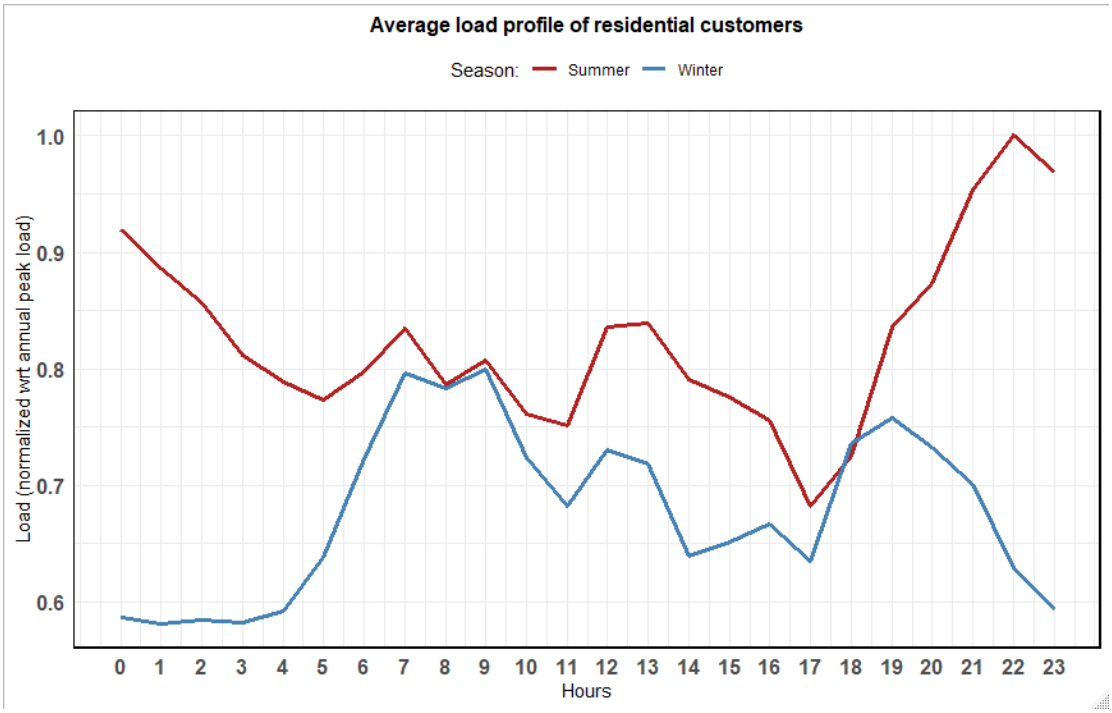

Figure 3. Average normalized load profile for residential customers for summer and winter months

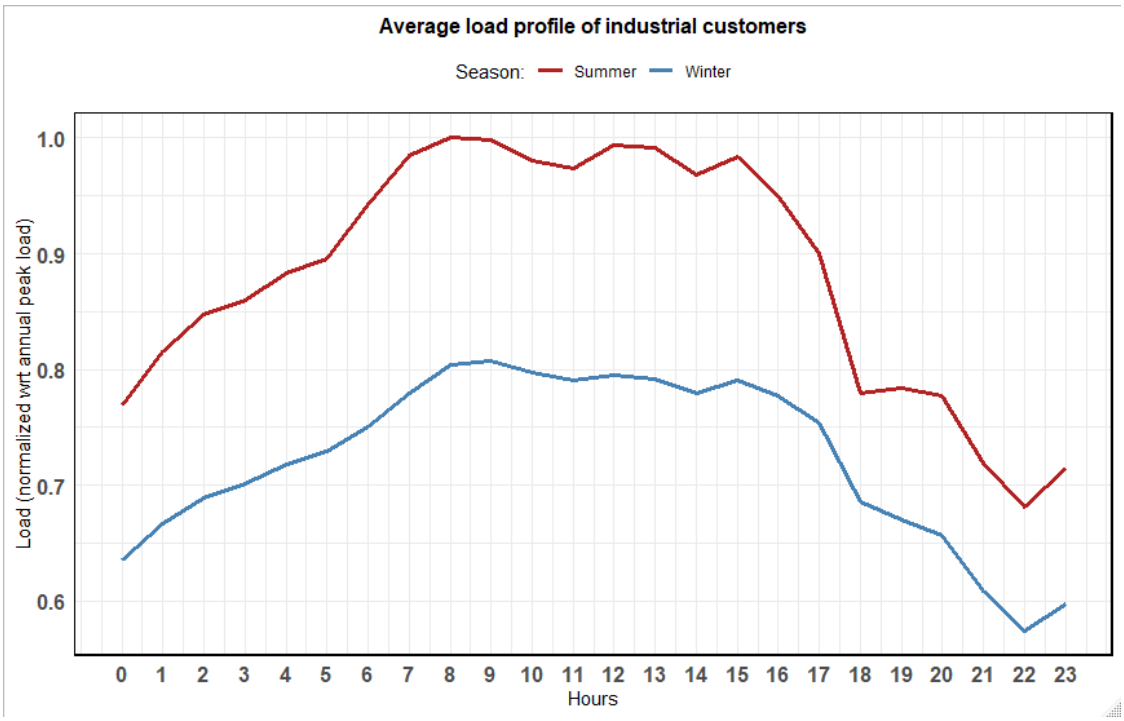

Figure 4. Average normalized load profile for industrial customers for summer and winter months

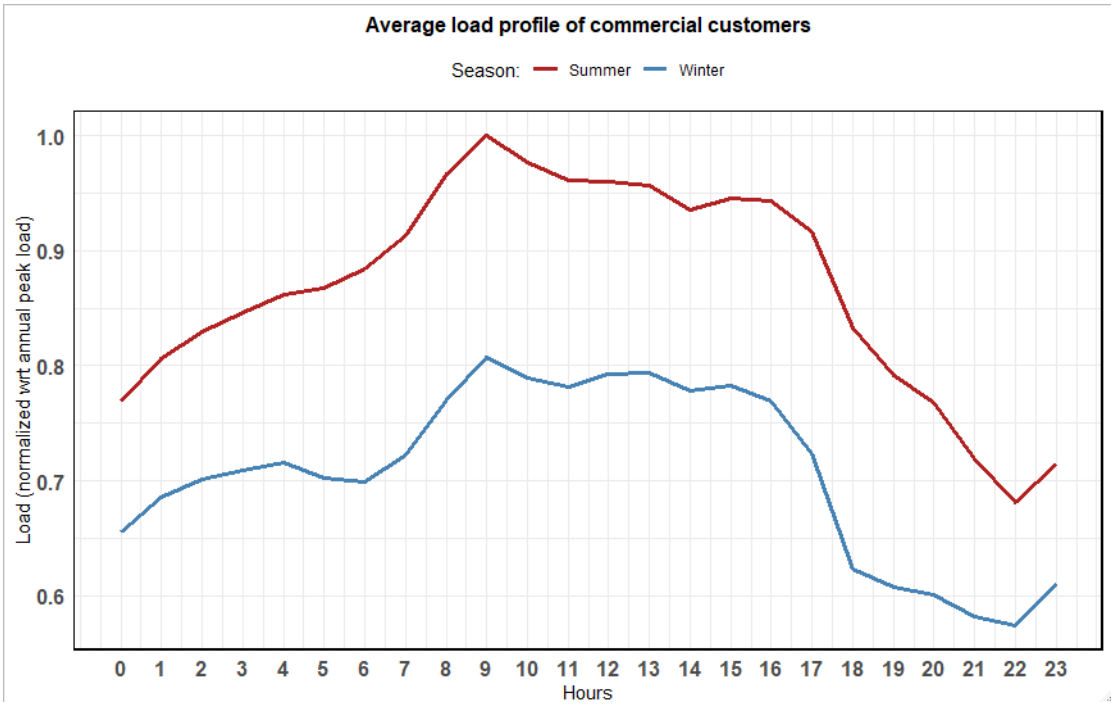

Figure 5. Average normalized load profile for commercial customers for summer and winter months.

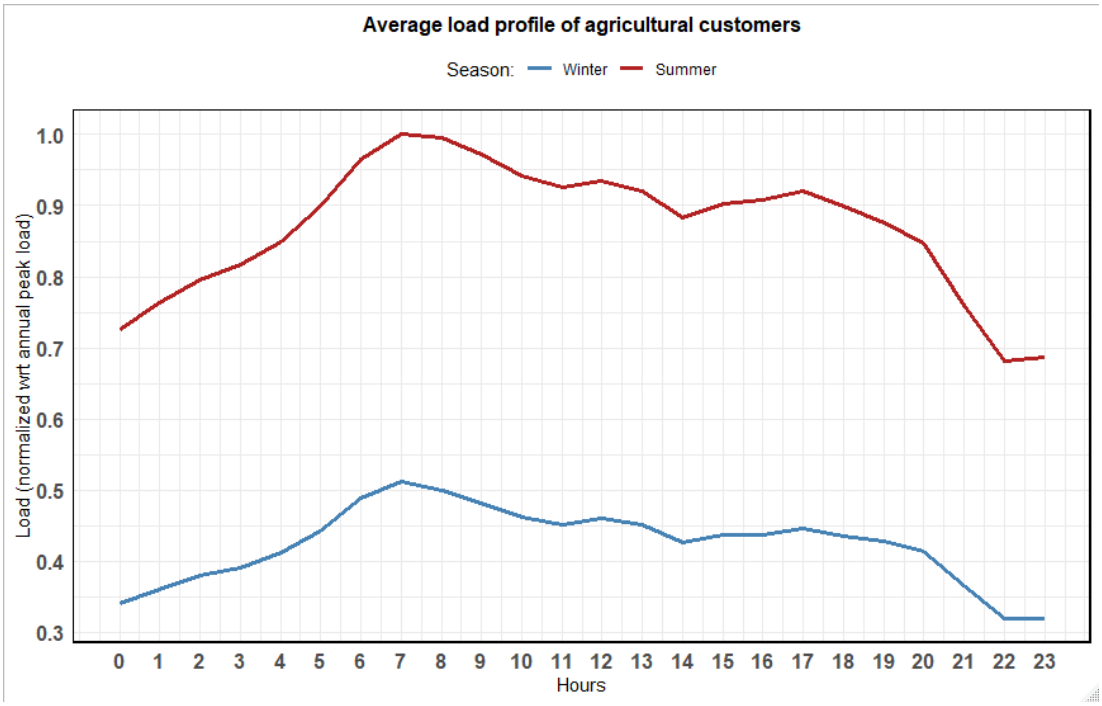

Figure 6. Average normalized load profile for agricultural customers for summer and winter months

The customer class profiles are then rescaled to the average load for the three feeders to analyze the seasonal load distribution of a feeder, and these show the daily contribution to the overall load profile per feeder, as shown in Figure 7 and Figure 8 for summer and in Figure 9 and Figure 10 for winter.

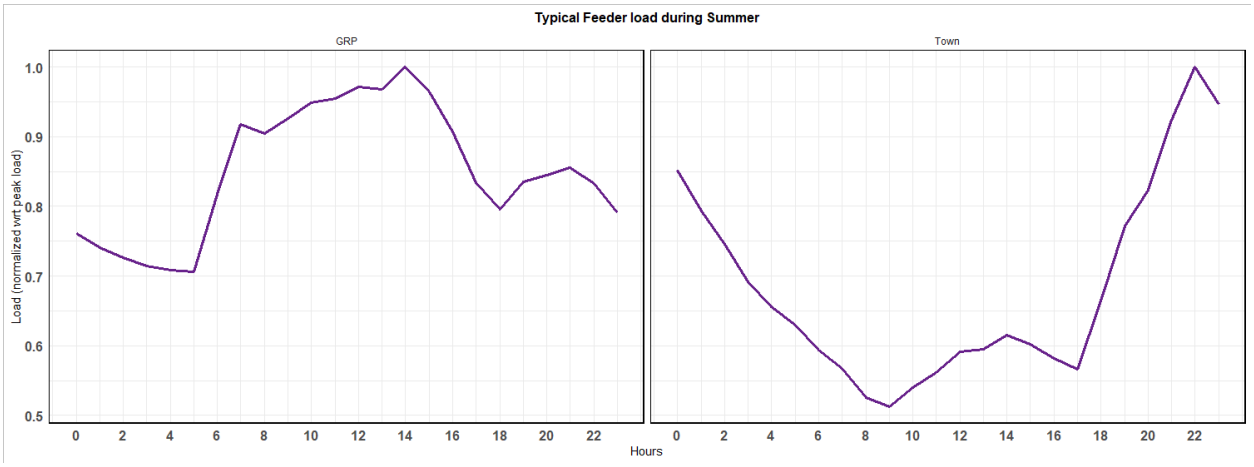

Figure 7. Average normalized load profile for GR Palayam and TOWN feeders for summer

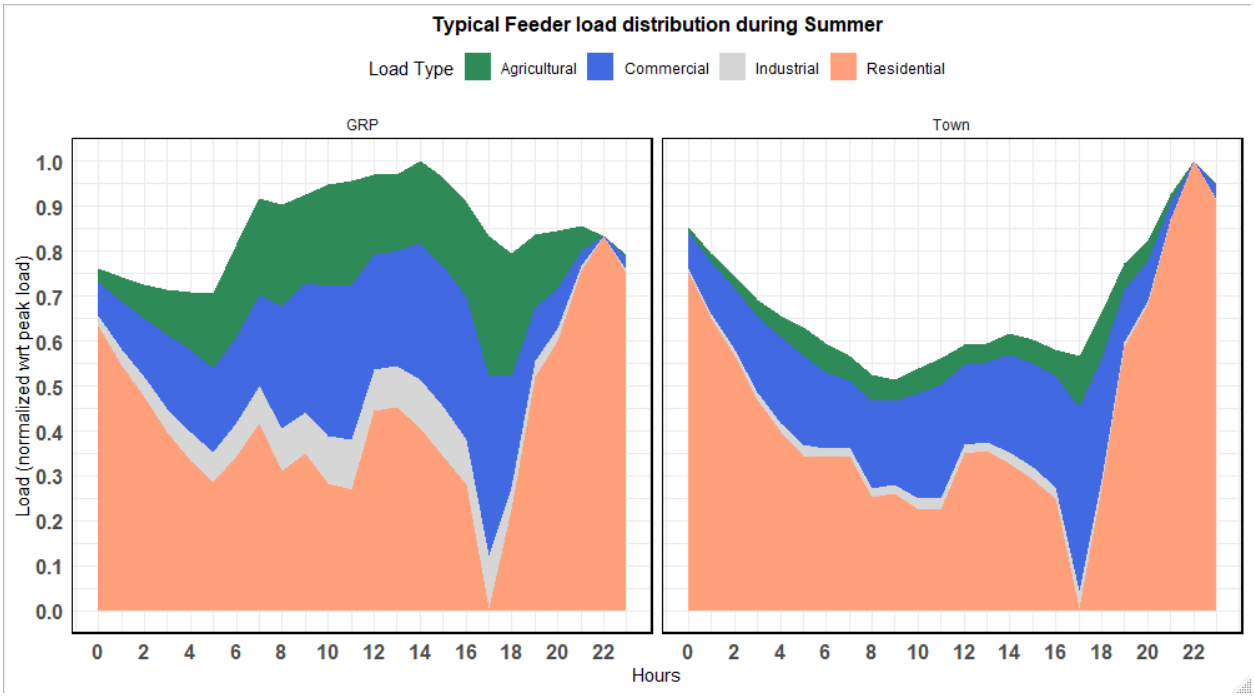

Figure 8. Average normalized load with specific contribution from each load sector (e.g., agricultural, commercial, industrial, and residential) for GR Palayam and TOWN feeders for summer

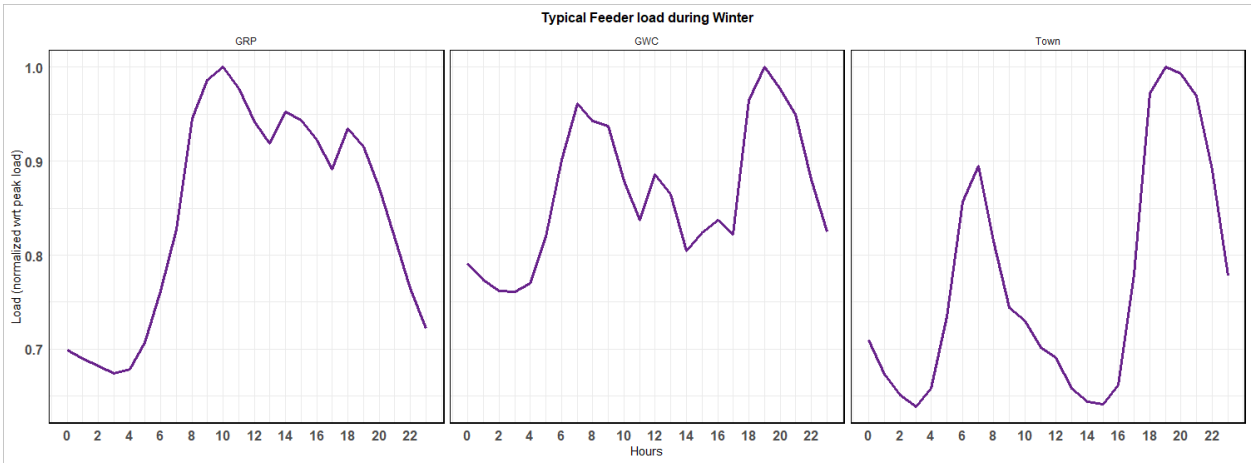

Figure 9. Average normalized load profile for GWC, GR Palayam, and TOWN feeders for winter

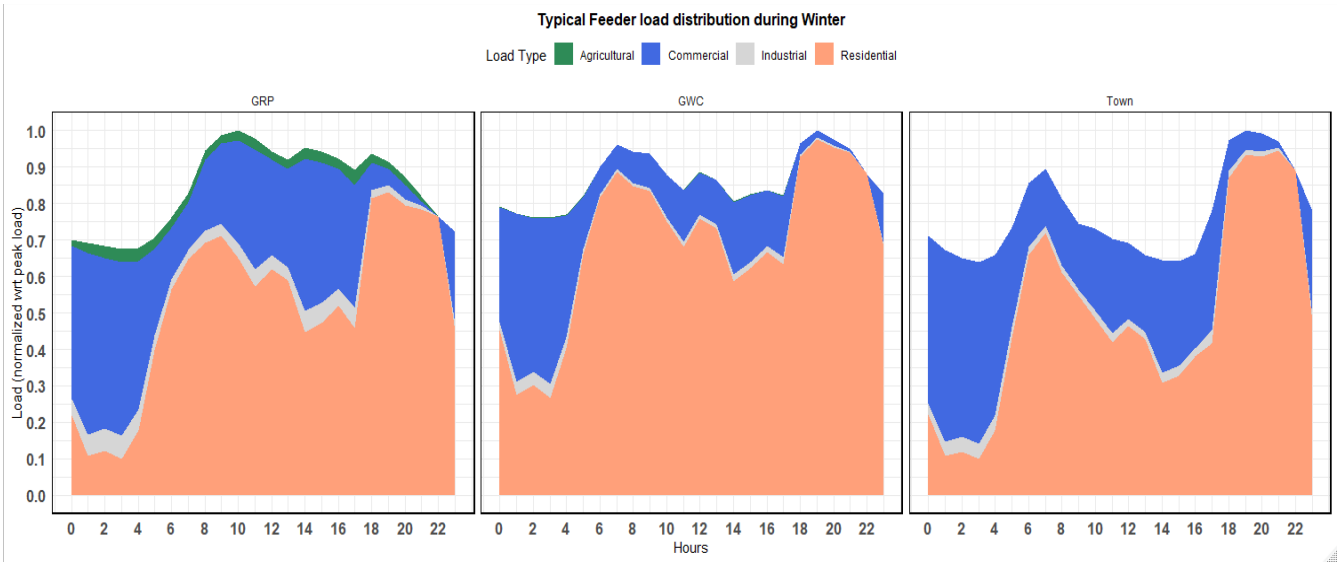

Figure 10. Average normalized load with specific contribution from each load sector (e.g., agricultural, commercial, industrial, and residential) GWC, GR Palayam, and TOWN feeders for winter

The hourly estimated load for different load sectors and seasons were then interpolated using linear approximation to estimate the power at every 15-minute time step for the complete study period of 2018. This data was later used for running power-flow analysis on each feeder in later sections of the report. The limited data used here produces valuable load profiles for the analysis, however, it would be recommended to use more SCADA feeder level data (e.g. for 10's to 100's of feeders) to produce more accurate results beyond the three feeders that were available for this analysis.

4 Solar PV Modeling and Integration Challenges

With ambitious renewable energy targets in India, the uptake of distributed solar PV is expected to increase. Increased solar PV can cause multiple technical challenges for distribution network planning and operation, and these challenges fall into the following categories:

- **Power Quality:** Distribution networks have traditionally been designed for one-way power flow, from the substation to the customer point of connection. One of the challenges of distribution network load flow is the voltage drops across assets (e.g., lines, transformers, and so on) from the substation to the end of line. Distributed solar generation results in injections of power in remote end-of-line regions of the network and can result in raising end-of-line voltages, and may result in difficulties in managing the voltage profile of the network [18]. Reverse power flow may become more prevalent, which in itself is not a problem, but in extreme scenarios may cause excessive loading of system assets and result in problems in legacy voltage regulation equipment not equipped for two-way flow of current and protection infrastructure

- **Asset Loading:** With increased solar generation on the distribution network, the traditional power flows across the network will start to change. Depending on the correlation of solar generation with traditional load consumption, this may either decrease asset loading (in the case of coincident consumption and solar production) or increase reverse power flow and asset loading (in the case of low coincident consumption and solar production and large installed solar capacity). Again, reverse power flow in and of itself is not a negative phenomenon, but it can cause problems for distribution network protection assets in maintaining safe operation of the network.

- **Protection:** Reverse power flow and injection of power in traditional load areas of the distribution network can cause challenges to system protection in detecting and isolating system faults and can create sources to continue to feed faults once assets have isolated sections of the network [19].

4.1 PV Modeling

To model solar PV systems in TANGEDCO, NREL obtained solar irradiance data for Chennai from [20]. This was used to model solar output for residential customers across Chennai. OpenDSS was used to translate irradiance data to power output for solar systems. PV systems were sized based on PV annual energy production relative to customer annual energy consumption, as shown in the equation below:

$$\%\ \text{Energy Covered by PV} = \frac{\text{Annual PV Production (kWh)}}{\text{Annual Energy Consumption (kWh)}} \times 100$$

This metric gives percentage of energy production to energy consumption for each customer. For example, 100% would indicate that a customer had produced as much energy as they had consumed for the year. This metric *does not* indicate the coincidence of production and consumption.

4.2 PV Grid Support Functions: Voltage Support

The inverter of PV systems can increasingly provide different forms of grid support in the areas of frequency support, voltage ride-through, and VAR provision for voltage control among other functions. These grid support functions (GSFs) can be mandated by utilities to help alleviate integration problems from solar PV and help bring about a more efficient and secure network. New interconnection standards are mandating that new inverters come with these capabilities [21], [22]; however, new interconnection

standards do not indicate how utilities should best implement and/or require these GSF from new customer installations. In India, the Bureau of Indian Standards, part of the Ministry of Consumer Affairs, Food & Public Distribution is responsible for solar inverter standard development (i.e., smart inverter functionality), and local regulators would be responsible for mandating smart inverter functionality is required to be used in interconnections. This report explores areas of grid support, namely those that give voltage support to the network through VAR provision and watt control. There are three principal control algorithms to provide reactive and active power support:

- **Power Factor:** In this control mode, reactive power production is directly proportional to the active power, and the relationship is set by the power factor of the inverter (where $p.f. = {}^{P}/_{S}$ where *p.f.* is power-factor, *S* is apparent power, *P* is active power). Typically, an inductive power factor is mandated to help alleviate voltage rise caused by active power injections.

- **Volt-VAR Control:** In volt-VAR control, VAR output typically has a droop output, where reactive power is directly proportional to voltage up to a point where VAR output saturates at a set voltage (e.g., maximum VAR output might be 0.44 p.u. of the inverter rating and might reach this at 1.05 p.u. voltage). In volt-VAR control, VAR is typically given priority over active power (i.e., active power may be reduced given the inverter ratings for a required VAR output).

- **Volt-Watt Control:** In volt-watt control, active power output typically has a droop output where active power reduction is inversely proportional to voltage, with this control only commencing at high voltages, or voltages above distribution network operating bounds.

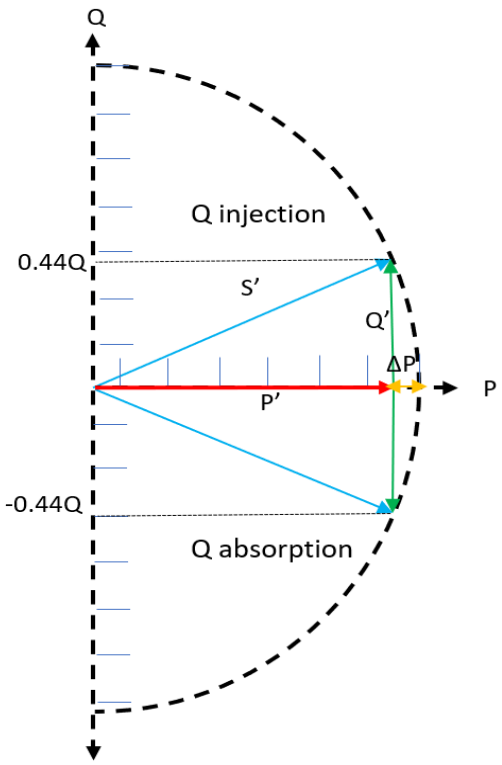

Figure 11. Inverter capability curve

Volt-VAR control provides greater flexibility, as it only injects or absorbs as much reactive power as is needed based on the inverter's point of common coupling (PCC) voltage. The inverter capability curve, as shown in Figure 11, helps in better understanding the functioning of the volt-VAR control mode of operation. In this figure, the semicircle represents the kVA rating of the inverter, which is always constant, irrespective of the real or reactive power injection at any given time point. The blue arrows represent two time instances when maximum reactive power injection and absorption is required from the inverter based on the PCC voltage. If the solar irradiance is also high at the same instance and inverter capacity limited, then a small amount of real power might be curtailed to supply the required reactive power in the VAR or reactive power priority mode. This curtailment can occur more frequently if the customer has an undersized inverter compared with the DC rating of the PV panels, also commonly referred to as "clipping." But, as it will be shown in Section 8, the total energy curtailed over the entire year is insignificant compared with the energy lost due to the clipping effect of an undersized inverter.

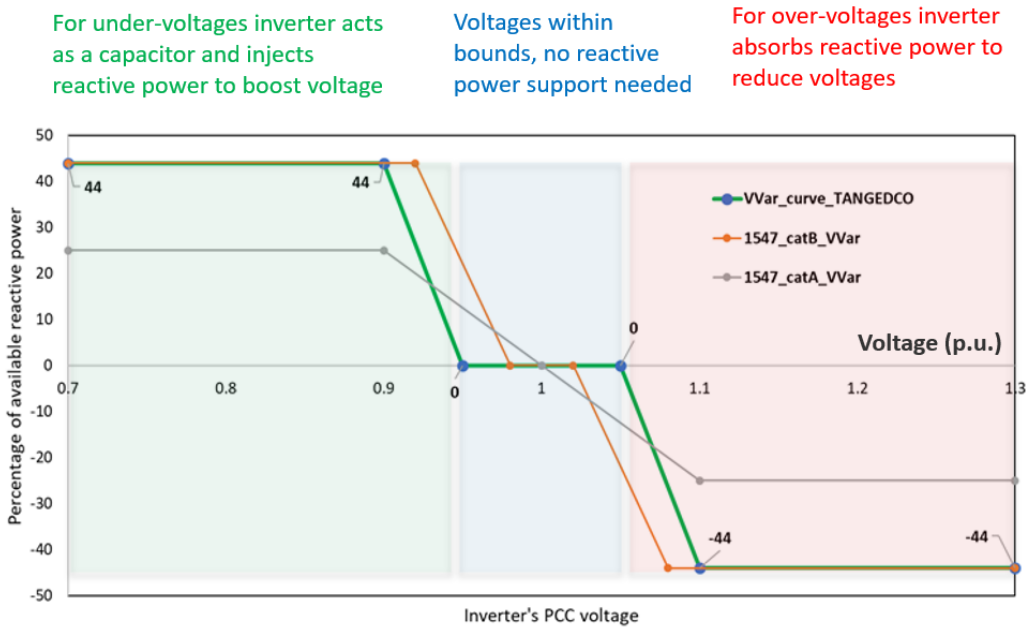

Figure 12. Volt-VAR curve regions of operation

Figure 12 shows some of the commonly used volt-VAR grid support curves in the United States based on the IEEE 1547-2018 standard [21]. The Category B volt-VAR curve shows three distinct regions of operation. When the PCC voltage is below 0.98 p.u., the inverter starts injecting reactive power like a capacitor bank, and when the voltage is above 1.02 p.u., reactive power is absorbed to reduce voltages. The maximum reactive power required is limited to 44% of the inverter's kVA rating, which further helps in reducing the energy curtailed. Also, if the voltages are close to the nominal value within a dead band of ±0.02 p.u., then no reactive power support is required. The curve used for TANGEDCO's feeders was based on the IEEE 1547 curve; however, the voltage limits were modified to match the voltage thresholds (+/- 10%) used in TANGEDCO, rather than those used in the United States (+/- 5%) [23].

While the impacts of using the volt-VAR GSF are discussed in detail in Section 8, it is worthwhile to look at the two interesting volt-VAR use cases that have been presented there. The inverter can not only provide reactive power support while injecting real power, but also during those times when it is not injecting real power. In this latter use case, the inverter can act as a distributed voltage regulating device, which solely

improves voltages without any potential adverse grid impacts. As seen in Figure 13, in the first use case, the inverter only provides reactive power when it is injecting real power as well.

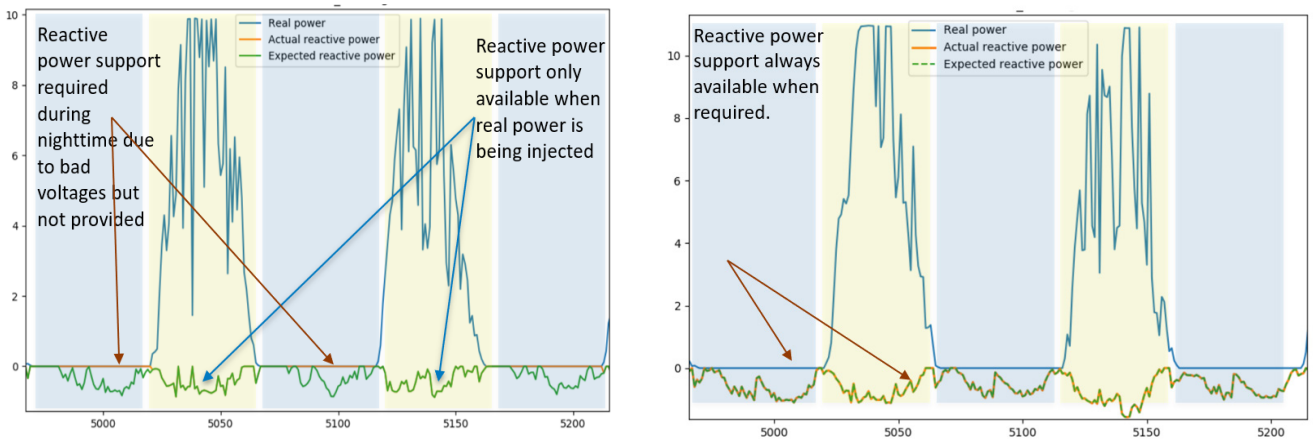

Figure 13. Volt-VAR use cases: limited daytime VAR support (left) and continuous VAR support (right) for two days of data

PCC voltage deviations from nominal and into volt-VAR operating regions show that reactive power support is required. In the second use case, the inverter provides reactive power support even during those times in which there is no solar production and can help in further improving the grid voltage profile.

4.3 PV Hosting Capacity

The hosting capacity of a distribution network is a metric that indicates the amount of solar PV (i.e., number of systems and/or total installed capacity) that a network can safely accommodate before running into network operational problems related to either power quality, asset loading, or protection limitations. Many studies have been conducted on the hosting capacity of distribution networks around the world with the results of each being highly localized and specific to the network under analysis [24], [25]; however, one observation generally seen in these studies is that with increased PV capacity present on the network, the voltage rise (i.e., a violation of the upper bound on system voltages) is typically the first problem to be seen, followed by asset overloading.

A traditional problem with many power-flow analyses is that hosting capacity can be extremely sensitive to network violations, the definition of which also varies across distribution network utilities. There is a large variation of hosting capacity definitions. The constraint limiting the hosting capacity of solar PV can come in the form of number of power quality violations, the depth and duration of violations, and the stochasticity (i.e., randomness) of where the capacity is allocated among other metrics. The variation of all of these constraints and variables produce different results.

Given these problems associated with the strict definition of hosting capacity, the proposed work in the next section looks at the associated risk to the network (either improved or otherwise) of different hosting capacity levels (i.e., adoption and capacity levels) of solar rooftop PV. The associated risk is created by an in-depth examination of network load-flow metrics.

5 Distribution System Analysis Metrics

This section details the analysis metrics to assess the power quality in terms of a risk. Several new distribution metrics are introduced to help analyze the health of the network. These developed metrics are later used to assess change in risk of the network when PV capacity is introduced.

5.1 Metrics for Assessing Power Quality Risk

The integration of DER and emerging technologies on the load side (e.g., solar PV, electric vehicles, energy efficient lighting, and so on) all introduce potential risks to distribution network planning and operation. Of key importance is how the prevalence of these technologies impacts the power quality and loading of the network and the potential need for network upgrades. Power quality can be defined as the reliability and adequacy of key system variables such as supply voltage, frequency, and waveform analysis (such as harmonics). Acceptable power quality can be described by the voltages being close to nominal or staying within prescribed standard ranges, low distortion and harmonic content and frequency close to nominal or within prescribed ranges. While there are many metrics for assessing the value of power quality, there are few that seek to quantify the risk or severity of power quality across an entire distribution feeder or network.

A principal problem with distribution system analysis is the strict definition of network violations, particularly when it comes to voltage violations and the overloading of distribution assets. In actuality, the severity of a violation is dependent on several factors, including:

- The depth of the violation (i.e., how far from bounds is the value; a 1.15 p.u. voltage violation is 0.05 p.u. out of bounds considering +/- 10%)
- The duration of the violation, either consecutive or nonconsecutive
- The importance of the asset: This can be classified by the voltage level or by the number of customers the equipment serves.

Capturing these elements in tandem for engineering analysis allows classification of the importance of a disturbance to power quality. There is a need to combine these parameters for any violation into a single metric, and to be able to aggregate those metrics to assess the overall quantification of power quality. To demonstrate the problem clearly, examine the following scenarios:

- Medium-voltage feeder three-phase line serving 1,000 customers experiences an overloading of 105% for a duration of 5 seconds;
- Low-voltage three-phase distribution transformer serving 20 customers experiences an overvoltage of 1.16 p.u. for a duration of 30 minutes; or
- 300 low-voltage residential customers experience under-voltages of 0.89 p.u. for 3 hours of nonconsecutive time on a daily basis.

The severity and risk of each of these power quality scenarios is dependent on the three elements discussed earlier, being the duration of the event, the severity of the event, and the importance of the asset (classifying potentially by voltage or number of customers served). This report proposes several power

quality metrics to help resolve this problem and enable distribution system engineers to make informed operational, planning, and investment decisions to improve the reliability and power quality of the distribution system. The proposed risk metrics and analysis leverage QSTS power-flow simulation to quantify component-level and aggregated risk by accounting duration, magnitude, and number of customers served and/or effected by the risk and assets impacted. The proposed metrics to quantify risk are explained below.

5.1.1 System Average Risk Duration Indices (SARDI)

These metrics give the percentage of time duration under consideration for which the average customer is at risk of power interruption because of a thermal and/or voltage violation. We can compute these metrics individually for line overload, transformer overload, and voltage violations, helping us to identify which one is critical. It is similar to the system average interruption duration index (SAIDI) reliability metric, which is the ratio of the sum of customer minutes of interruption to the total number of customers served [26]. The difference in this case is that the customers are not actually interrupted but are put at risk because of either a voltage violation, a line overload, a transformer overload, or any combination of them. Equation (1) gives the SARDI for voltage violations.

$$\text{SARDI}_{voltage} = \frac{\sum_{t=0}^{T} N_{VAC}^{t} \times \Delta T \times 100}{N_c \times T} \tag{1}$$

Here N_{VAC}^{t} is the number of unique customers (i.e., avoiding double-counting customers impacted by multiple violations) affected by a voltage violation in the network at time t. The way we compute the number of customers affected is that we list downward customer IDs for all voltage violations for a time t and count the number of unique customers from that list to make sure we do not overcount customers. $\Delta T, T, and\ N_c$ represent the measurement time step or simulation time step, the total time period under consideration, and the total number of customers present in the distribution network, respectively. We are considering a violation any voltage magnitude above and below 10% from 1.0 p.u. for analysis purpose in this report.

Similarly, we can compute the SARDI metric for line and transformer-related violations (loading above 100%) as given in Equations (2) and (3).

$$\text{SARDI}_{line} = \frac{\sum_{t=0}^{T} N_{LAC}^{t} \times \Delta T \times 100}{N_c \times T} \tag{2}$$

$$\text{SARDI}_{transformer} = \frac{\sum_{t=0}^{T} N_{TAC}^{t} \times \Delta T \times 100}{N_c \times T} \tag{3}$$

Here, N_{LAC}^{t} and N_{TAC}^{t} are the number of customers affected by line overload and the transformer overload respectively at time t. The aggregated SARDI metric would consider all the technical violations at once and quantifies the aggregated risk.

$$\text{SARDI}_{aggregated} = \frac{\sum_{t=0}^{T} N_{AC}^{t} \times \Delta T \times 100}{N_c \times T} \tag{4}$$

N_{AC}^{t} represents the number of customers affected by all the thermal and voltage violations for time t.

To go even further, we may need to determine which element is more vulnerable for each of these violations. The component level risk can be assessed with the help of the following metrics.

5.1.2 Nodal Voltage Risk Index (NVRI)

An NVRI measures the average voltage violation severity (deviation from either upper or lower limits) weighted by the fraction of customers present downward of node n. The severity factor γ_t^n is based on how far the voltage magnitude is from the desired threshold value at time t for node n. It will be zero when voltage is within upper and lower voltage limit for a given node.

$$\text{NVRI}_n = \frac{N_{DC}^n \times \sum_{t=0}^{T} \gamma_t^n \times \Delta T}{T \times N_c} \tag{5}$$

$$\gamma_t^n = \begin{cases} V_n^t - V_{upper} \text{ if } V_n^t \geq V_{upper} \\ V_{lower} - V_n^t \text{ if } V_n^t \leq V_{upper} \\ 0 \qquad \text{otherwise} \end{cases} \tag{6}$$

Here, N_{DC}^n, γ_t^n, ΔT, N_c, V_{upper}, $V_{lower,}$ and V_n^t represent the number of downward customers for node n, the weighting factor at time t for node n, the simulation time step, the total number of customers, the upper voltage limit, the lower voltage limit, and the nodal voltage, respectively, at time t.

5.1.3 Line Loading Risk Index (LLRI)

An LLRI measures the average line overloading severity weighted by the fraction of customers present downward of line l. The severity factor α_t^l is based on how far the line loading magnitude is from the thermal limit at time t for line l. It will be zero when the line loading is below the thermal limit for a given line.

$$\text{LLRI}_n = \frac{N_{DC}^l \times \sum_{t=0}^{T} \alpha_t^l \times \Delta T}{T \times N_c} \tag{7}$$

$$\alpha_t^n = \begin{cases} l_t - 1.0 \text{ if } l_t \geq 1.0 \\ 0 \qquad \text{otherwise} \end{cases} \tag{8}$$

Here, N_{DC}^l, α_t^l, ΔT, N_c, and l_t represent the number of downward customers for line l, the weighting factor at time t for line l, the simulation time step, the total number of customers, and the line loading, respectively, at time t for line l.

5.1.4 Transformer Loading Risk Index (TLRI)

A TLRI measures the transformer overloading severity weighted by a fraction of customers present downward of transformer Tr. The weighting factor β_t^{Tr} is based on how far the transformer loading magnitude is from the thermal limit at time *t* for transformer *Tr*. It will be zero when transformer loading is below the thermal limit for a given transformer.

$$\text{TLRI}_{Tr} = \frac{N_{DC}^{Tr} \times \Sigma_{t=0}^{T} \beta_t^{Tr} \times \Delta T}{N_c} \tag{9}$$

$$\beta_t^{Tr} = \begin{cases} Tr_t - 1.0 & \text{if } Tr_t \geq 1.0 \\ 0 & \text{otherwise} \end{cases} \quad (10)$$

Here, N_{DC}^{Tr}, β_t^{Tr}, ΔT, N_c, and Tr_t represent the number of downward customers for transformer Tr, the weighting factor at time *t* for transformer *Tr*, the simulation time step, the total number of customers, and the transformer loading at time *t* for transformer *Tr,* respectively.

5.1.5 Customer Risk Index (CRI)

The CRI measures average severity experienced by a customer c and is experessed below:

$$\text{CRI}_c = \frac{\sum_{t=0}^{T} \gamma_t^{n_c} + \alpha_t^{l_c} + \beta_t^{Tr_c}}{T} \quad (11)$$

Here, $\gamma_t^{n_c}$, $\alpha_t^{l_c}$, $\beta_t^{Tr_c}$ are the weighting factor associated with nodal voltage violation, the line overload, and transformer overload, respectively, for which customer *c* is directly affected.

5.2 Metrics for Assessing Efficiency

In addition to the power quality metrics that capture violations, of additional importance are metrics that capture the efficiency, that is, the network losses. The following metrics describe the overall efficiency of the network in terms of power delivery to the end customer from the feeder head.

5.2.1 Energy Efficiency Index (EEI)

These metrics measure efficiency of energy transfer from the distribution network feeder head down to the end-of-line customer and can be computed separately for different groups of distribution system assets and for the entire system. Equations (12), (13), and (14) compute the efficiency for line elements, transformers, and system-wide.

$$\text{EEI}_{line} = \frac{\sum_{t=0}^{T} \sum_{l=1}^{N_l} \left(S_t^l - R_t^l\right)}{\sum_{t=0}^{T} C_t} \times 100 \quad (12)$$

$$\text{EEI}_{transformer} = \frac{\sum_{t=0}^{T} \sum_{l=1}^{N_{Tr}} (S_t^{Tr} - R_t^{Tr})}{\sum_{t=0}^{T} C_t} \times 100 \quad (13)$$

$$\text{EEI}_{System} = \frac{\sum_{t=0}^{T} \sum_{l=1}^{N_l} (S_t^l - R_t^l) + \sum_{t=0}^{T} \sum_{l=1}^{N_{Tr}} (S_t^{Tr} - R_t^{Tr})}{\sum_{t=0}^{T} C_t} \times 100 \quad (14)$$

Here, $S_t^l, S_t^{Tr}, R_t^l, R_t^{Tr}, C_t, N_l, N_{Tr}, T$ are the sending end power of line l at time t, the sending end power of transformer Tr at time t, the receiving end power of line l at t, the receiving end power of transformer Tr at time t, the circuit power at time t, the number of line elements, the number of transformers, and the total simulation time period, respectively.

5.2.2 Line Efficiency Index (LEI)

The LEI can be computed for all line elements in the distribution network. It is a measure of efficiency for individual line segments and can be computed using Equation (15). This metric can be used to help identify lines that are especially contributing toward overall system losses.

$$\text{LEI}_l = \frac{\sum_{t=0}^{T} S_t^l - R_t^l}{\sum_{t=0}^{T} S_t^l} \times 100 \tag{15}$$

5.2.3 Transformer Efficiency Index (TEI)

The TEI can be computed for all transformer elements in the distribution network. Transformer losses are generally made up of no-load losses and load losses. Transformer losses in the core are a function of harmonics, as core losses are proportional to the frequency, meaning high-frequency harmonics can increase core temperatures and increase the losses; the impact of harmonics are not captured in the modeling effort here. It is a measure of efficiency for individual transformer and can be computed using Equation (15).

$$\text{TEI}_{Tr} = \frac{\sum_{t=0}^{T} S_t^{Tr} - R_t^{Tr}}{\sum_{t=0}^{T} S_t^l} \times 100 \tag{16}$$

5.3 Metrics for Assessing Loss of Life of Transformers

Transformers are a vital asset on the distribution network, and the operation of the network can significantly impact not only the loading and losses for this equipment but also their long-term life. To create a holistic risk analysis, including the impact of the network operation on transformer life, is of key importance.

Transformer life is fundamentally a function of loading, ambient temperature, and internal temperature, but also the quality and maintenance of the asset (e.g., ensuring regular changing of insulating oil). Transformer winding insulation life is mainly determined by the hot-spot temperature of winding. ANSI/IEEE C57.91 guidance for computing hottest-spot temperature at time t follows (17), where $\theta_H, \theta_A, \theta_{TO}, \theta_G$ represent hottest-spot temperature, ambient temperature, top oil temperature rise above ambient temperature, and winding hottest-spot temperature rise above top oil temperature [27].

$$\theta_H(t) = \theta_A(t) + \theta_{TO}(t) + \theta_G(t) \tag{17}$$

The steady state top oil temperature rise above ambient temperature θ_{TOS} can be computed using Equation (18)

$$\theta_{TOS} = \theta_{TO@FL}\left(\frac{K^2 + 1}{R + 1}\right)^n ; K = \frac{S}{S_{rated}} \tag{18}$$

$\theta_{TO@FL}, K, R, n, S, S_{rated}$ represent the top oil temperature rise at full load, the ratio transformer loading to nameplate rating, the ratio of loss at rated load to no-load loss, and the exponential power of loss versus top oil temperature rise (a constant). For the transient calculation, the top oil temperature rise after t hours can be computed as:

$$\theta_{TO}(t) = \theta_{TOS}\left(1 - e^{\frac{-t}{\tau}}\right) + \theta_i e^{\frac{-t}{\tau}} \tag{19}$$

where τ, θ_i are the thermal time constant for rated load and initial top oil temperature (the initial temperature is unknown but can be determined by using an iterative method).

The hottest-spot temperature rise above top oil temperature can be computed using Equation (20).

$$\theta_G(t) = \theta_{G@FL} K^{2m} \quad (20)$$

$\theta_{G@FL}, m$ represents the hottest-spot temperature rise above rated load and exponential power winding loss versus winding gradient (a constant for the transformer).

The transformer insulation loss of life (noted as LOF) follows Arrhenius reaction rate theory according to IEEE Std. C57.91 and can be computed using Equation (21).

$$LOF(\theta_H) = 100 \times t \times 10^{-(A+B\theta_H)} \quad (21)$$

LOF is the percentage loss of life of insulation, θ_H is hottest-spot temperature of the transformer winding, and A and B are constants from the life expectancy curve.

We assumed the following (Table 6) for all transformers to compute insulation loss of life from IEEE Std. C57.115-1991 Appendix C.

Table 6. Transformer Parameters for Computing Insulation Loss of Life

Parameters	Value
Top-oil rise over ambient at rated load	36
Hottest-spot conductor rise over top oil temperature at rated load	28.6
Ratio of load loss at rated load to no-load loss	4.87
Exponential power of loss versus top-oil rise	1
Thermal time constant for rated load in hour	3.5
Exponential power of winding loss versus winding gradient	1
Loss of life logarithmic co-efficient	-13.391
Loss of life logarithmic co-efficient	6,972.15

An overall flowchart for computing the transformer insulation loss of life is presented in Figure 14.

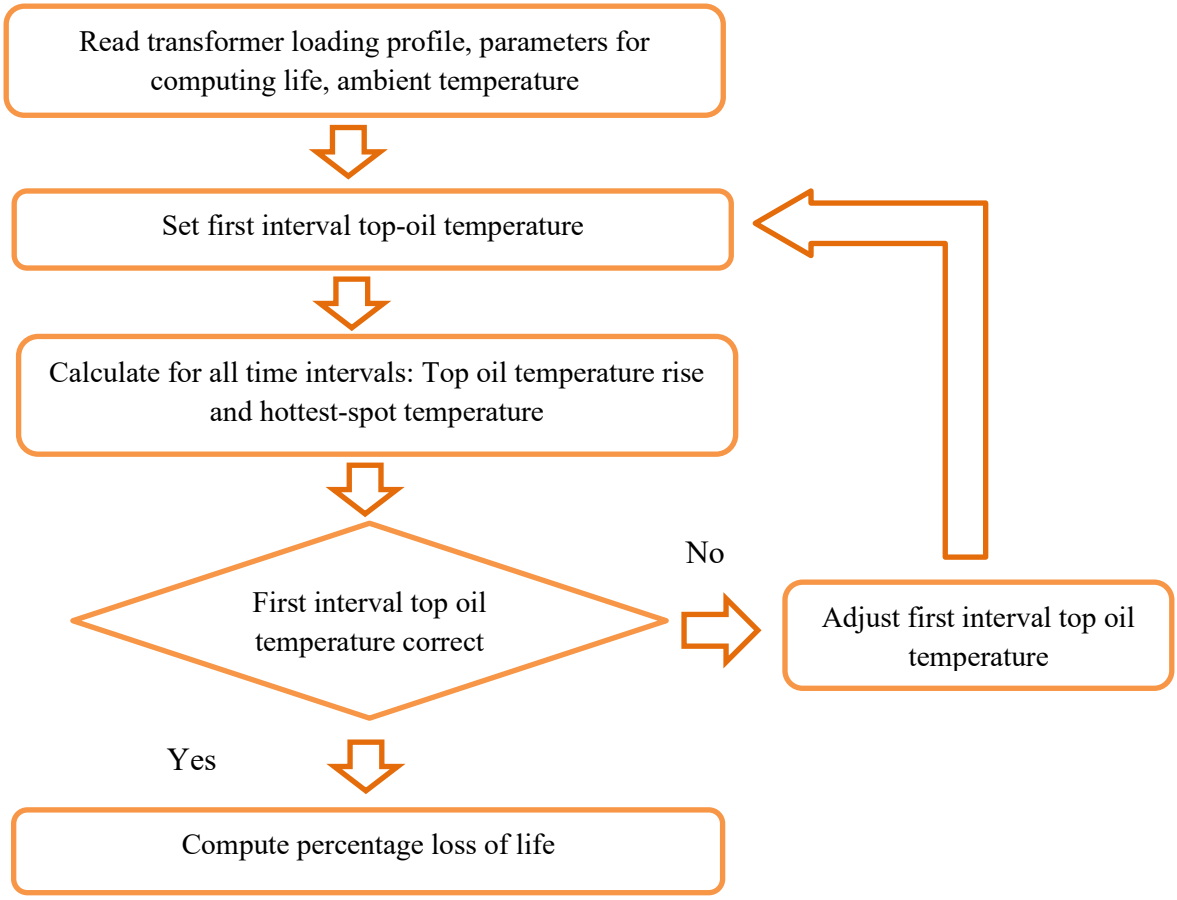

Figure 14. Flowchart for computing transformer insulation loss of life

5.4 Metrics Specific to Assessing DERs

In addition to power quality metrics, other metrics that will be specific to DER characteristics are introduced in this section. In this study, the focus is on the impact of distributed PV on distribution feeders. One of the important metrics specific to PV deployment is overgeneration (power export), either at a customer level or at a transformer-asset level.

5.4.1 System Net Export (SNE)

The system net export (SNE) metric is the percentage of energy generation exported at the feeder head because of distributed PV over a given time period with respect to the energy delivered to the load in absence of PV. PV_t^C is the PV generation at time t in whole distribution circuit.

$$\text{SNE} = \frac{\sum_{t=0}^{T} -C_t \ \ if \ C_t < 0 \ else \ 0}{\sum_{t=0}^{T} PV_t^C} \times 100 \qquad (22)$$

5.4.2 Transformer Net Export (TNE)

The TNG metric is the percentage of net export at each transformer because of distributed PV over a given time period with respect to energy delivered to the load in absence of PV. PV_t^{Tr} is the PV generation at time t downward of Transformer Tr.

$$\text{TNE}_{Tr} = \frac{\sum_{t=0}^{T} -Tr_t \;\; if \; Tr_t < 0 \; else \; 0}{\sum_{t=0}^{T} PV_t^{Tr}} \times 100 \tag{23}$$

Here TR_t is the transformer primary side active power at time t.

5.5 Risk-Based Capacity Assessment Using Distribution System Metrics

Unlike traditional distribution analysis, which is done by analyzing important time steps, to understand the impact of increasing PV penetration in distribution systems, time series analysis is required [19]. PV hosting capacity analysis is a commonly used analysis approach to understand the impact of PV in the distribution feeder. PV hosting capacity is defined as the PV capacity that can be accommodated in the distribution feeder without adversely impacting voltage, protection, line, and transformers with no feeder upgrades [28]. Evaluating how much PV can a feeder accommodate is not a simple task and depends on many variables. Some hosting capacity analysis in the past relied on analysis from few time steps (such as peak load time, peak generation time) to estimate how much PV can be incorporated. The key drawbacks were the inability to account for time series behavior of load and PV generation and only look at the worst-case scenario, which is very unlikely to occur. Recently, dynamic PV hosting capacity is becoming more popular, attempting to address the drawbacks of traditional hosting capacity analysis.

The risk-based capacity assessment approach is like the dynamic hosting capacity approach in that both attempt to capture time-series interaction. The key difference is that the risk-based approach is suitable for any kind of distribution system analysis and not limited to PV. The metrics discussed at the beginning of this chapter are at the heart of risk-based capacity assessment.

5.5.1 PV Hosting Capacity Analysis Using Risk-Based Metrics

The criteria determining when to stop adding PV in a distribution feeder varies among distribution utilities. Voltage violation, thermal violation, efficiency, transformer loss of life, and overgeneration caused by distributed PV are major drivers for determining PV hosting capacity.

Metrics described at the beginning of this chapter can be used to estimate PV hosting capacity depending on the risk tolerance level of the utility. For example, the aggregated system average risk duration index (SARDI-aggregated) can be used to determine the trajectory of risk associated with voltage and thermal violations as PV penetration increases.

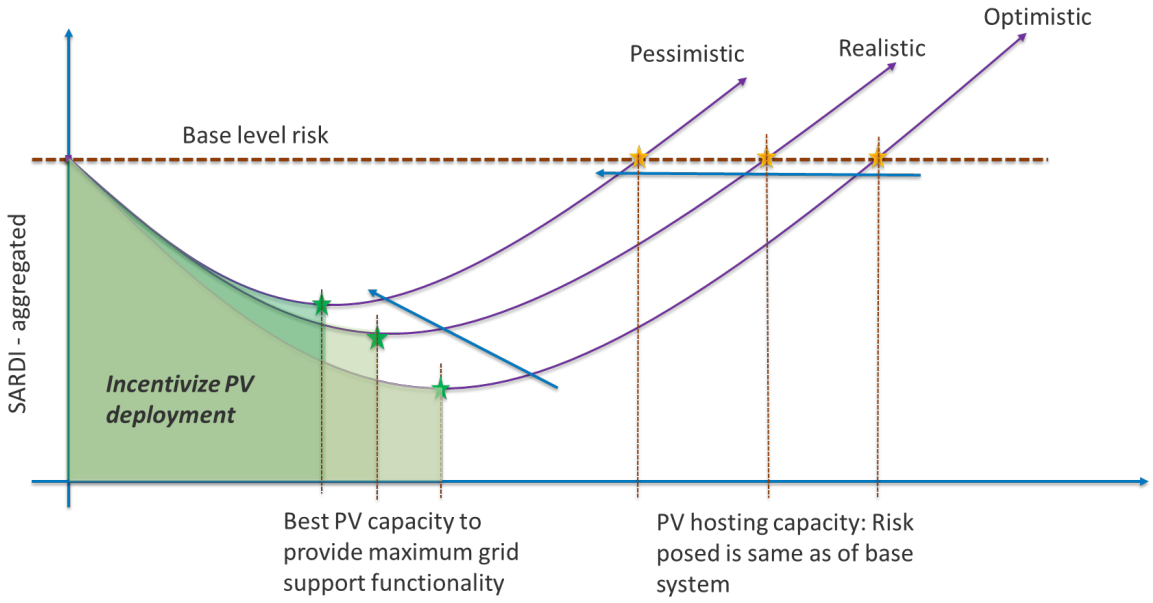

Figure 15. Conceptual graphic of risk level versus increasing hosting capacity

As shown in Figure 15, there is a PV capacity level where the overall risk level is decreased from the case without PV that provides an overall benefit to the utility. The PV capacity at which the risk posed is the same as the base-level risk could be described as the utilities' safe point to stop adding or incentivizing exporting PV. Beyond this point, the utility has a net increase in risk that may need to be mitigated.

6 Distribution Network Analysis Framework

Distribution network analysis plays a fundamental role in enabling distribution system planning to implement the best practices in terms of assessing the health of the network, making changes to the system operation, changing interconnection standards, and building out and upgrading network assets. Increased adoption of DERs and changing consumer energy consumption patterns are challenging the distribution planning process and increasing the need for holistic distribution network analysis.

6.1 DER Impact Analysis Framework

NREL has developed a comprehensive and insightful framework for distribution network analysis that leverages a suite of metrics proposed in Section 5. Figure 22 shows the framework for distribution system analysis.

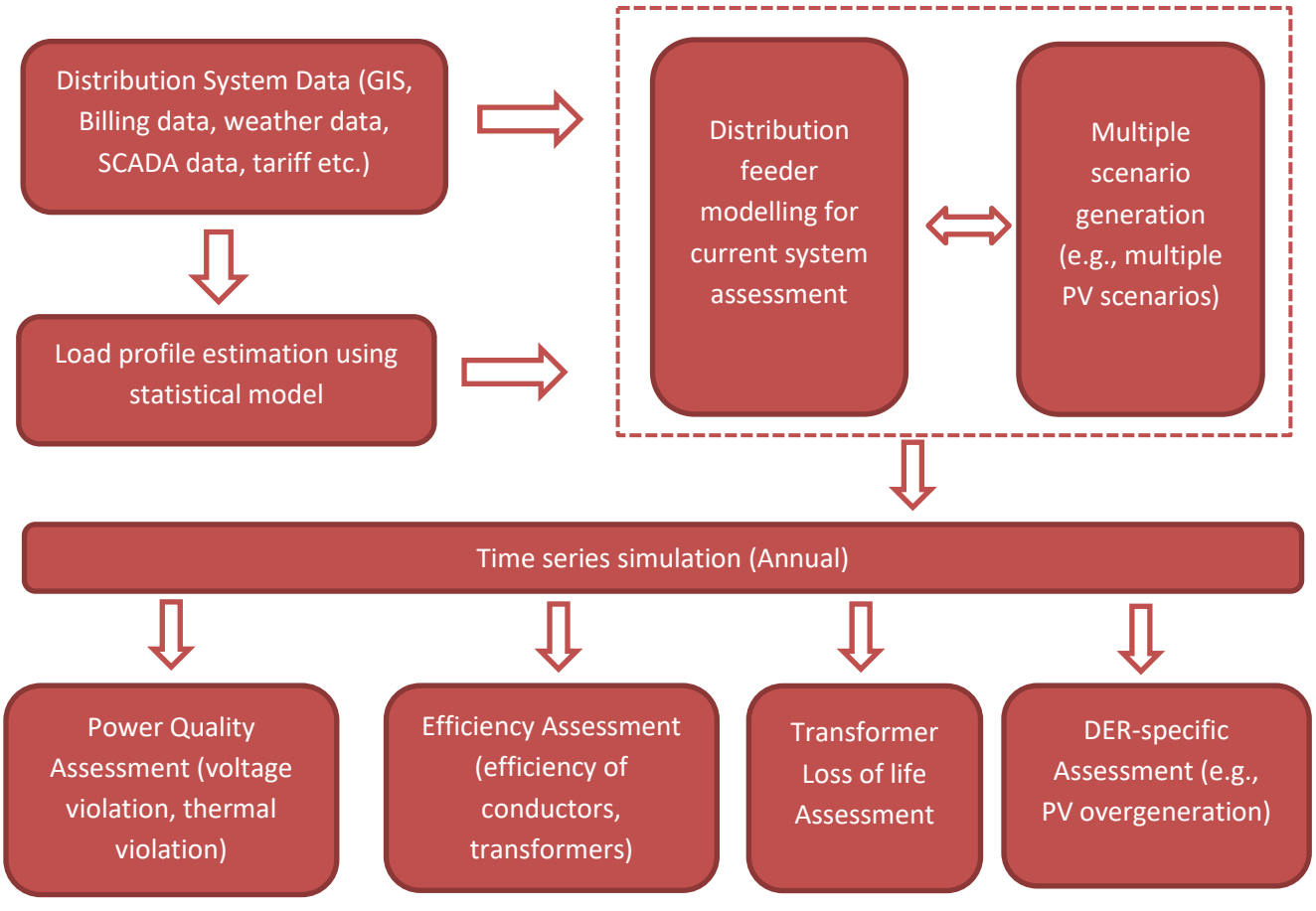

Figure 16. Framework for distribution network analysis

The proposed framework utilizes data available from the distribution utility to develop network models, generate scenarios, and perform the analysis. Data is utilized from the GIS at TANGEDCO to develop OpenDSS feeder models. The conversion process from GIS to the OpenDSS file format (.dss) is explained in detail in Section 2. Load profiles are required for running time-series power flow simulations. A statistical model to estimate load profile for four consumer classes, namely residential, commercial, industrial, and agricultural identified using the tariff type was developed to this need, the details of which

are in Section 3. The statistical model utilized bimonthly energy consumption data of all customers for 2018, in addition to time-series temperature data, holiday indices, and customer tariff types to estimate the 15-minute resolution load profile for each customer class. The details behind the load profile generation are explained in Section 3. Distribution feeder models are then ready-to-run OpenDSS files. To analyze the impact of emerging technologies, multiple scenarios can be generated. Each scenario will have their own .dss file. Although this framework can be used for any technologies applicable to the distribution system, in this report, the focus is on the impact of distributed PV on distribution feeders. Multiple PV scenarios are conducted on the distribution system feeder models and are analyzed using the time-series power flow simulation tool and assessed for power quality, efficiency, transformer loss of life, and PV overgeneration.

Utilities need to understand the impact of distributed PV on their system before making decisions on how much PV can be safely accommodated on their system. Most of the PV impact analysis study focuses on snapshot power-flow analysis by focusing on worst-case time stamps (e.g., peak load time, maximum generation time, and so on), ignoring the impact at other times. The framework here utilizes holistic metrics that consider time series across the year to analyze performance of the distribution system. The metrics used are described in detail in Section 5.

6.1.1 How Are PV Scenarios Defined?

PV scenarios are defined based on two separate solar penetration metrics. The first metric represents the fraction of customers installing PV to the total number of customers expressed in percentage (*No. Customers*), and the second metric represents the annual PV energy production as a fraction of each customer's total energy consumption (*Self-Generation*). Each scenario is defined as a combination of these two metrics, that is, *No. of Customers*%-*Self-Generation*%. For example, the **10%-100%** PV scenario means 10% of total customers have installed PV, and each of the PV units are sized in such a way that energy produced by the individual PV unit over the entire year is equal to 100% of the annual energy consumption of the customer without PV. To give an example of PV sizing, in the **10%-100%** PV scenario, a consumer with 1,000 kWh annual energy consumption (without PV) would have to install a 0.456 kW solar panel based on a capacity factor of 25%, that is:

$$\frac{1000kWh*\mathbf{100}}{100\times0.25\times365\times24} = 0.456\ kW\ of\ PV\ \text{- assuming 25\% annual PV capacity factor}$$

6.1.2 Simulation Details

NREL performed simulations on three TANGEDCO feeders, namely GR PALAYAM, GWC, and TOWN, for 2018, using a time resolution of 15 minutes. For each PV scenario, customers are chosen at random with uniform distribution. The assumptions made in the distribution feeder model are explained in Section 2.

6.2 Interconnection Assessment Framework

NREL also developed a tool to analyze PV interconnection requests for TANGEDCO to allow the distribution planning team to perform initial assessment on new PV applications. The process for assessing PV interconnection request is shown in Figure 17. The framework takes the PV interconnection request (information on PV capacity, location, phase) and adds the PV system to the current distribution system model. Time-series simulation analysis is performed on the updated model. The simulation period can be daily, monthly, or yearly, depending on the interest. The tool allows the user to visualize the change in risk, efficiency, overgeneration, voltage profile, and line and transformer loading for a given PV request.

This can allow TANGEDCO to make an assessment on new interconnections, accepting, rejecting, or recommending changes to the application. The tool will allow TANGEDCO to make rapid analysis of new interconnection requests and increase the speed and reliability of the process.

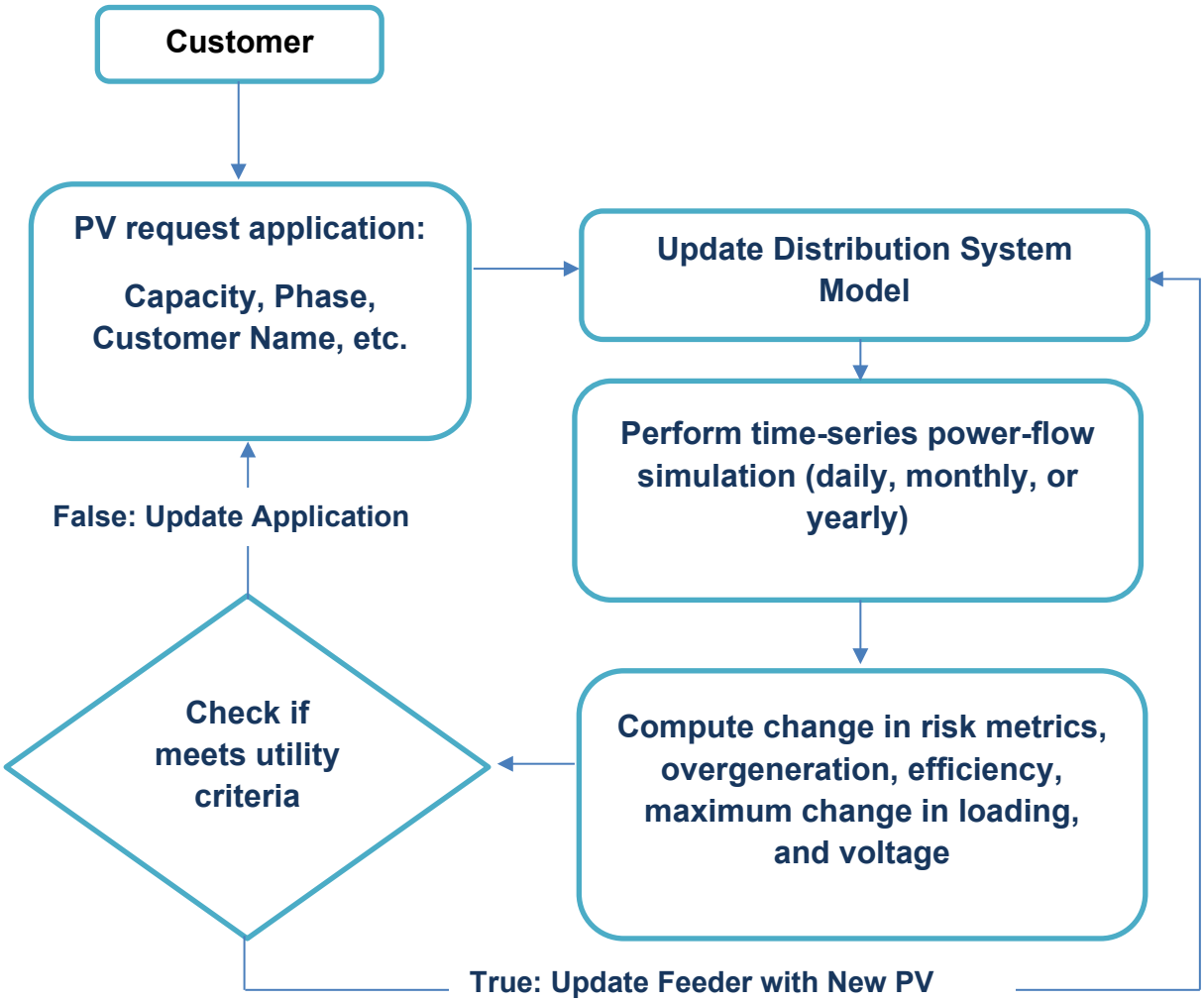

Figure 17. Framework for PV interconnection request assessment

7 Tamil Nadu Feeder Results and Analysis for High-PV Penetration Scenarios

NREL conducted an PV impact analysis on three TANGEDCO feeders, namely GR PALAYAM, GWC, and TOWN for 2018. These feeders were used to examine multiple PV penetration scenarios. This section provides a detailed analysis of the impact of distributed PV on distribution systems, as well as their impacts on overall network load shapes. Distributed PV examined in this section is modeled without any reactive power or active power control with respect to system voltages (e.g., power factor or volt-VAR control), and voltage support from PV systems is considered in Section 8.

7.1 PV Penetration Scenarios

Multiple PV penetration scenarios are examined to analyze the sensitivity of the network to increased levels of PV adoption. PV penetration/adoption rates are examined in increments of 10% of customers having PV systems on their premise. A base case scenario is used to define the current status of the network and is equivalent to 0% of customers having PV systems. PV penetration scenarios are used as defined in Section 6 (i.e., the scenarios are defined as the percentage of customers who have adopted solar PV and the percentage of PV annual energy production to customer annual energy consumption) and these two metrics define the scenarios (e.g., *No. of Customers*%-*Self-Generation*%). For all PV scenarios, PV capacity is defined in such a way that energy generated by PV throughout the year is the same as customers' annual energy consumption without PV. For most customers this results in relatively modest PV capacities. The average PV capacities for customers in GR PALAYAM, GWC and TOWN feeders is around 1 kW, 1.5 kW and 1.2 kW respectively. To avoid very high PV capacity resulting from this methodology, particularly for commercial, industrial, and agricultural customers, all required customers with computed required PV capacity greater than 20 kW are capped at 20 kW. The percentage number of customers is incremented in steps of 10% between 0% and 100% to generate the PV scenarios. Note customers for PV adoption are selected with a uniformly random distribution.

7.2 Impact on Load Shapes

Feeder load shapes give us information about how load consumption changes over time and is insightful into changes in asset utilization, both in terms of temporal and frequency of use. A detailed methodology on load profile estimation by class (i.e., residential, commercial, industrial, and agricultural) for TANGEDCO is presented in detail in Section 3. The following analysis examines how increased PV penetration impacts the diurnal load consumption pattern, introduces reverse power flow, and changes the utilization of the network (examined through load duration curves).

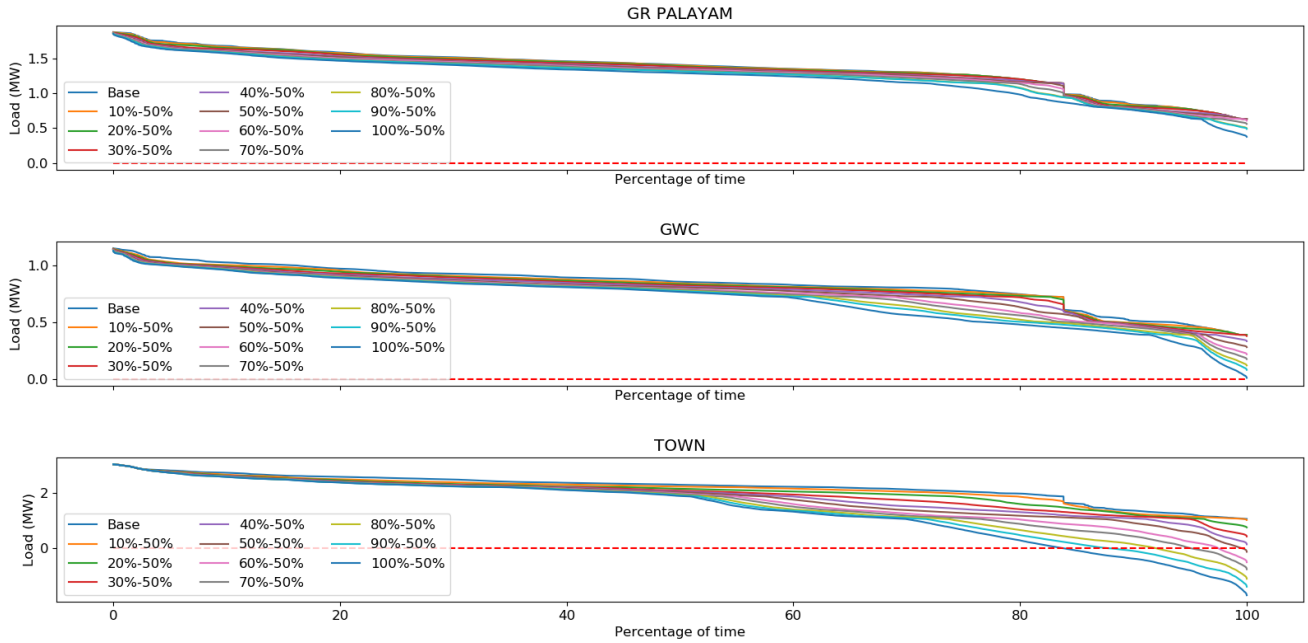

Figure 18. Annual load duration curve for TANGEDCO feeders in various PV scenarios

Customers in all three feeders were divided into four classes for this analysis: residential, commercial, industrial, and agricultural. Categorization was based on tariff types and more detail can be found in Section 3.

7.2.1 Load Duration Curve

Load duration curves present the magnitudes of load consumption data arranged in descending order from the highest magnitude to the lowest, rather than a traditional chronological temporal view. Load duration curves gives the duration for which different magnitudes can be expected to last over the total time period examined. Figure 18 shows the load duration curve for three TANGEDCO feeders. The load duration curve allows for some basic analysis on the impacts of increased PV generation, for example TOWN feeder will experience overgeneration (i.e., back feeding or reverse power flow from the distribution feeder) for 18% of year in the 100%–50% case scenario, whereas GR PALAYAM and GWC feeders will not experience reverse power flow at the feeder level). Another important aspect to look at is how much peak load has been reduced because of PV. In TOWN feeder, the peak occurred at nighttime, so PV did not reduce the peak; however, for GR PALAYAM and GWC, the peak occurred during daytime, which allowed PV to reduce the peak by up to 25 kW and 23 kW in 100%–50% PV scenario (i.e., a peak load reduction of approximately 1.33% and 2%) for GR PALAYAM and GWC respectively. It is worthwhile to mention that PV deployment increased the percentage of time for which the top 10% and 5% load hours occur for all three feeders compared to the base case when there is no PV in the system. The increase is almost 5% for the top 10% hours and 3% for the top 5% hours in all three feeders.

7.2.2 Average to Peak Power Ratio

The average to peak power ratio is defined as the ratio of average power consumed in a given duration to the maximum power consumed during the same duration. A high average to peak power ratio indicates that the load curve is relatively flat, whereas a low average to peak power ratio implies that the load curve has larger magnitude changes.

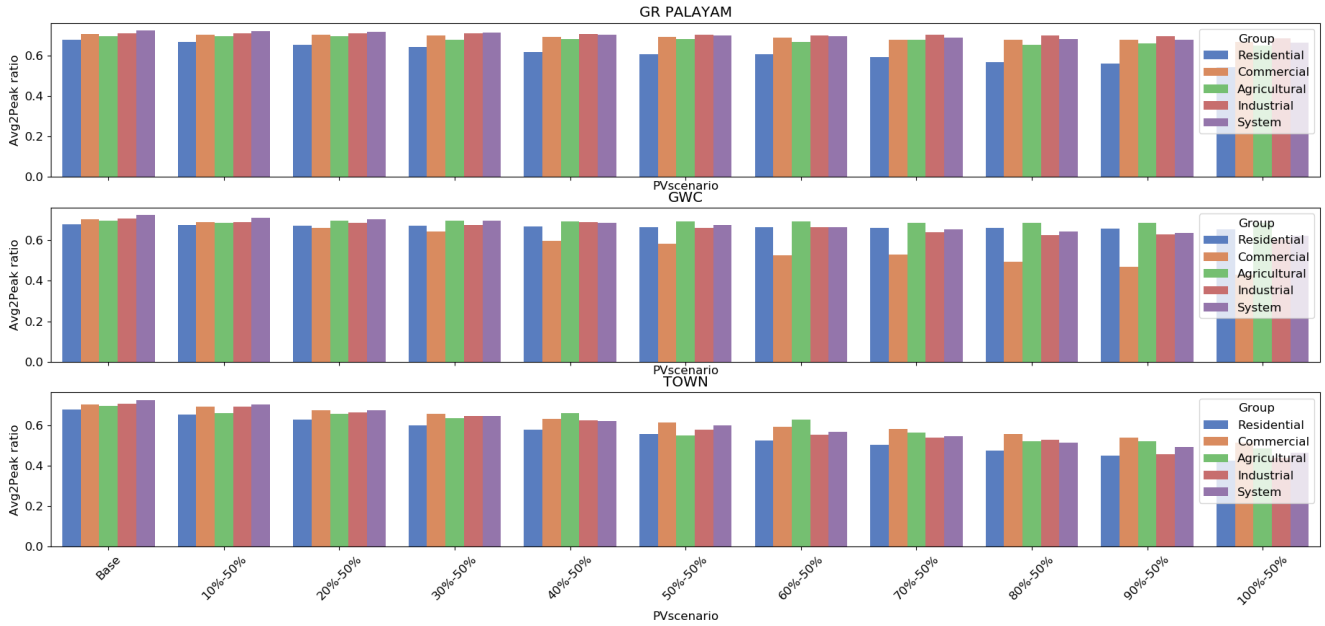

Figure 19. Annual average to peak power ratio variation for different consumer classes, as well as for the entire system in the three TANGEDCO feeders for various PV scenarios

Figure 19 shows the impact on annual average to peak power ratio for four consumer classes, as well as the entire system in three TANGEDCO feeders because of distributed PV. Average to peak power ratio tends to decrease with PV because of the minimal impact on the peak load and maximum reduction on consumer's energy consumption. The decrement in average to peak power ratio of residential customer group tends to be higher in all three feeders. This is because all three feeders have high numbers of residential customers, and they are more likely to install PV even when customers are randomly chosen in different PV scenarios. If the customers in a group do not have PV, average to peak power ratio would remain constant in all PV scenarios (for example, the Agricultural group in the GWC feeder).

7.2.3 Coincidence Factor

The coincidence factor is the ratio of system peak load to the sum of peak loads of individual groups. This metric is the reciprocal of the diversity factor. Often used in load analysis in distribution planning to estimate the sizing of network assets from the customer point of connection up to the medium voltage network. Figure 20 shows a coincidence factor in three TANGEDCO feeders for various PV scenarios. The load groups are highly coincident in nature. In GWC and TOWN the coincident factor tends to increase with PV penetration, and this is because the system peak remains unaffected as it happens at night; however, individual noncoincident peaks are reduced by PV.

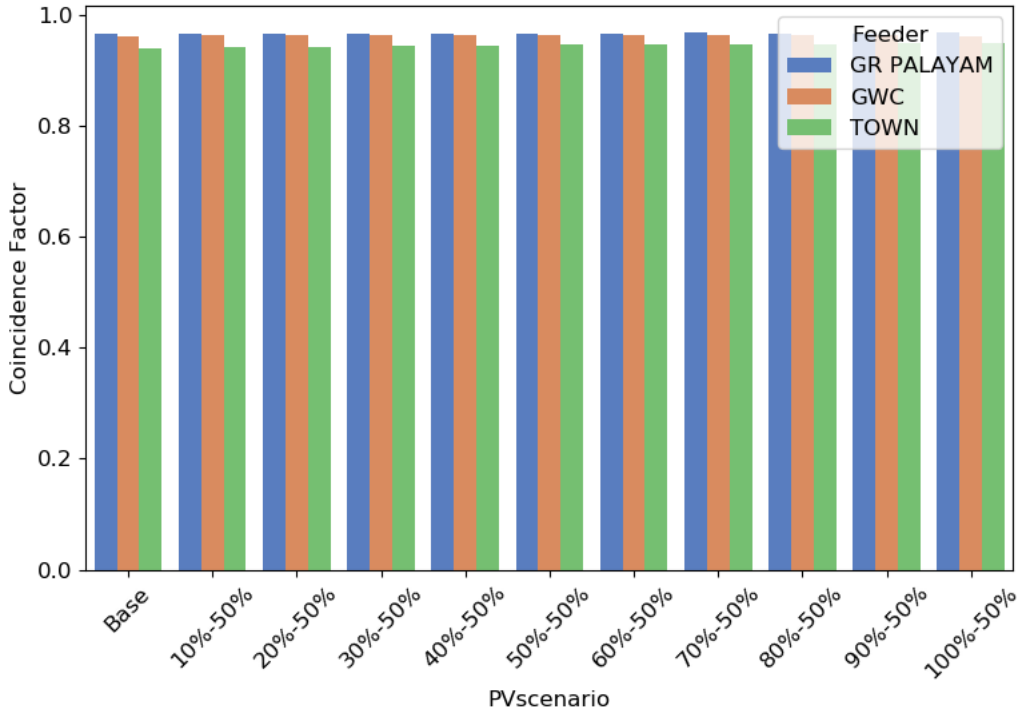

Figure 20. Coincidence factor of TANGEDCO feeders for various PV scenarios. Note PV has very minimal effect on peak load reduction as PV generation at the peak almost zero.

7.2.4 Responsibility Factor

Responsibility factor is defined as the load class peak that occurs at the same time as system peak divided by peak of each load class. This metric helps in demand-side evaluation by providing information of how much each load class is coinciding with the peak load. Figure 21 shows the responsibility factor of all consumer classes in three feeders at various PV scenarios. The responsibility factor tends to remain fairly constant for all PV scenarios because PV has little or no impact on system and individual peak reduction. It is important to note that unity responsibility factor of a group means that the peak of the group coincides with the system peak. If the responsibility factor is 1, the class peak is completely coincidental with the system peak; if this is less than 1 the class peak is not coincident with the system peak.

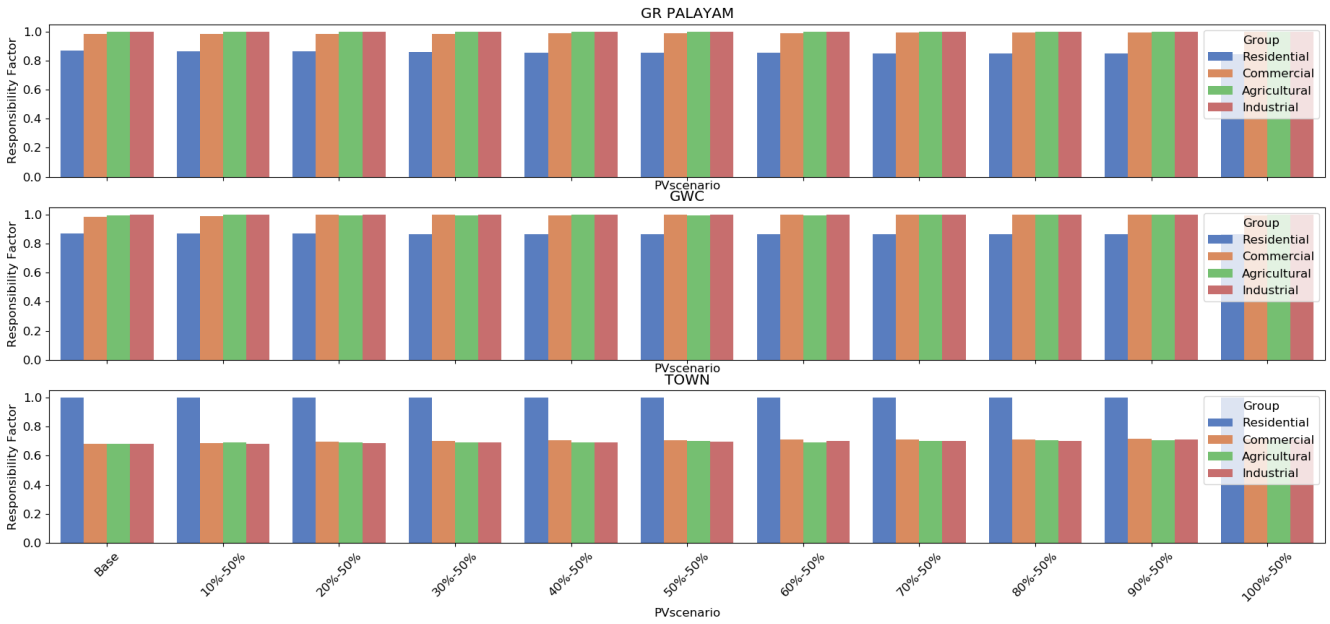

Figure 21. Responsibility factor of four consumer classes in TANGEDCO feeders for various PV scenarios

7.3 Impact of Distributed PV on TANGEDCO Distribution Feeders

To understand the impact of distributed PV on TANGEDCO distribution feeders, three feeders (GR PALAYAM, GWC, and TOWN) are used to simulate 10 PV scenarios for 2018, running annual time-series simulations at 15-minute resolution. The feeders are analyzed at increasing increments of 10% of customers having on-site PV generation. Running time-series static power-flow at each 15-minute increment, the total data set is used to analyze the impact of increased distributed PV on power quality, overall network efficiency, impact on asset lifetime, and overall PV overgeneration.

7.3.1 Analysis of Power Quality Risk With Distributed PV

Increasing PV penetration changes the loading of distribution lines and transformers and changes the overall voltage profile. Depending on the coincidence of PV generation with load consumption and the magnitude of generation, the presence of PV systems can increase or decrease system loading. Increased loading of system assets generally only occurs in cases with low coincident demand and PV production, and high enough PV capacities to cause excess generation well beyond original consumption levels resulting in reverse power flow. Increased PV generation always serves to raise system voltages, and generally this impact is observed well before the increased asset loading is realized. Raising system voltages will only be of concern if the original voltages were close to the high end of the required voltage bounds.

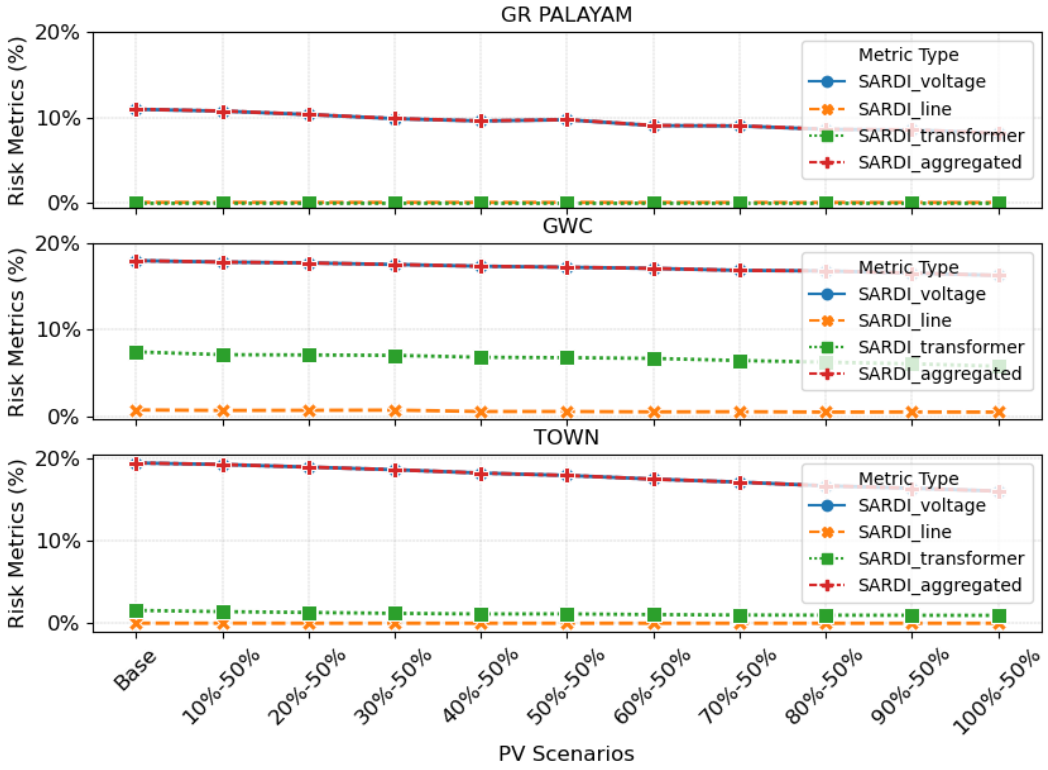

Figure 22. SARDI in three TANGEDCO feeders (2018)

Transformer and line loadings that exceed 100% for a long period of time and voltages outside of the recommended limits (i.e., greater than 1.1 p.u. or less than 0.9 p.u.) result in problems for system operation and are violations of power quality standards. Figure 22 plots the SARDI associated with voltage violations (SARDI_voltage), line violations (SARDI_line), transformer violations (SARDI_transformer) along with the aggregate risk for three TANGEDCO feeders for 2018. All three feeders have non-zero risk metrics in the base scenario (the scenario without PV). More specifically, transformer violations exist in two feeders (GWC and TOWN), and voltage violations exist in all three feeders without PV, with the feeders experiencing voltage violations below the lower bound (i.e., less than 0.9 p.u.). Line loading is lower than 100% in all three feeders indicated by the zero magnitude of the SARDI_line metric in base scenario.

Increasing PV penetration reduces the risk associated with the voltage violation, line violation and transformer violation in all three feeders by increasing the voltage for parts of the network that were initially experiencing violations below 0.9 p.u. voltage. Self-generation from PV results in customers decreasing their net load and improves the voltage profile of the feeder. Only as PV penetration levels increase significantly, reverse power-flow from excess PV generation increases loading on both lines and transformers.

Figure 23 shows the Nodal Voltage Risk Indices (NVRI) for all nodes overlaid on a spatial map of the network for 2018 for the three PV scenarios.

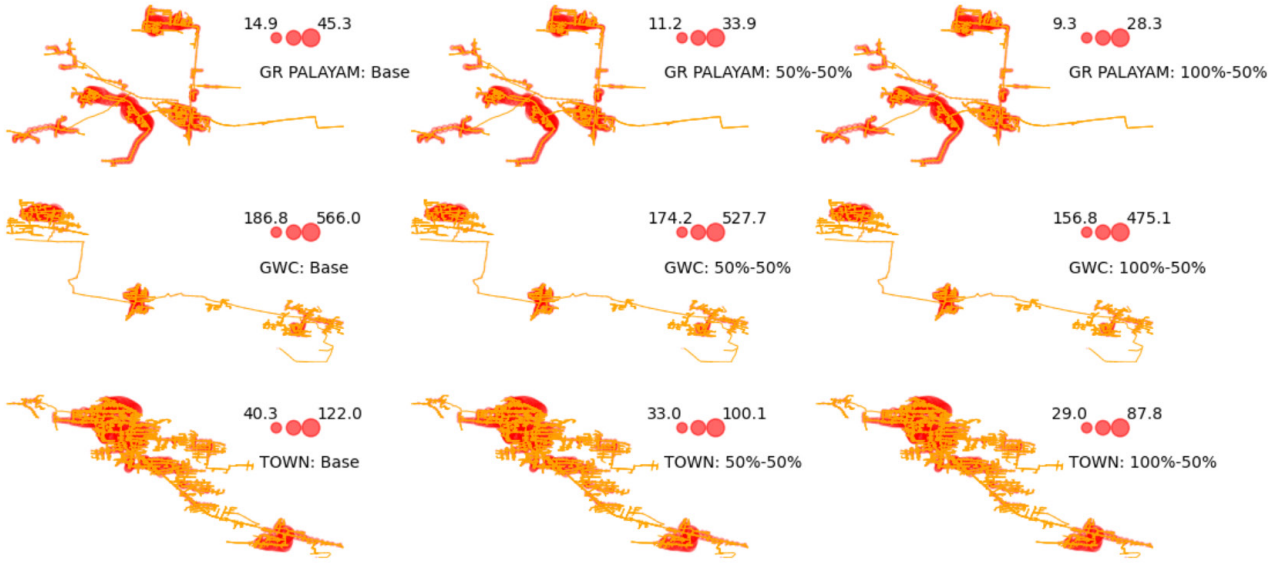

Figure 23. Scatter plot of NVRI in TANGECO feeders in three different PV Scenarios ('Base', '50%-50%' and '100%-50%') 2018; actual magnitude is multiplied by 1,000

The NVRI of a node is a measure of the average depth of the voltage violation for a given time period (a year in this case) multiplied by the fraction of customers present downward. It gives relative idea of overall risk associated with nodes for the whole year. The risk associated with a node is not just a function of the magnitude of the overvoltage or undervoltage at each node but also how many customers are being served and will be affected because of it. Nodes in GWC pose more risk than nodes in TOWN and GR PALAYAM feeders as indicated by the higher magnitude. The NVRI decreases with increasing PV penetration in all three feeders.

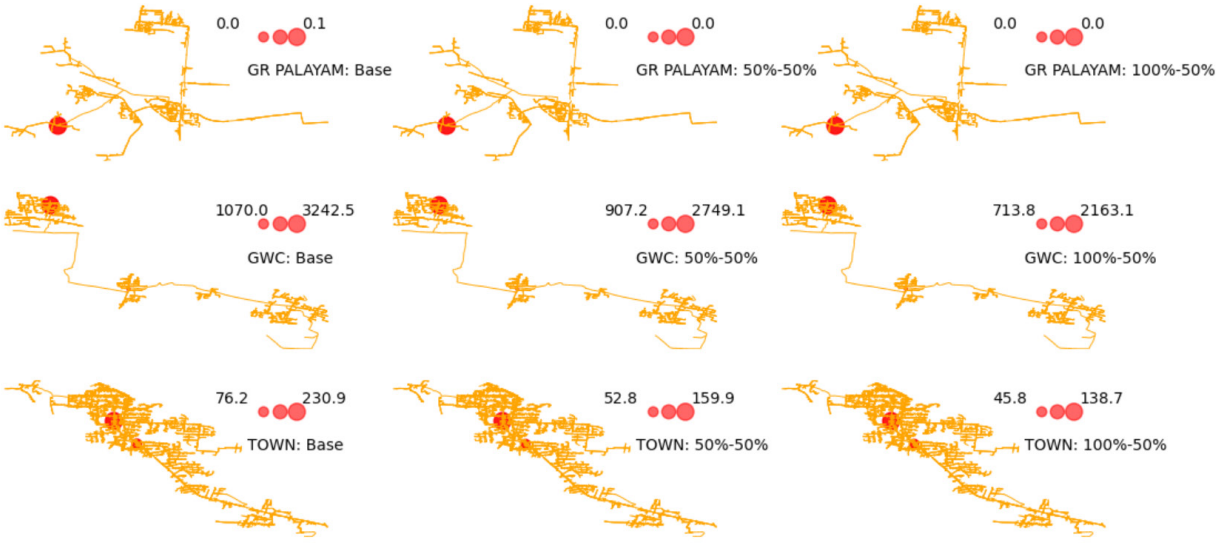

Figure 24. Scatter plot of Transformer Loading Risk Indices (TLRI) in TANGECO feeders in three different PV scenarios ('Base', '50%-50%' and '100%-50%') for 2018; actual number multiplied by 1,000

Figure 24 shows the TLRI of all transformers in three TANGEDCO feeders for three scenarios: Base, 50%-50% and 100%-50%. Like NVRI, the TLRI is a measure of the average depth of transformer loading violation for a given time period multiplied by the fraction of customers the transformer is serving. The risk associated with a transformer is not only dependent on how much overloading it is experiencing, but also depends on how many customers are being affected by it. The TLRI of transformers is much higher in GWC compared to GR PALAYAM and TOWN, indicating that transformers are more heavily loaded for that feeder. The TRLI is also shown to reduce with increase in PV penetration for low to medium penetration levels.

Figure 25 and Figure 26 show the line loading risk indices (LLRIs) of all lines and customer risk indices (CRIs) for all customers in three TANGEDCO feeders for three 2018 scenarios: Base, 50%-50%, and 100%-50%. The LLRI is a measure of the average depth of a line loading violation for a given time period multiplied by the fraction of customers it is serving, and CRI is a measure of the average sum of depth of all three violations affecting a customer. LLRI is lower for the 50%-50% PV scenario, whereas higher for the 100%-50% scenario in GR PALYAM feeders, it reduces with increasing PV penetration in both GWC and TOWN feeders.

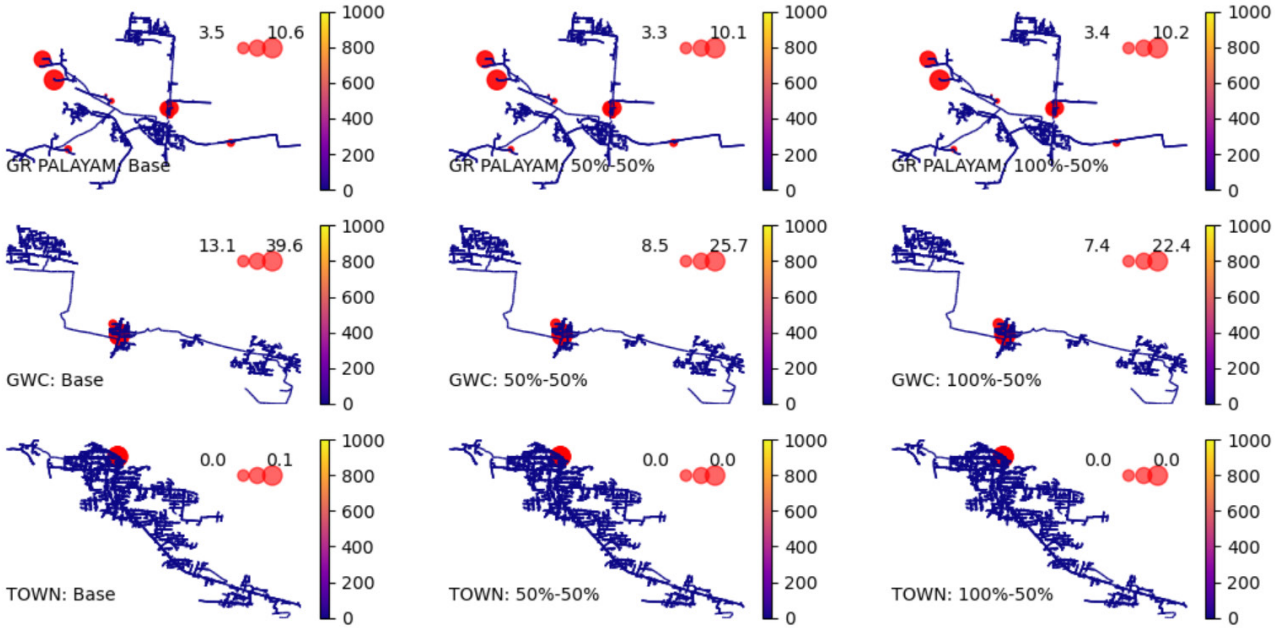

Figure 25. Scatter plot of Line Loading Risk Indices (LLRI) in TANGECO feeders in three different PV scenarios ('Base', '50%-50%' and '100%-50%') for 2018; actual number multiplied by 1,000

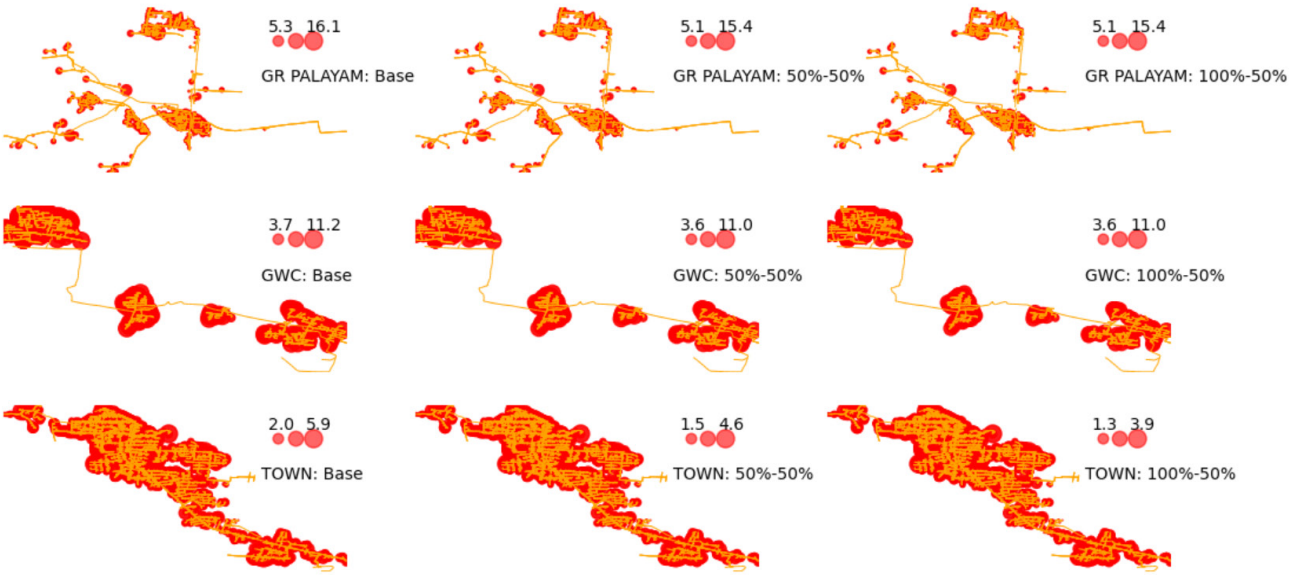

Figure 26. Scatter plot of Customer risk indices CRI) in TANGECO feeders in three different PV scenarios ('Base', '50%-50%' and '100%-50%') for 2018; actual number multiplied by 1,000

The higher LLRI in the 100%-50% PV scenario is because of the increased loading caused by the reverse power flow. CRI is higher in GWC and GR PALAYAM compared to TOWN.

Figure 27–Figure 30 show the time-series plots of NVRI, LLRI, TLRI, and CRI metrics for all three feeders for three different scenarios. LLRI, TLRI, and CRI metrics are lowest in the 100%-50% PV scenario for all three feeders, indicating PV generation helped reduce loading on lines and transformers imposing less risk to lines, transformers, and customers. NVRI is also lowest in the 100%-50% PV scenario for all three feeders because the local generation tends to increase the voltage at the PCC, thus eliminating the undervoltage issue that was already present in the system without PV.

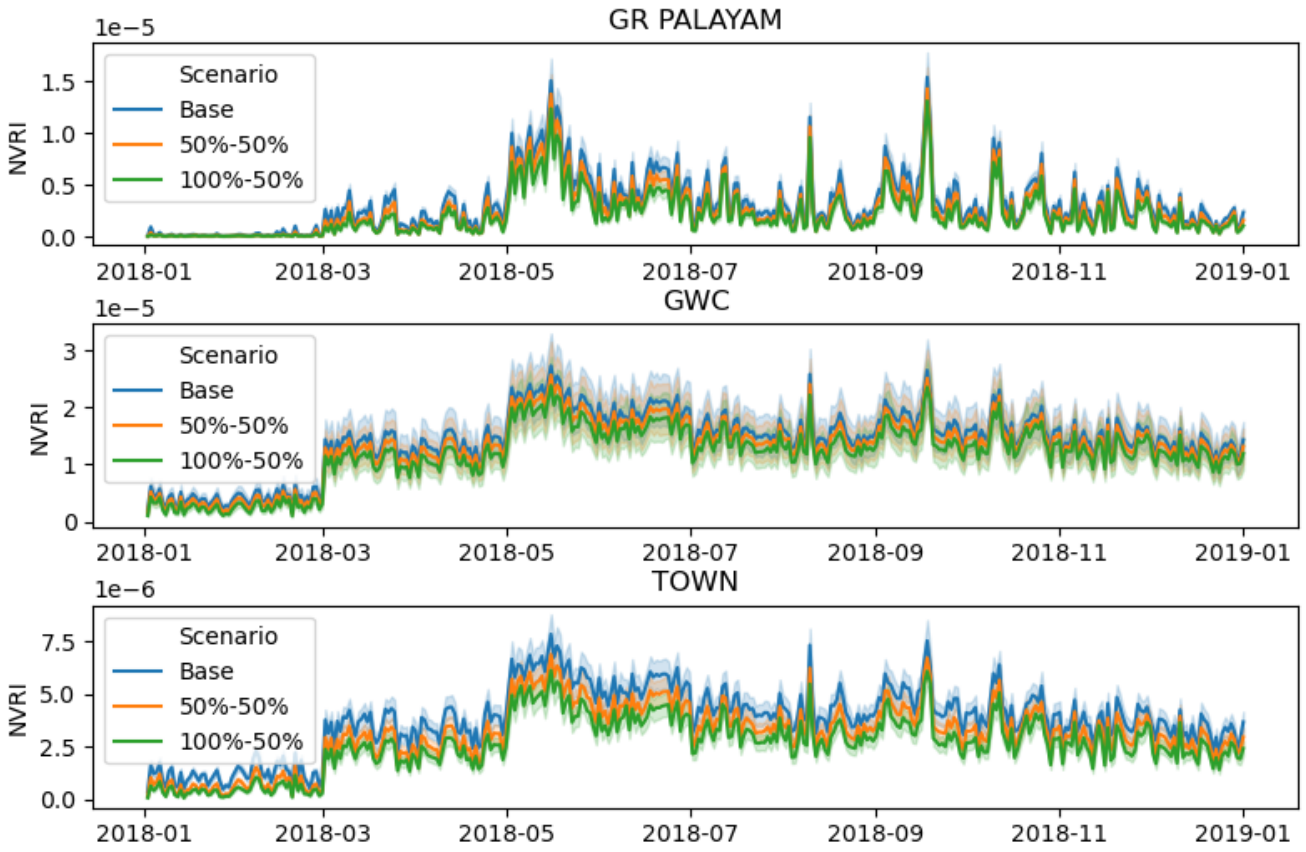

Figure 27. Daily variation of NVRI in TANGECO feeders (for 2018 in three PV scenarios: 'Base', '50%-50%' and '100%-50%' scenarios) ordered top to bottom (GR PALAYAM, GWC, TOWN). Shading shows the mean (stronger shaded lines) and distribution of daily variation of NVRI.

The time-series loading pattern is reflected in the daily variation of asset-level system violation risk metrics. The NVRI metric improved for both the 50%-50% and the 100%-50% PV scenarios in all three feeders, and the variation follows the risk pattern observed for the base case. This has to do with the improved voltage profile caused by the increased PV penetration throughout the year. LLRI improved for both PV scenarios in all three feeders throughout the year; and the risk is higher in summer compared to other seasons corresponding to higher loads. The reason for reduced line risks with increasing PV penetration is due to the reduction in loading caused by local PV generation. A similar pattern can be observed for TLRI and CRI metrics across all feeders for all PV scenario. It is important to note that although NVRI, LLRI, CRI, and TLRI metrics are shown to reduce with increasing PV penetration levels, higher PV sizes than those used in this study may cause reverse power-flow increasing loading on transformers, lines thereby increasing system risk.

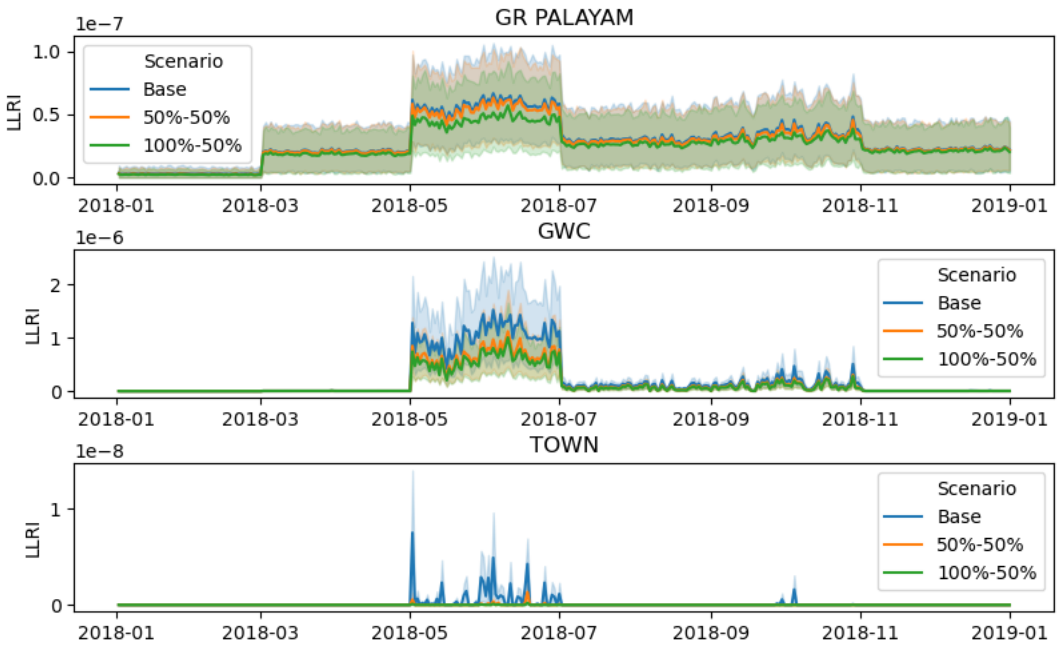

Figure 28. Daily variation of LLRI in TANGEDCO feeders (for 2018 in three scenarios: 'Base', '50%-50%' and '100%-50%' scenarios), ordered top to bottom (GR PALAYAM, GWC, TOWN)

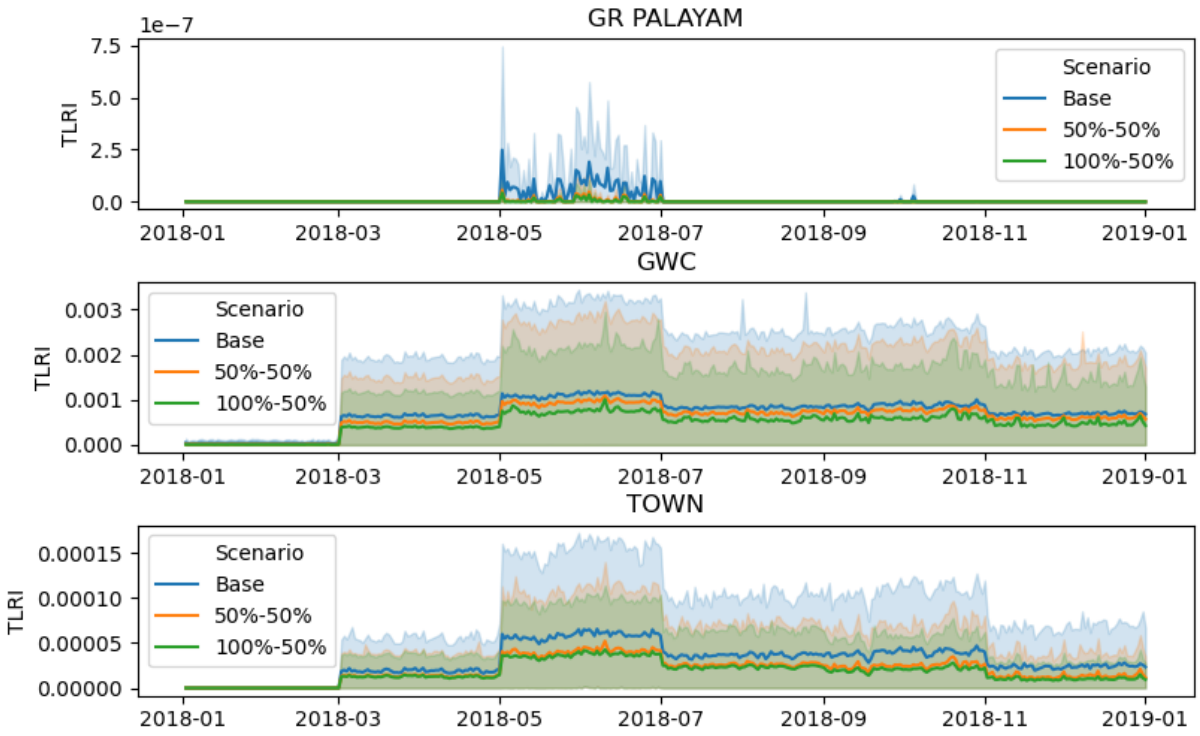

Figure 29**. Daily variation of TLRI in TANGEDCO feeders (for 2018 in three PV scenarios: 'Base', '50%-50%' and '100%-50%' scenarios), ordered top to bottom (GR PALAYAM, GWC, TOWN)**

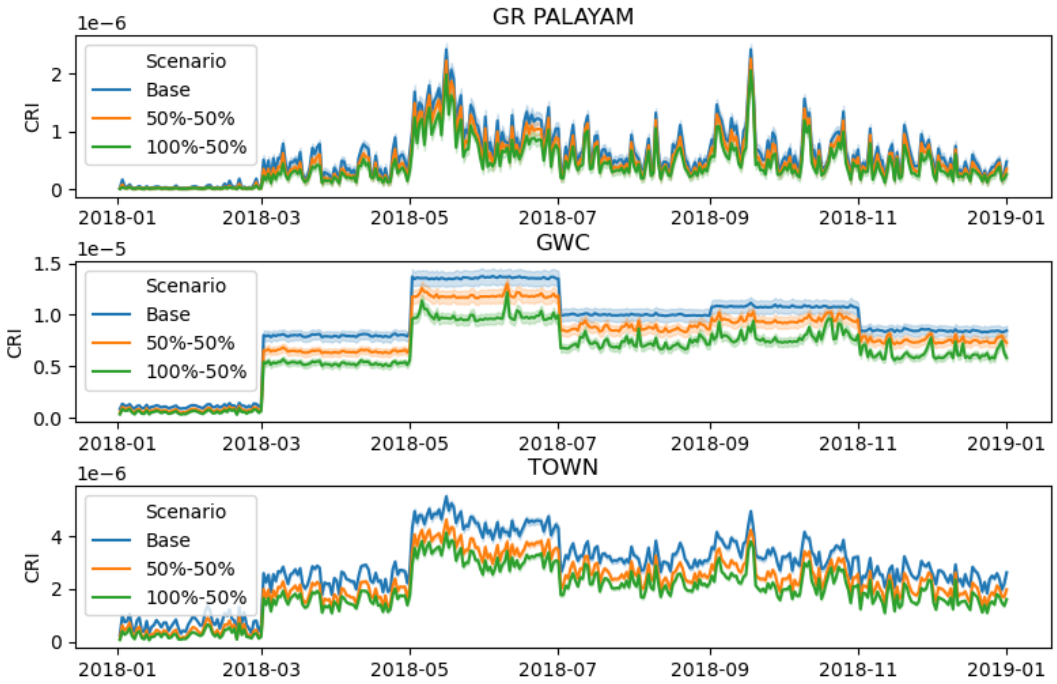

Figure 30. Daily variation of CRI in TANGECO feeders (for 2018 in three PV scenarios: 'Base', '50%-50%' and '100%-50%' scenarios), ordered top to bottom (GR PALAYAM, GWC, TOWN)

7.3.2 Analysis of Efficiency Metrics With Distributed PV

A major concern for distribution utilities is reducing power losses on their feeder (conductors and transformers) as it results in lost revenue. Power loss in conductors and transformers is a function of current (amps) experienced across each asset and impedance (e.g., resistance in Ohms). Impedance is impacted by temperature, aging, and other factors. In this study, assets are modeled as having constant impedance, such that power loss does not vary with temperature and asset life. The current flowing through these assets is a result of the customer energy consumption patterns. Distributed PV alters customers' consumption patterns, the magnitude of which is determined by load, solar coincidence, and correlation. This section examines how PV impacts the efficiency of the distribution feeders. The efficiency metrics used herein are described in detail in Section 5.

Figure 31 shows the efficiency of conductors, transformers, and the overall feeder for all three feeders for each PV scenario. Overall losses are higher in transformers than in conductors for GR PALAYAM and TOWN whereas for GWC it is the opposite case, which is indicated by the lower efficiency. The efficiency tends to remain constant up to a certain PV penetration level after which starts to reduce. This effect is due to the increase in loading at higher PV penetration levels. Apart from these system-level metrics, asset level efficiency metrics were examined (e.g., transformers and lines).

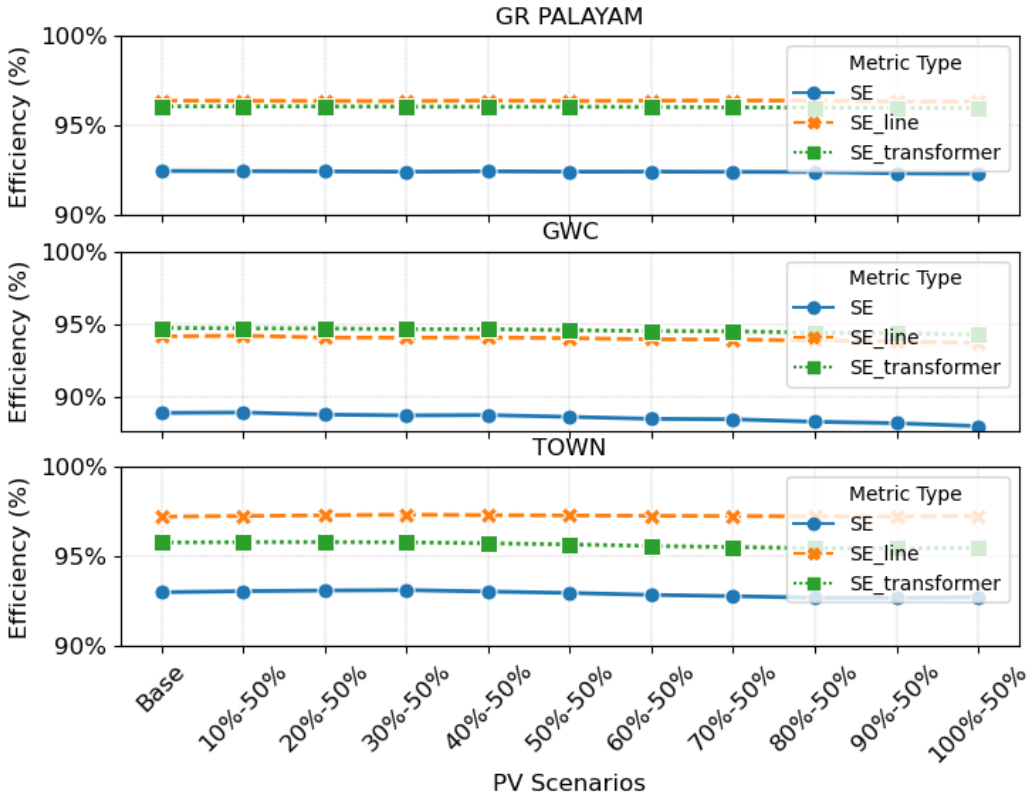

Figure 31. System efficiency metrics in TANGEDCO feeders (2018)

Figure 32 shows the annual efficiency of all distribution transformers overlaid on the network map for all three feeders in three different PV scenarios. Notice that transformers with an efficiency less than 96% are colored black. The results indicate that more transformers will have lower efficiency with increasing PV penetration in all three feeders.

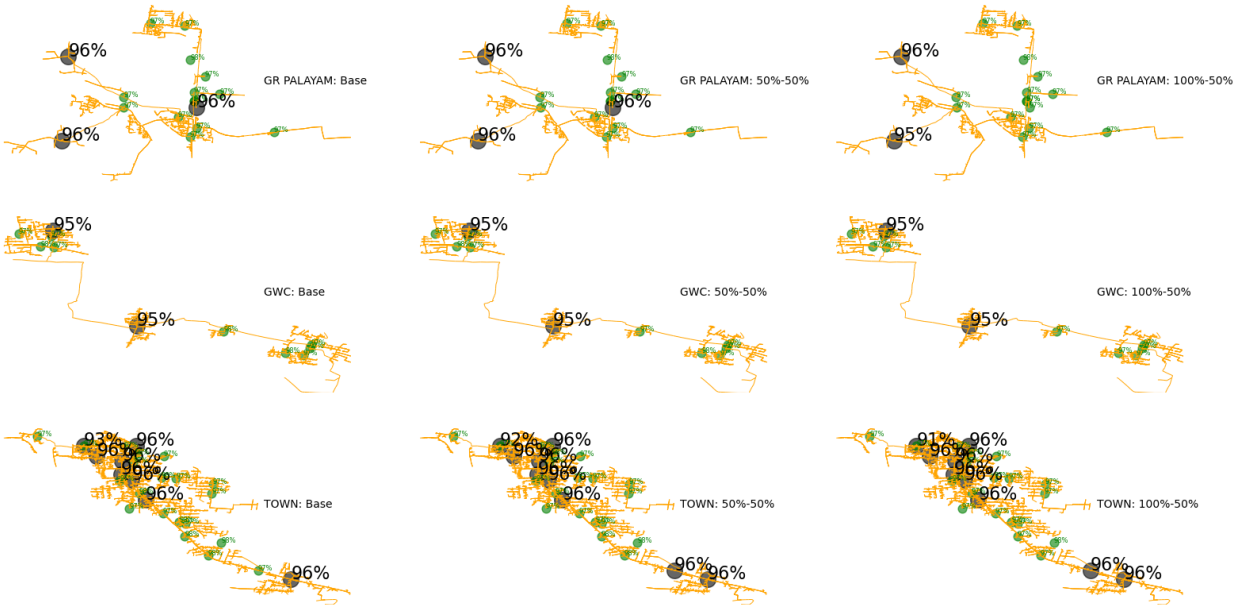

Figure 32. Scatter plot of efficiency of distribution transformers in TANGEDCO feeders in three different PV scenarios ('Base', '50%-50%' and '100%-50%') for 2018

The annual efficiency of all line elements for three TANGEDCO feeders in three different PV scenarios is shown in Figure 33. The efficiency of individual line elements remains high, although cumulative losses are also high as shown by lower efficiency metrics of the conductors in Figure 31. Some conductors exhibit much lower efficiency, represented by a darker color in GWC.

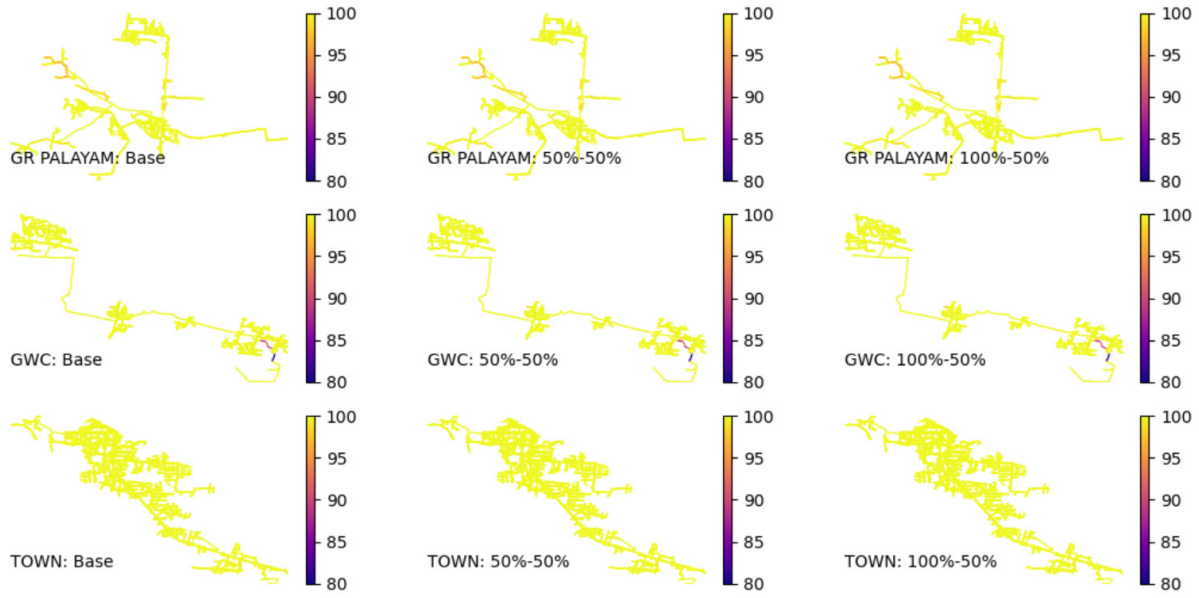

Figure 33. Heatmap of conductor efficiencies in TANGEDCO feeders in three different PV scenarios ('Base', '50%-50%' and '100%-50%') for 2018

Figure 34 and Figure 35 show the time-series variability of efficiency of all lines and conductors in three different PV scenarios across three feeders.

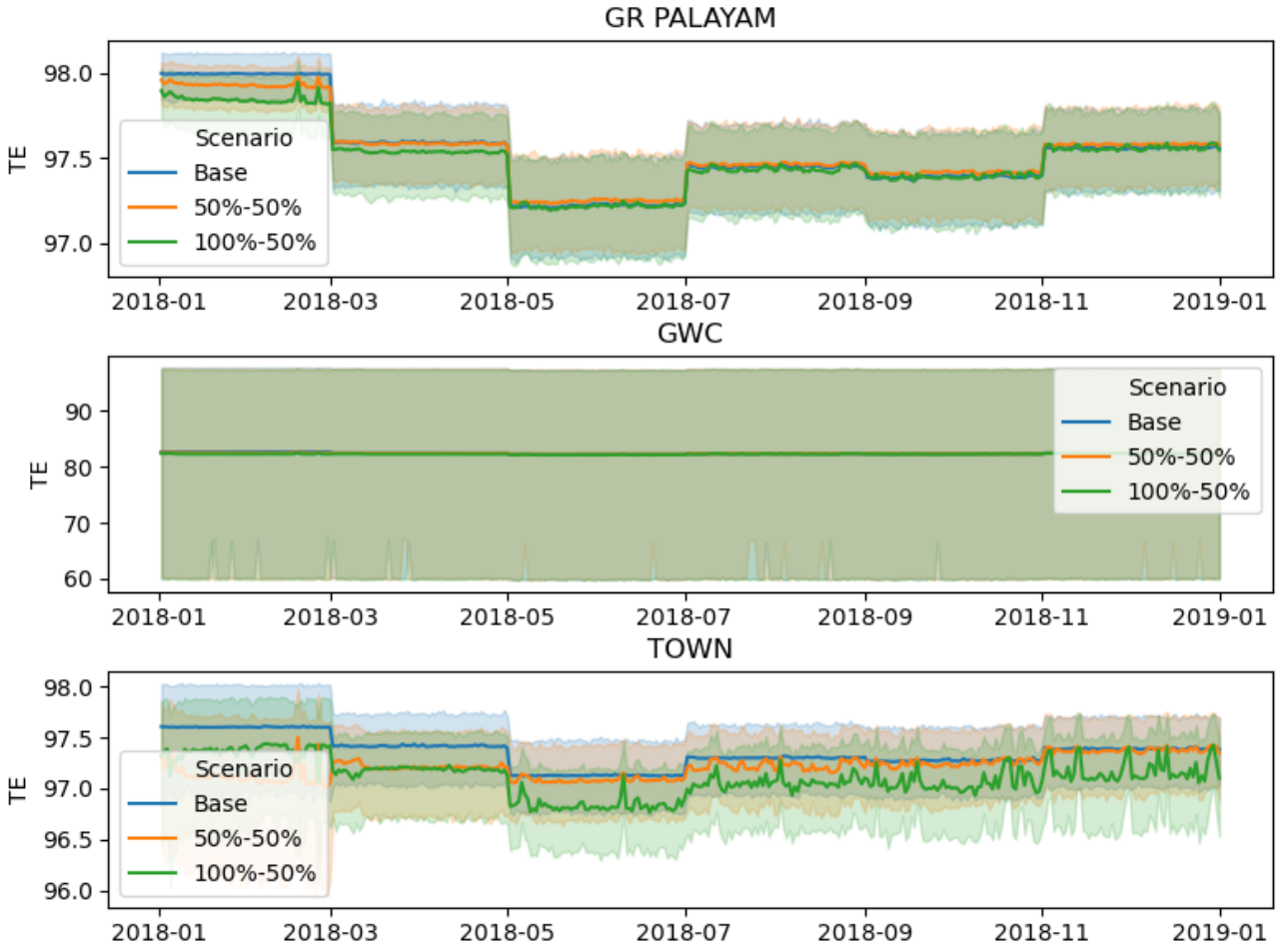

Figure 34. Daily variation of conductor efficiency in TANGEDCO feeders (for 2018 in three PV scenarios: 'Base', '50%-5%' and '100%-50%' scenarios), ordered top to bottom (GR PALAYAM, GWC, TOWN)

The darker lines represent the mean efficiency value. The efficiency is lower at the time of higher loading and higher at the time of light loading. Transformer efficiency dropped for the 100%-50% PV scenario in all three feeders. PV improves the line loading (which, here, means reduced loading) in all feeders as seen by increased average efficiency.

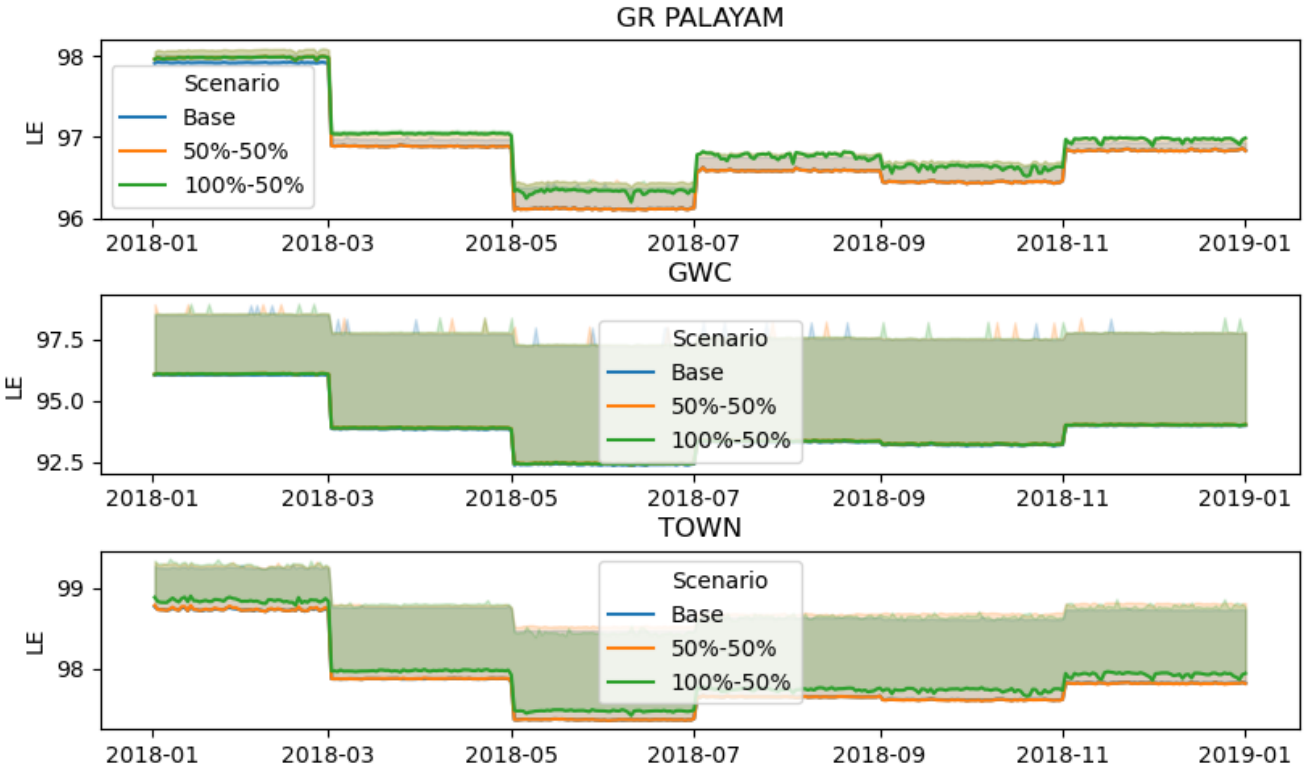

Figure 35. Daily variation of transformer efficiency in TANGEDCO feeders (for 2018 in three PV scenarios: 'Base', '50%-50%' and '100%-50%' scenarios), ordered top to bottom (GR PALAYAM, GWC, TOWN)

7.3.3 Analysis of Loss of Life of Distribution Transformers

Distribution transformers are an expensive distribution utility asset prone to life reduction due to excess loading. Efficient operation of transformers over their lifetime reduces upgrade costs and improves system reliability. Along with violation risks and efficiency impacts, utilities should also look at how emerging technologies are affecting transformer life.

Distribution utilities operate their systems with a large percentage of distribution transformers that have been in service for multiple years. Understanding how emerging technologies will affect transformer life enables system planning on future network upgrades. Estimating transformer loss of life is complicated and is a function of several factors, including: ambient temperature conditions, maintenance frequency, asset loading, and so on. In this analysis, loading and environmental temperatures are used to investigate the impact on transformer insulation life, which gives us a relative loss-of-life estimate. More details on how this is calculated is described in Section 5.

Figure 36 shows a plot of transformer loss of life at incremental PV penetrations across the three TANGEDCO feeders. PV penetration in general improves the average transformer loss of life by reducing loading, mostly in the afternoon when the outside temperature is high, and by reducing the hot-spot temperature of the transformer winding.

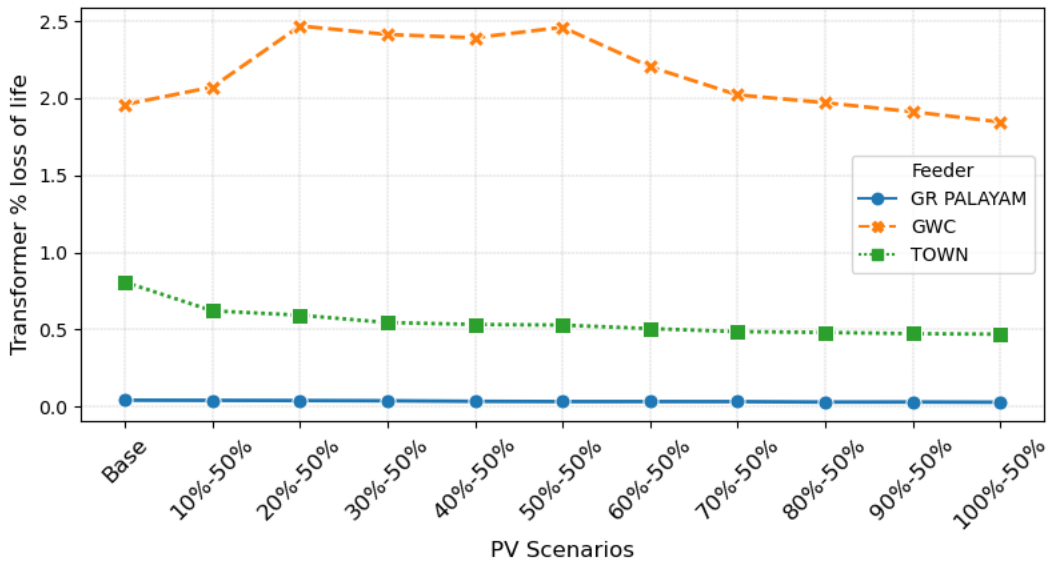

Figure 36. Average transformer loss of life in TANGEDCO feeders for 2018

Individual transformer loss of life for all three feeders in three PV scenarios is plotted over the network layout for 2018 in Figure 37.

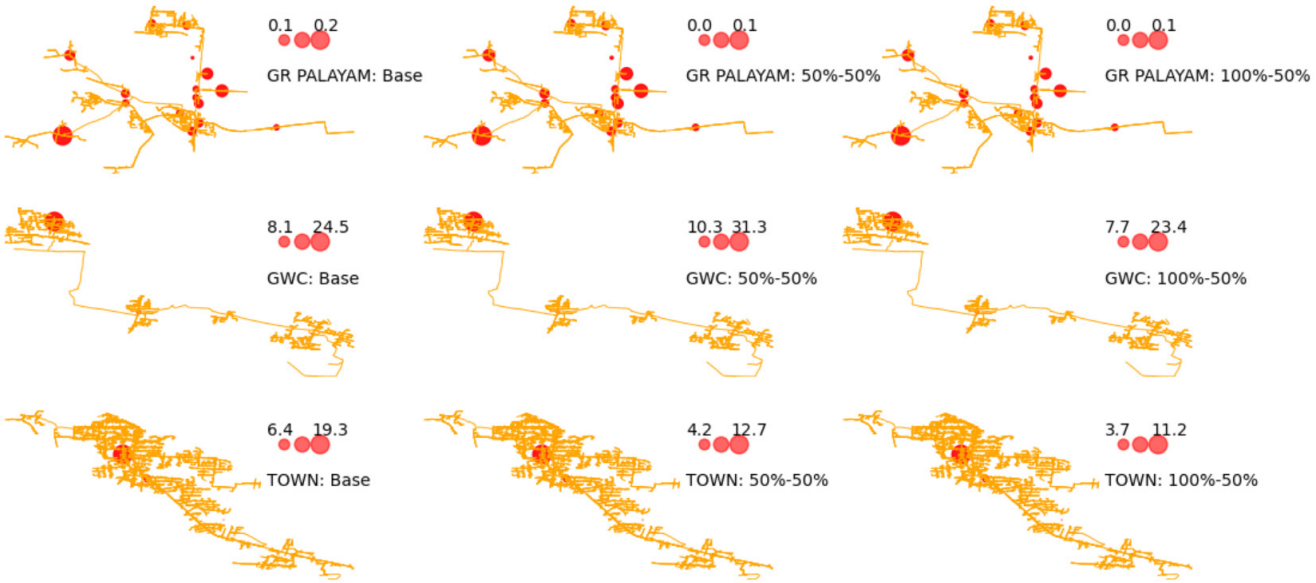

Figure 37. Scatter map of transformer loss of life over network map for three feeders in three different PV scenarios ('Base', '50%-50%' and '100%-50%') for 2018

In GR PALAYAM, transformers experience lower loss of life, the rate of which reduces with increased PV penetration. The maximum loss of life is 0.1% in 100%-50% PV scenario, compared to 0.2% in the base case. In GWC and TOWN the transformer loss of life is significantly higher in a single transformer which is heavily loaded. In general transformer loss of life improves with increasing PV penetration. Figure 38 shows the daily variability of transformer loss of life in the same feeders for three PV scenarios.

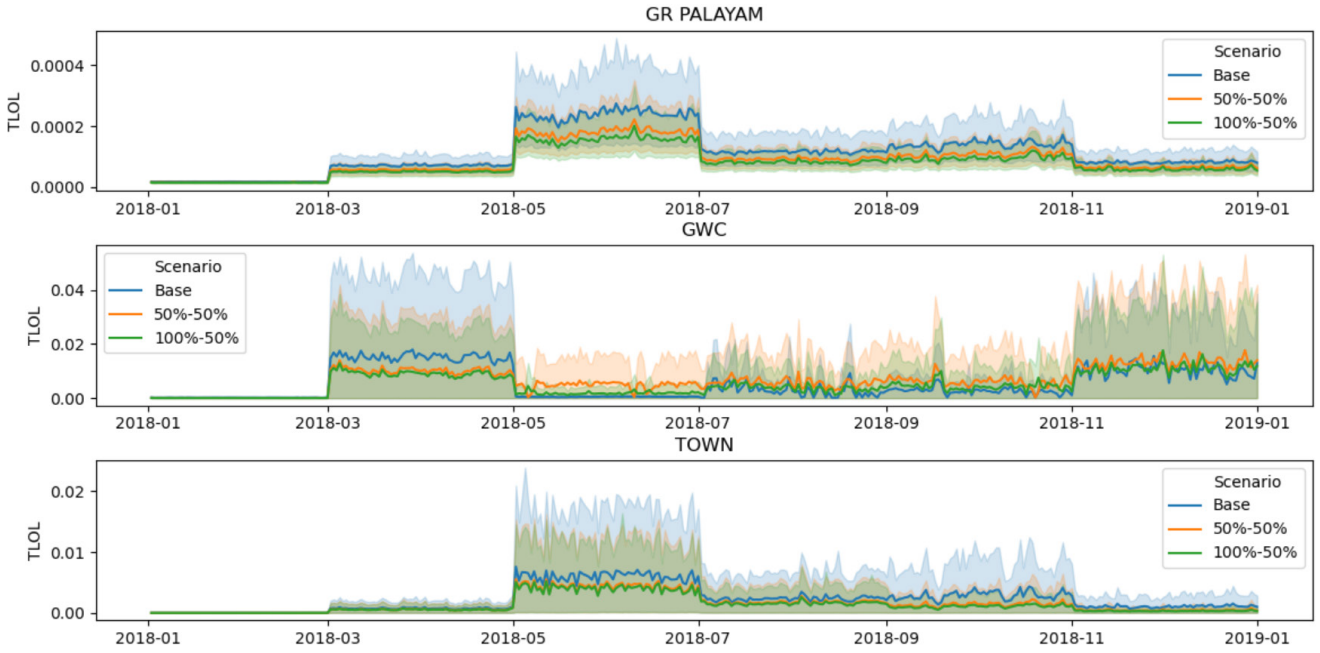

Figure 38. Daily variation of transformer loss of life time series in TANGEDCO feeders (for 2018 in three scenarios: 'Base', '50%-50%' and '100%-50%' scenarios), ordered top to bottom (GR PALAYAM, GWC, TOWN)

The mean transformer loss of life is lower for both the 50%-50% and the 100%-50% PV scenarios in all three feeders throughout the year. The key observation is that transformer loss of life is related to the coincidence of solar generation and load consumption: the lower the coincidence, the higher potential for high PV penetrations to increase transformer loss of life.

7.3.4 Analysis of PV Overgeneration With Distributed PV

When the power production from PV is greater than power consumption at a given time, this causes reverse power flow, where power is fed back to the utility. Understanding how much energy is being generated and at what time allows distribution utilities to make decisions on how to plan and operate in the presence of overgeneration. How much PV can be adopted in a distribution feeder can be limited by net export if there is a limit on back feed at the distribution substation.

Figure 39 shows a plot of the percentage of PV net export in three TANGEDCO feeders at increasing PV penetration levels. For GR PALAYAM and GWC feeders no net export is observed whereas TOWN feeder net export is observed after 30%-50% PV penetration level.

Net export is highly dependent on the customer breakdown at each distribution transformer and the load and PV production coincidence. Figure 32 shows a scatter map of PV net export for all transformers in three TANGEDCO feeders in three different PV scenarios.

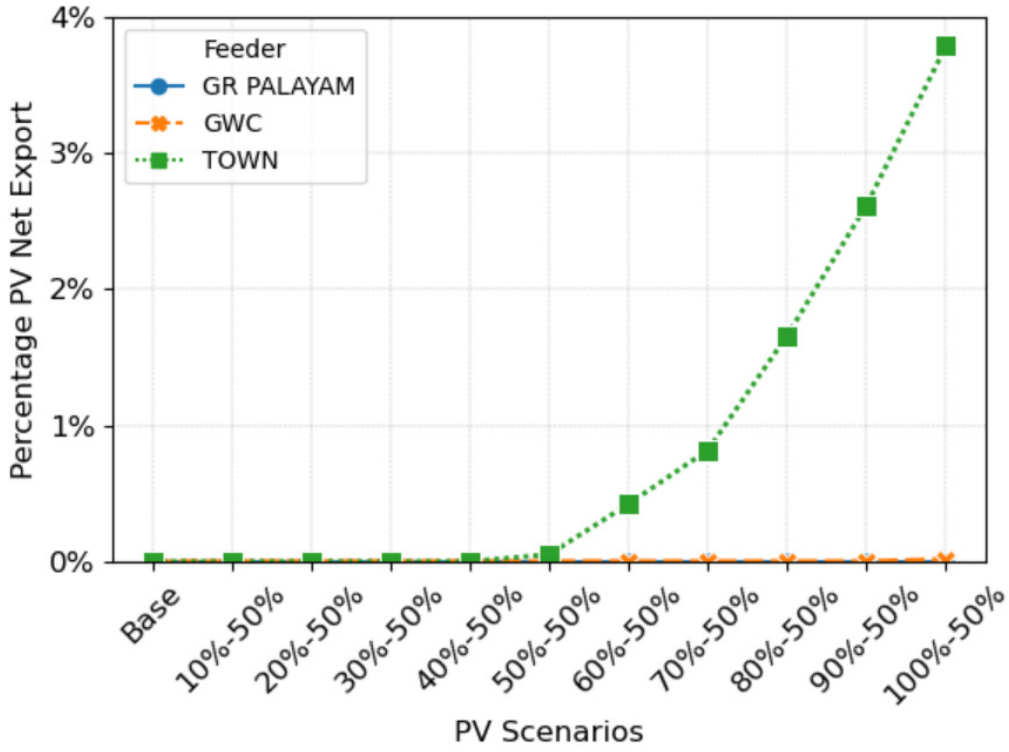

Figure 39. PV net export with increasing PV penetration in TANGEDCO feeders in 2018

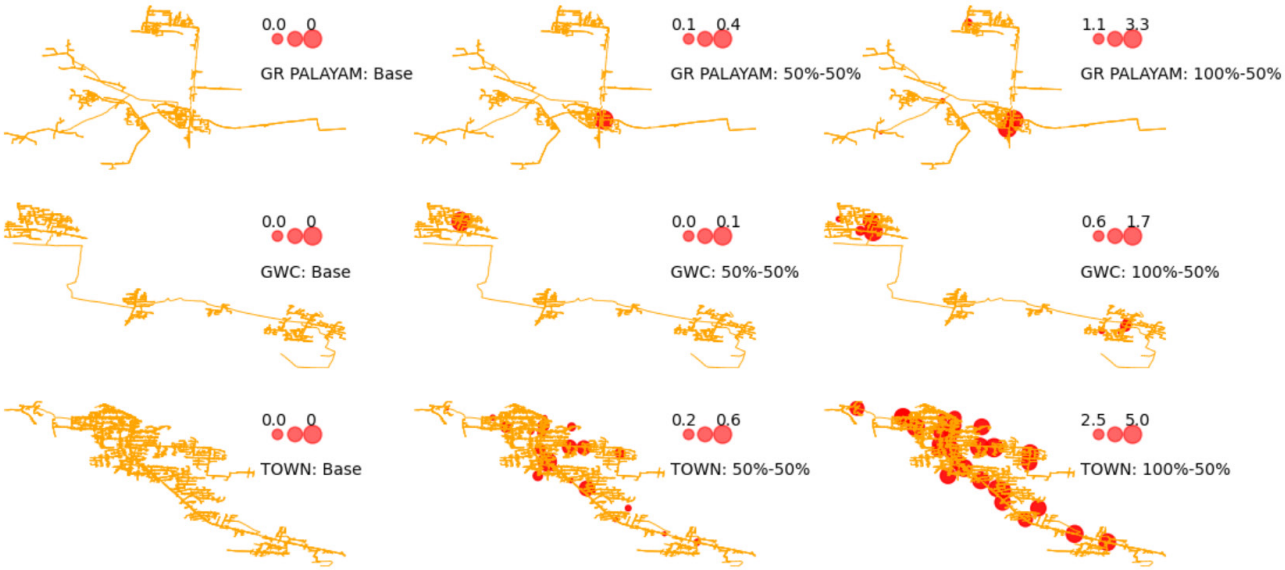

Figure 40. Scatter map of PV net export for all transformers in three feeders in three different PV scenarios ('Base', '50%-50%' and '100%-50%') for 2018

PV net export at a single distribution transformer is a function of the number of PV installations on that transformer, the capacity of those systems, and the magnitude and coincidence of production with energy consumption. The location of PV systems was chosen with a uniform random distribution throughout the

feeder so the proportion of PV installed will be different on each transformer for a given PV scenario. The reason for lower net export at the substation level compared to the distribution transformer level is because generation from one transformer can be consumed by the load on a neighboring network section, avoiding back feed at the substation level.

Figure 41 shows the daily variability of net export at all distribution transformers with the solid line representing the mean value for three feeders in three PV scenarios. The net export is higher at times when solar generation is higher, and load is lower for all three feeders.

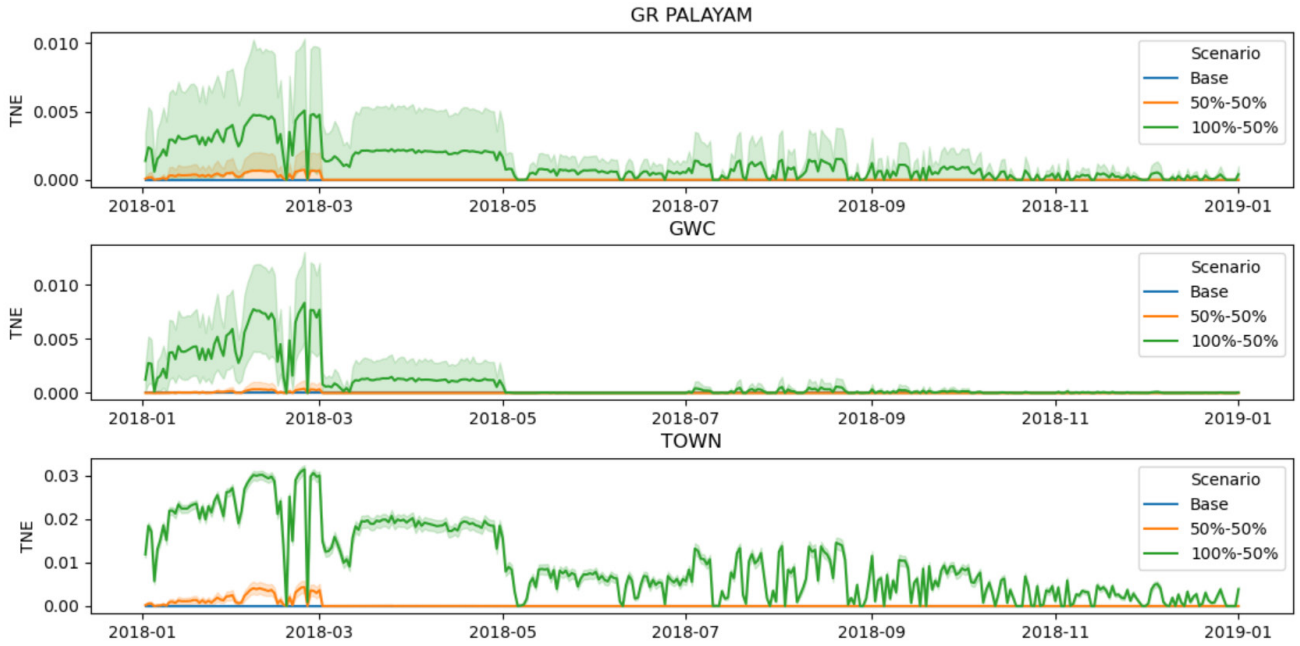

Figure 41. Daily variation of net export at distribution transformers with increasing PV penetration in TANGEDCO feeders (for 2018 in three scenarios: 'Base', '50%-100%' and '100%-100%' scenarios), ordered top to bottom (GR PALAYAM, GWC, TOWN)

8 Impact of GSFs

In Section 4.2, this report discussed GSFs that can be provided by inverters for voltage support. In this section, we discuss the impact of using those GSFs on the three modeled TANGEDCO feeders. Support functions, such as volt-VAR control, can help increase the amount of PV generation that can be safely accommodated on the network and improve power quality. A more in-depth discussion on the potential benefits of using the volt-VAR GSF will be presented for one of the three feeders (GWC feeder), while the change in system impact metrics with the volt-VAR GSF is presented for all three feeders.

8.1 Analysis of Power Quality Risk with Distributed PV

Volt-VAR curves use droop control to output reactive power, help control local voltages, and keep those voltages within bounds. At low voltages, the system injects VARs to increase system voltages back toward nominal, and at high voltages, the system absorbs VARs to decrease system voltages back toward nominal. As described in Section 4.2, when the system is producing active power output close to the inverter limits to keep producing VARs, volt-VAR GSF is used in *reactive power priority* to maintain reactive power output. Reactive power priority can lead to curtailment of energy produced by reducing active power output to prioritize reactive power needs. This can have a direct impact on the economic benefits achievable from the installed PV systems by the consumer. Both the maximum reactive power injection or absorption limits and the voltage values when the inverter should start providing reactive power support can have an impact on the total amount of energy curtailed. Thus, it is essential to correctly define volt-VAR curves to minimize unnecessary curtailment. Commonly used Volt-VAR curves in the United States, as defined by IEEE 1547.1 and Rule 21 in California, are based on ANSI C84.1-2016 limits (i.e., +/- 5% voltage bounds) [21], [23]. Voltage bounds in TANGEDCO are +/- 10%, so for this analysis, volt-VAR curves were created to match the thresholds used by TANDEDCO. The curve used for the analyses presented here can be seen in Figure 42. This figure also shows the volt-VAR category A and category B curves specified in the IEEE 1547-2018 standard, which helps in easily identifying the similarities and differences of the curve used here with other commonly used curves.

The custom TANGEDCO volt-VAR curve maximum reactive power support set-points are the same as the IEEE 1547-2018 category B volt-VAR curve, see Figure 34. The dead band has been enlarged, so for the inverter PCC voltages within the dead band the inverter is not required to provide any reactive power support. Beyond the dead band, however, the reactive power absorption and injection requirements increase gradually until the maximum saturation value of 44% of available reactive power if the PCC voltage reaches the ±10% voltage thresholds. The percentage of available reactive power is equivalent to the percentage of the inverter's kVA rating here as *reactive power priority* is used. Also, it is important to highlight that this curve is not necessarily the most optimal curve for TANGEDCO's feeders. This curve simply builds upon the existing commonly used volt-VAR curves and tries to apply them to the voltage thresholds followed by TANGEDCO.

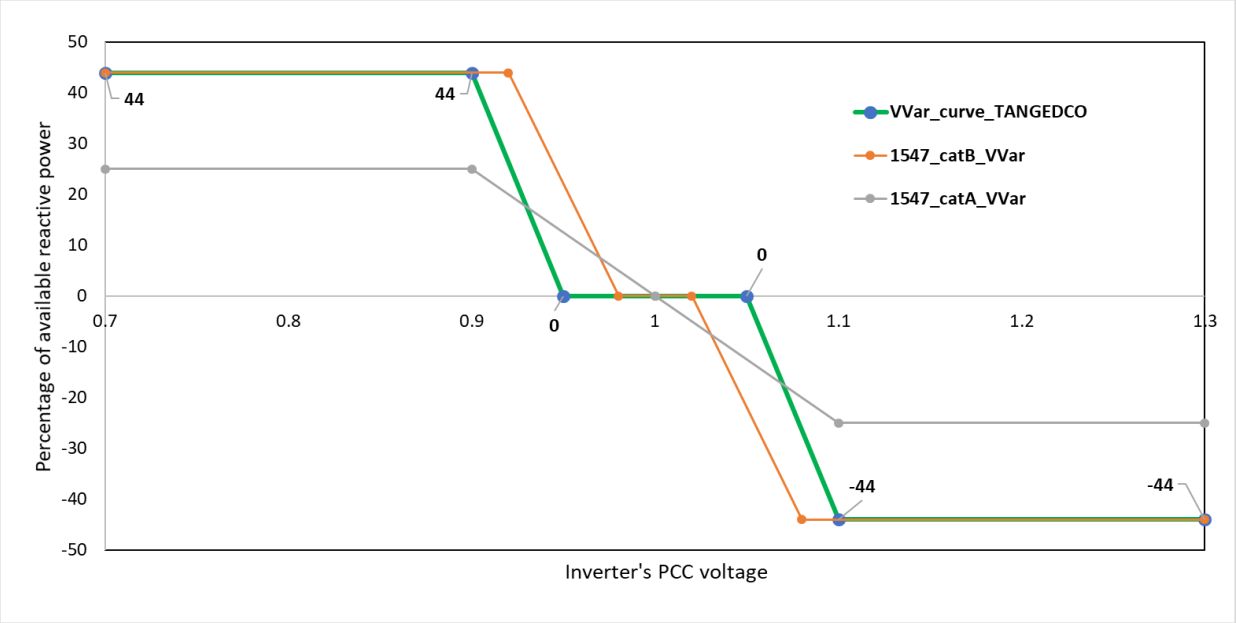

Figure 42. Volt-VAR GSF curve used for TANGEDCO

8.1.1 PV Penetration Scenario Considered for In-Depth Analysis

To determine the impact of volt-VAR support on system parameters, a relatively high PV penetration scenario was considered for the GWC feeder. In this scenario, 50% of the customers in the GWC feeder were deployed with PV systems, as shown in Figure 43. The PV systems were sized to generate 100% of consumer energy requirements over the entire year, and all PV inverters were assumed to be capable of providing volt-VAR GSF.

Figure 43. PV scenarios considered; 50% customers have PVs that satisfy 100% of their energy requirements

For this scenario, yearlong QSTS simulations were completed at 15-minute time steps for three use cases:

- *Unity Power Factor case (PF1)*: This is the traditional case in which the PV inverters were operated with the power factor set to 1. This means the inverters only inject real power and do not provide any reactive power support.

- *Volt-VAR with limited VAR support (VVAR lim)*: In this scenario, all inverters were operated with the volt-VAR GSF enabled using the curve shown in Figure 42. The reactive power support is only provided when the PV system is generating real power. This is the most commonly used volt-VAR setting, as the PV inverters are only expected to mitigate the violations they create. Thus, when their real power injection is zero, the reactive power support is also zero.

- *Volt-VAR with continuous VAR support (VVAR cnt)*: In this scenario, all the inverters were operated with the volt-VAR GSF enabled; however, the voltage support is kept enabled even when the PV system is not injecting real power. With this setting, the PV inverters can provide reactive power support to mitigate external network violations as well.

Along with these simulations, the base case is also simulated. The base case represents the existing GWC feeder without any added PV systems, and provides the reference against which the other PV use cases are compared.

8.1.2 Testing Volt-VAR GSF

The high PV penetration scenario considered here contains 971 PV systems. Running the three-phase unbalanced power flow on a large network with close to 2,000 buses and achieving convergence is challenging by itself, and the problem is further compounded by the presence of such a large number of

PV controllers. Each controller tries to inject or absorb reactive power based on its PCC voltage at every time point. This injection or absorption, in turn, changes the PCC voltage. These iterations continue until the convergence criteria is met. Furthermore, to ensure the results are accurate, the voltage and VAR change tolerance limits were reduced by an order of magnitude compared with the default OpenDSS tolerances. This further increased the number of iterations required at each time step and increased the simulation accuracy. Even with these constraints, the 50% PV penetration scenario simulation completed without any convergence issues. Thus, the results presented here are accurate and statistically relevant.

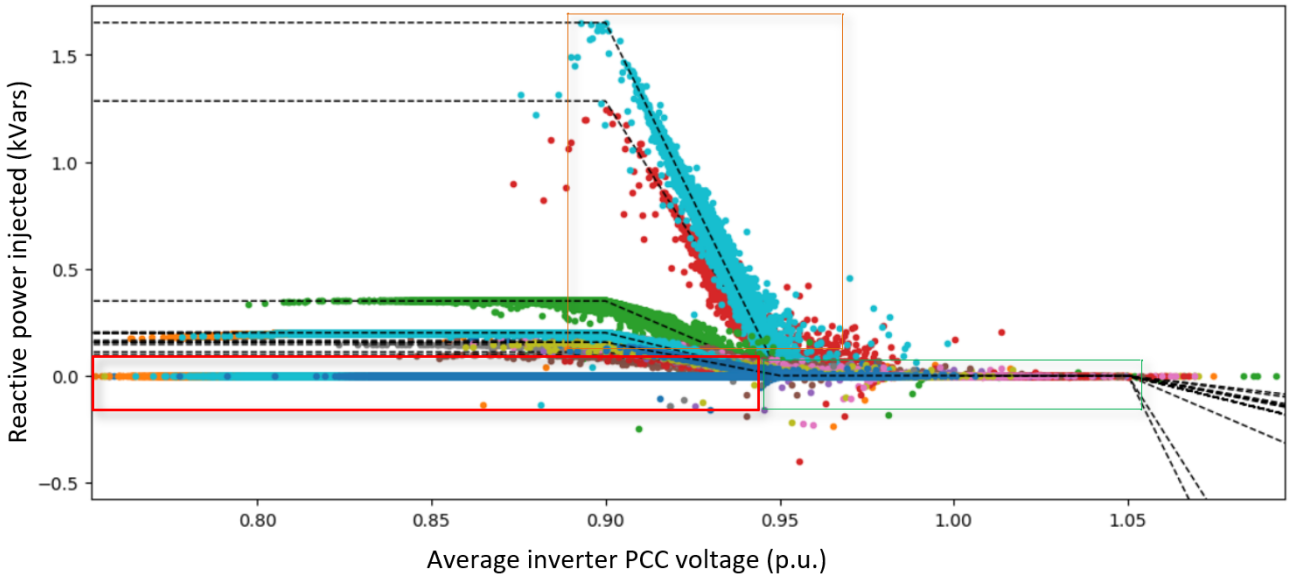

Figure 44. Scatter plot of inverter PCC voltage and reactive power injection for limited volt-VAR support

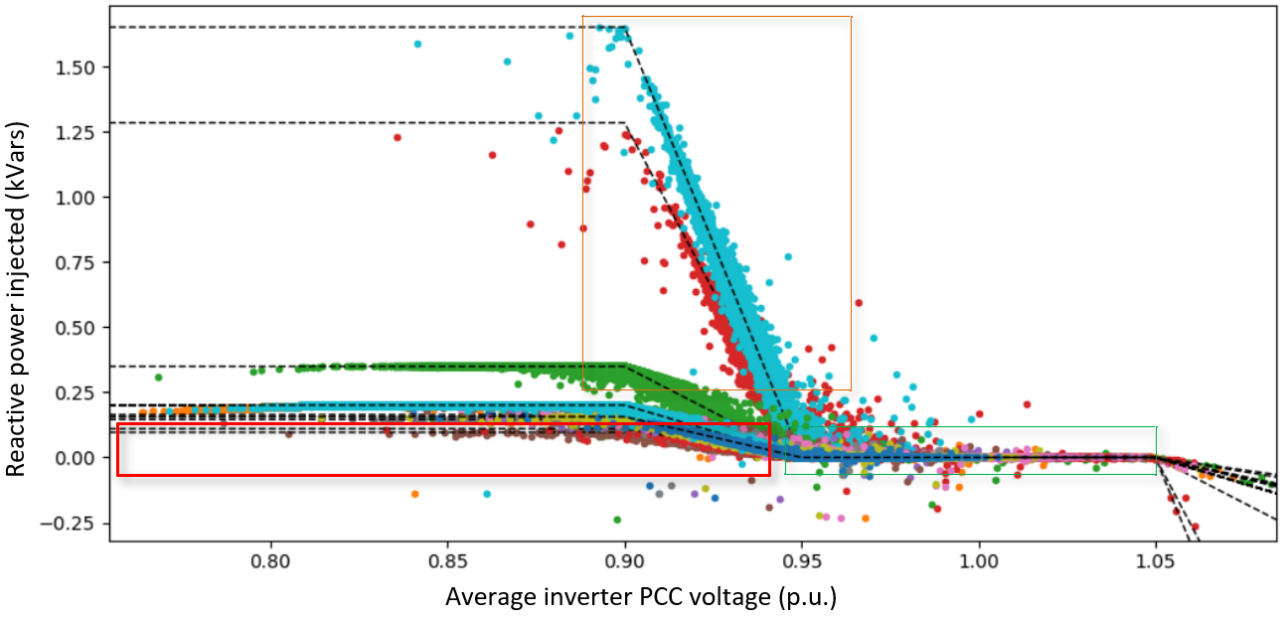

Figure 45. Scatter plot of inverter PCC voltage and reactive power injection for continuous volt-VAR support

Figure 44 shows the scatter plot of average PCC voltage and reactive power injection for 20/971 randomly chosen PV systems of the 50% PV penetration scenario. The PV inverters here were operated with volt-VAR GSF, but reactive power support was provided when real power was also being injected. For each PV system, the volt-VAR curve scaled to its kVA rating is also plotted as a dotted line. In Figure 36, three key results are highlighted using boxes. The orange box shows that the reactive power injection closely follows the volt-VAR curve based on the average PCC voltage; however, there are still a few points that do not lie close to the curve. This is expected, considering the large number of distributed controllers in the simulation. The green box shows the dead band and demonstrates negligible reactive power support is provided when voltages lie within the dead band as desired. The red box highlights those time points when inverter PCC voltages are outside the dead band, but reactive power support cannot be provided as there is no real power generation. Presence of a number of low voltage time points when PV inverters are not operating indicates that enabling reactive power support during these time points can reduce system violations.

Figure 45 shows the scatter plot of average PCC voltage and reactive power injection for the 20/971 randomly chosen PV systems of the 50% PV penetration scenario; however, in this scenario, reactive power support was always enabled. This is why there are no time points in the red box that were present in Figure 36. Also, the reactive power injections closely follow the volt-VAR curve. Volt-VAR at the distribution level may be advantageous due to the limitations and challenges in transporting VARs from the bulk system and substation down to grid-edge network sections.

The results presented here show that the QSTS simulations were completed successfully and all PV inverter reactive power injections closely followed their volt-VAR curves. Thus, the grid impact results and inverter operation statistics obtained from these simulations are accurate and are discussed subsequently.

8.2 Volt-VAR GSF Impact on System Parameters

In this subsection, we discuss the impact of volt-VAR GSF on grid parameters such as voltage and thermal loading of lines and transformers. Instead of just looking at the maximum and minimum values of these parameters at each time point, the net impact of all bus violations and overloading of all lines and transformers were determined as described in each subsection.

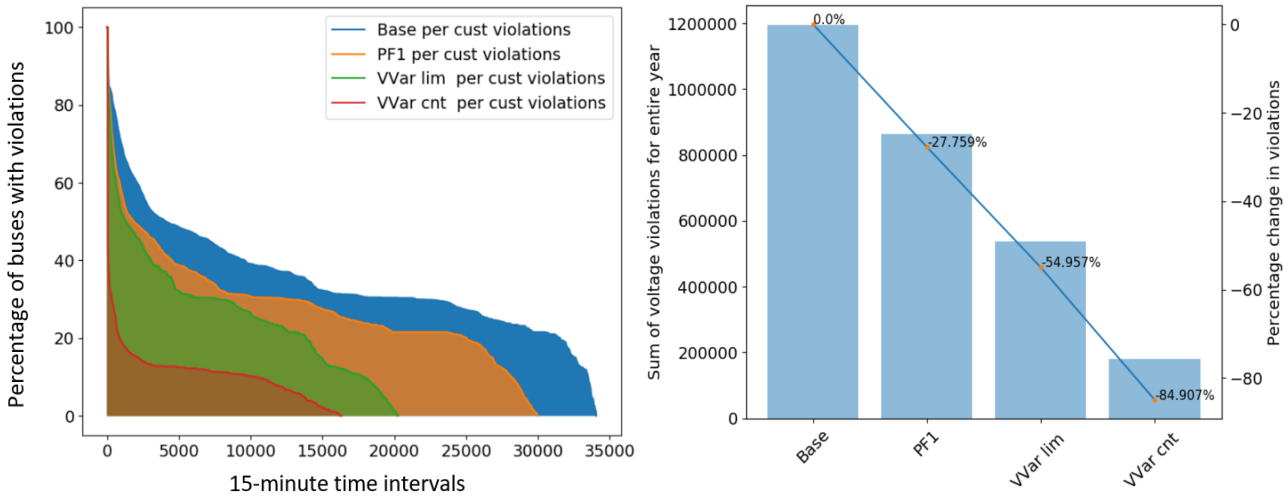

Figure 46. Duration curves of the percentage of buses with violations (left) and percentage change in percentage of buses with violations compared with base (right) for 50% PV scenario

- *Impact on voltages:* The net impact on feeder voltages was obtained by determining the percentage of buses with voltage violations (V_{bus}) (voltage outside ±10% of nominal) and the severity of violations (V_{sev}^{bus}) at all time points using equations (1-2). Using these two quantities, the impact of adding PV controllers on voltages across the feeder over the entire year was determined.

$$V_{bus}(t) = \frac{1}{N}\left(\sum_{i=1}^{N} n_i\,(t)\right) * 100, (1)$$

$$where,$$

$$N\ is\ the\ number\ of\ buses\ in\ the\ feeder$$

$$n_i\,(t) = \begin{cases} 1, if\ v_{b_i}(t) > v_U\ or\ v_{b_i}(t) < v_L \\ 0, otherwise \end{cases}$$

$$v_U\ is\ the\ overvoltage\ threshold\ (1.1\ p.u.)$$

$$v_L\ is\ the\ undervoltage\ threshold\ (0.9\ p.u.)$$

$$v_{b_i}(t)\ is\ the\ voltage\ at\ bus\ b_i\ at\ any\ time\ t$$

$$V_{sev}^{bus}(t) = \sum_{i=1}^{N} s_i(t), (2)$$

$$where,$$

$$s_i\,(t) = \begin{cases} v_{b_i}(t) - v_U, if\ v_{b_i}(t) > v_U \\ v_L - v_{b_i}(t), if\ v_{b_i}(t) < v_L \\ 0, otherwise \end{cases}$$

Figure 46 and Figure 47 show the duration curve of the percentage of buses with violations and severity of violations for the base case with no PV and the PV scenarios. It can be clearly seen that the base case with no PV scenario has significantly more voltage violations than the scenario with PV systems. Both the percentage of buses with violations and violation severity are higher for the base case. The scenario shown in green for the limited volt-VAR case shows a further reduction in voltage violations due to the reactive power support available from the PV inverters. The continuous volt-VAR support scenario shows the steepest reduction in voltage violations as reactive power support is available at all time points. Along with the severity and number of buses with violations, the number of time intervals with violations was also reduced. The voltage violations in the base case are caused by system under-voltages; PV generation helps bring these systems within bounds.

The net change in voltage violations over the entire year can be determined by summing up $V_{bus}(t)$ and $V_{sev}^{bus}(t)$ for the entire year using (3) and (4).

$$V_{bus}^{net} = \sum_{t=1}^{T} V_{bus}(t) \quad (3)$$

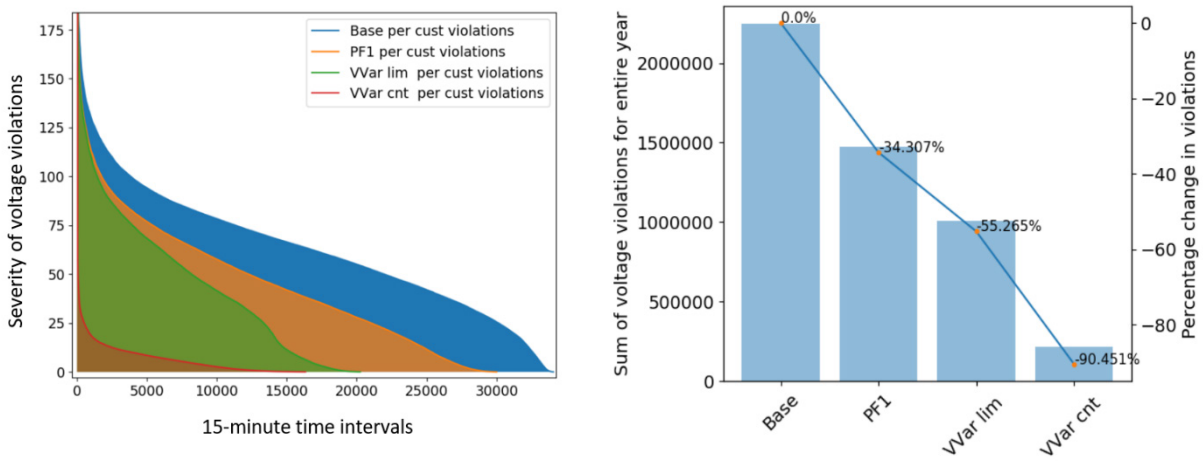

Figure 47. Duration curves of severity of voltage violations (left) and percentage change in severity of voltage violations compared with base (right) for 50% PV scenarios

$$V_{sev}^{bus\_net} = \sum_{t=1}^{T} V_{sev}^{bus}(t) \quad (4)$$

where T is the total time points simulated (35040).

Equations 3 and 4 were used to determine the percentage change in V_{bus}^{net} and $V_{sev}^{bus\_net}$ for all PV scenarios from the base with no PV scenario, and this percentage change is presented in Figure 47 and Figure 48. These figures show that adding PV systems leads to a steep reduction in voltage violations, and continuous VAR support can eliminate almost all voltage violations.

- *Impact on thermal loading of transformers:* The net impact on transformer thermal violations was obtained by determining the percentage of transformers with thermal violations (V_{xfmr}) (thermal loading greater than rated value) and the severity of violations (V_{sev}^{xfmr}) at all time points using Equations 5 and 6. Using these two quantities, the impact of adding PV controllers on transformer thermal loadings across the feeder over the entire year was determined.

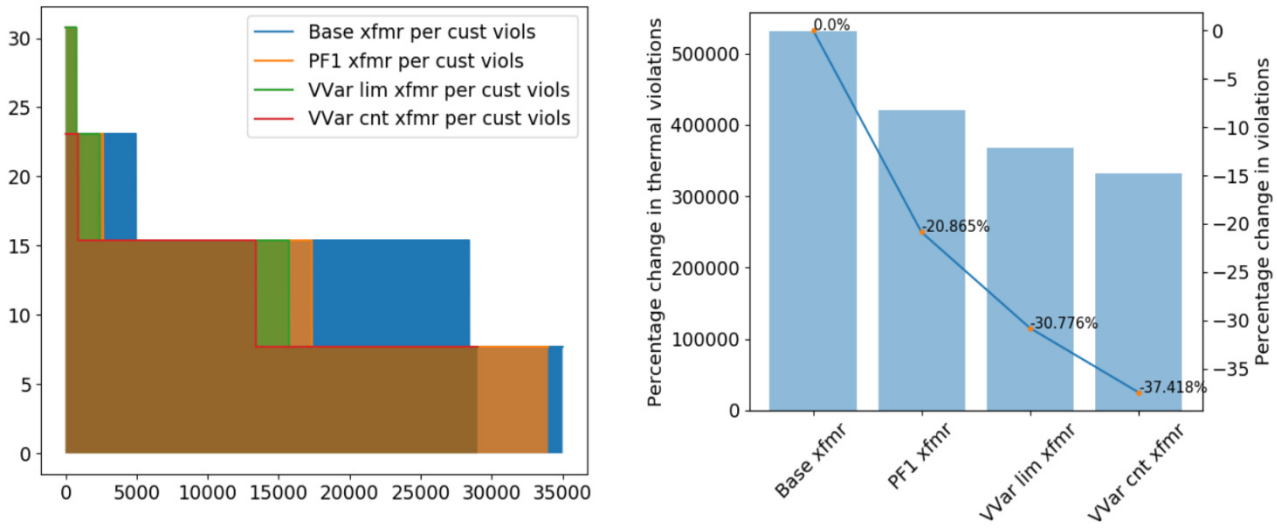

Figure 48. Duration curves of percentage of transformers with thermal violations (left) and percentage change in percentage of transformers with thermal violations compared with base (right) for 50% PV penetration

$$V_{xfmr}(t) = \frac{1}{X}\left(\sum_{i=1}^{X} x_i\,(t)\right) * 100, (5)$$

$$where,$$

$$X\ is\ the\ number\ of\ transformers\ in\ the\ feeder$$

$$x_i\,(t) = \begin{cases} 1, if\ l_{X_i}(t) > l_{U_i} \\ 0, otherwise \end{cases}$$

$$l_{U_i}\ is\ the\ rated\ ampacity\ of\ any\ transformer\ i.$$

$$l_{X_i}(t)\ is\ the\ current\ flowing\ through\ any\ transformer\ X_i\ at\ any\ time\ t$$

$$V_{sev}^{xfmr}(t) = \sum_{i=1}^{N} s_i(t), (6)$$

$$where,$$

$$s_i\,(t) = \begin{cases} l_{X_i}(t) - l_{U_i}, if\ l_{X_i}(t) > l_{U_i} \\ 0, otherwise \end{cases}$$

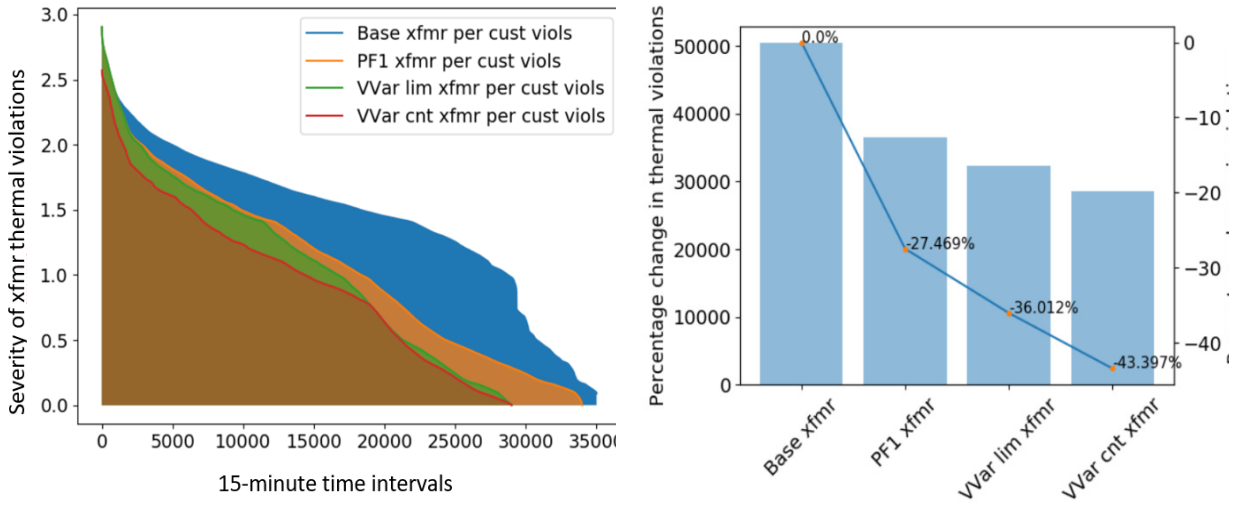

Figure 49. Duration curves of severity of transformer thermal violations (left) and percentage change in severity of transformer thermal violations compared with base (right) for 50% PV penetration

Figure 48 and Figure 49 show the duration curve of the percentage of transformers with violations and the severity of violations, respectively, for the base case with no PV and the PV scenarios. The reactive power support from PV inverters is only meant to support voltages and does not try to improve system thermal violations; however, these figures show that both the percentage of transformers with violations and violation severity reduces for the 50% PV penetration scenario with reactive power support. This is because more load is being served locally, and reactive power support reduces the kVA loading of the transformers.

The net change in line thermal violations over the entire year can be determined by summing up $V_{xfmr}(t)$ and $V_{sev}^{xfmr}(t)$ for the entire year using Equations 7 and 8.

$$V_{xfmr}^{net} = \sum_{t=1}^{T} V_{xfmr}(t) \quad (7)$$

$$V_{sev}^{xfmr\_net} = \sum_{t=1}^{T} V_{sev}^{xfmr}(t) \quad (8)$$

where T is the total time points simulated (35040)

Equations 7 and 8 were used to determine the percentage change in V_{xfmr}^{net} and $V_{sev}^{xfmr\_net}$ for all PV scenarios from the base no PV scenario. This is presented in Figure 48 and Figure 49, as well. In these figures, the actual percentage reduction in violations over the entire year has been quantified.

- *Impact on thermal loading of lines:* None of the lines in the GWC feeder experienced thermal violations in the base case with no PV or in any of the PV scenarios.

8.2.1 Clipping and Curtailment With Volt-VAR GSF

To provide voltage support when the inverters are operated in the reactive power priority mode, real power may have to be curtailed. This curtailment principally occurs during high irradiance and high voltage time periods above the upper voltage bound. So, if the PV system's PCC voltage is within permissible bounds or if the inverter has sufficient headroom to provide reactive power support, energy will not be curtailed.

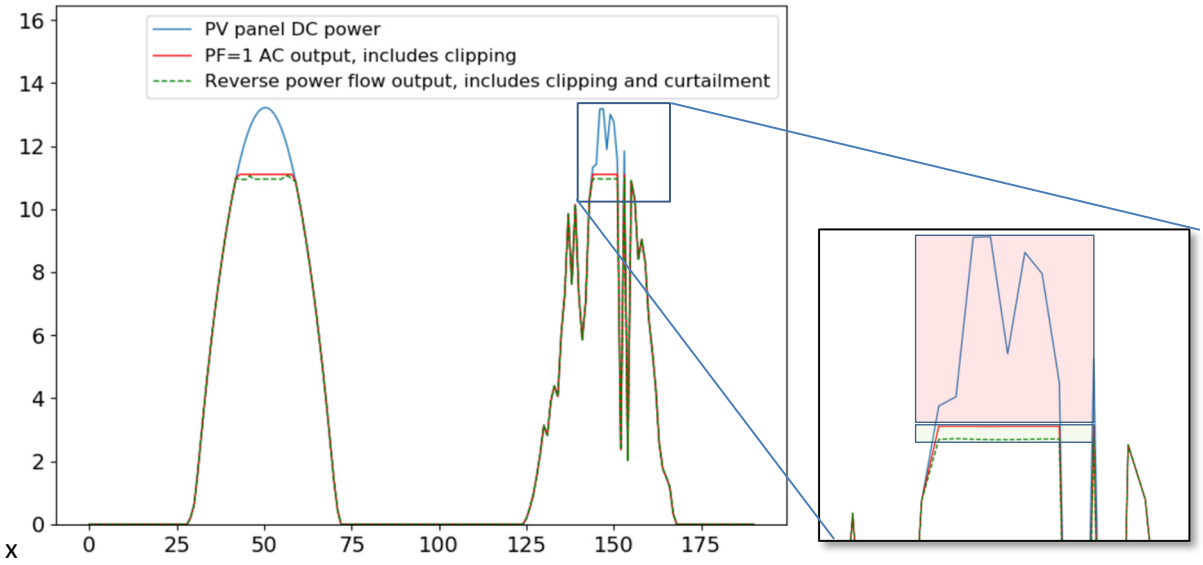

Figure 50. Clipping (area between red and blue lines) and curtailment (area between green and red lines) for a PV system with a DC to AC ratio greater than 1

Before presenting energy curtailment results, it is important to distinguish between "clipping" and "curtailment." Clipping refers to the energy curtailed because of the choice of the DC to AC ratio used by the consumer (Equation 9). The DC to AC ratio, in simple terms, refers to the ratio of the DC rating of the PV panels and the kVA rating of the inverter. Since peak irradiance only happens for few time points of the year, consumers may choose to have an underrated inverter (in respect to the DC panel capacity) to reduce capital costs of the system. Consequently, the PV panel's full DC power cannot be fully converted to AC power during those irradiance periods as the inverter's kVA limit is reached; here, voltage is reduced on the DC side to limit output to the inverter's rating.

Curtailment, on the other hand, refers to the energy curtailed because of the reactive power provided for voltage support by curtailing real power production (Equation 10). It is important to distinguish between the two, as only curtailment represents the part of the total available DC power curtailed for voltage support, and clipping is solely based on the consumer's choice of inverter size.

$$Clipping = \frac{Panel\ DC\ power - Inverter\ real\ power\ for\ PF1}{Panel\ DC\ power} \quad (9)$$

$$Curtailment = \frac{Inverter\ real\ power\ for\ PF1 - Inverter\ real\ power\ for\ VoltVar}{Inverter\ real\ power\ for\ PF1} \quad (10)$$

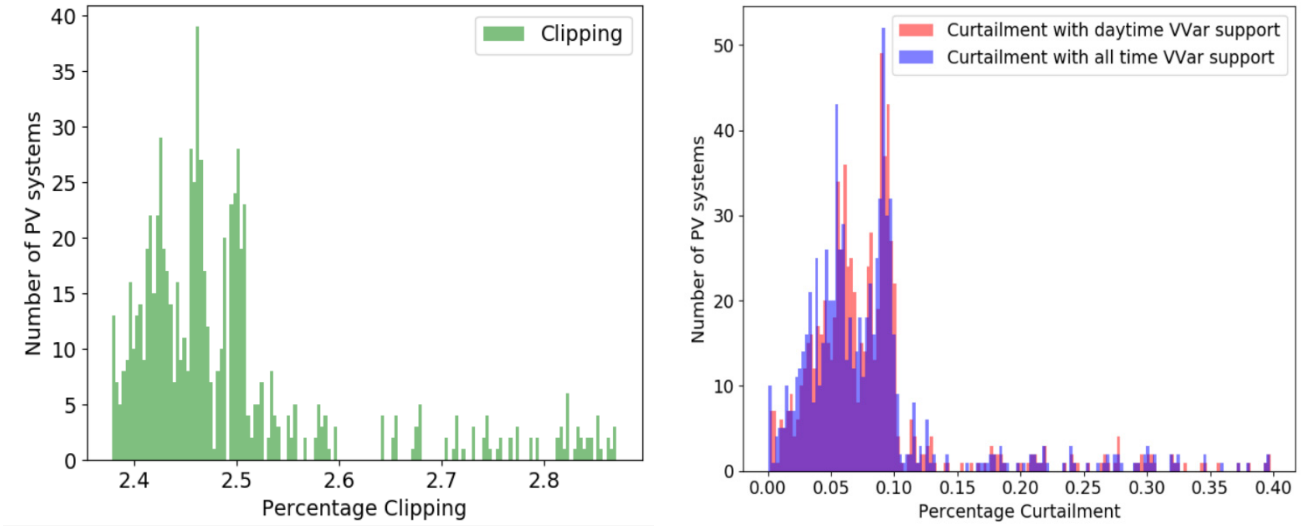

Figure 51. Clipping and curtailment values for 50% PV penetration scenario for GWC feeder

Figure 50 shows the clipping and curtailment observed for a PV system with a DC to AC ratio greater than 1. In this figure, the DC and AC power outputs are shown for 2 days. For commonly used DC to AC ratios and volt-VAR curves, annual clipping tends to be higher than the annual curtailment. The same was observed for GWC feeder, as the DC to AC ratio considered here was 1.11. Figure 51 shows the annual clipping and curtailment values observed for 80% of the smart inverter-connected PV systems for the 50% PV penetration scenario. Remaining inverters were either outliers or had minor convergence issues and their results are not included. Figure 42 shows that while clipping values for most inverters lie in the 2.4%–2.8% range, curtailment values lie between 0%–0.4%. Thus, the average energy curtailment a customer might experience to provide reactive power support would be much less than the energy clipped due to the choice of their inverter's DC to AC ratio, and it can be negligible.

8.2.2 Change in PV Inverter Operation With Volt-VAR GSF

The previous sections showed how the volt-VAR GSF reduced voltage violations dramatically while also reducing transformer thermal violations. The energy curtailed to provide reactive power support is also negligibly small; however, the additional reactive power support can impact the net apparent power output of the inverter. Increase in power output can increase the stress on the inverter's switches, which can increase the junction temperature and impact the inverter's life. Translating increased usage to life reduction is a much more involved process. Studies have shown that providing reactive power support does not have a big impact on the inverter's life [29].

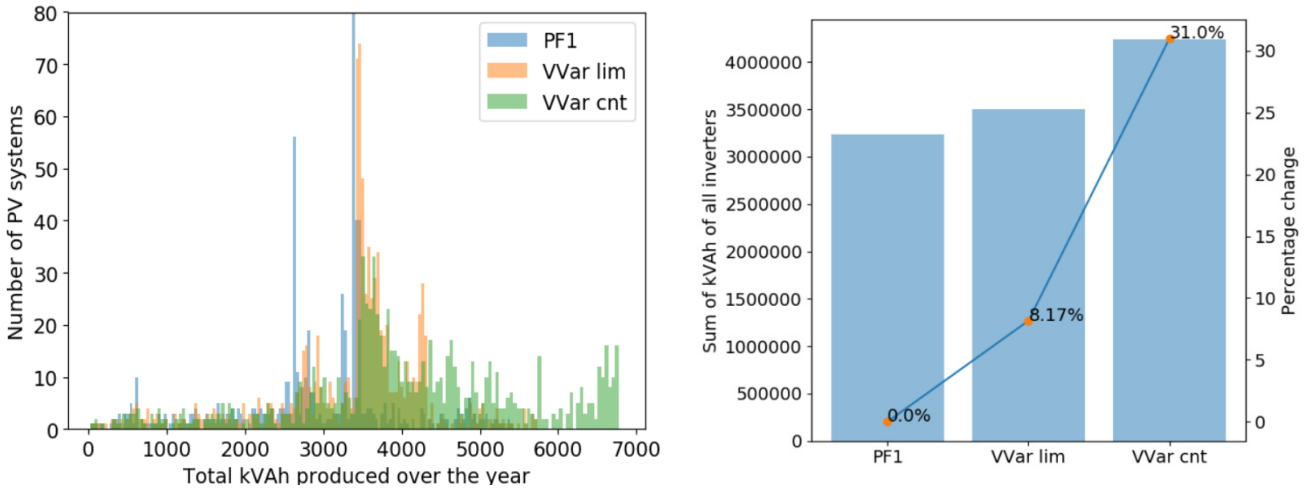

Figure 52. Change in kVA output of inverters for volt-VAR GSF use cases compared with PF=1 operation

The net change in kVA output of inverters and the increase in time points when the inverter operates can be more easily quantified. Figure 52 shows the annual kVA hours (kVAh) generated by each inverter. This figure also shows the percentage change in kVAh due to volt-VAR compared with the unity power factor scenario. On the other hand, Figure 53 shows the total number of time points for which inverters operated in each use case. As expected, the number of time points of operation is the same for PF=1, and limited volt-VAR use cases as reactive power support is not provided when real power is not generated during daytime hours. The time points of operation increase for the continuous VAR support volt-VAR use case. The increase is directly dependent on the time points when voltages are outside bounds when the inverter is not injecting real power or at nighttime. These increased time points may or may not impact inverter life significantly depending on ambient temperature and inverter characteristics. More research is needed to determine this impact. However, from Figure 52 and Figure 53, it can be seen that volt-VAR GSF increased kVAh output by 8%–31% and time points of operation by 0%–68% for the 50% PV penetration scenario of the GWC feeder compared with the unity power factor operation.

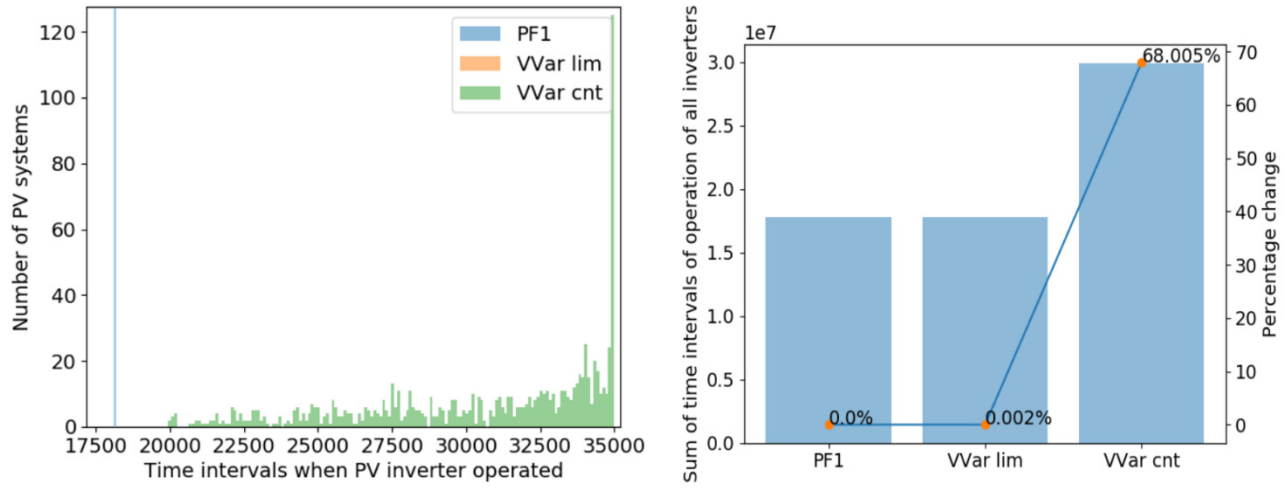

Figure 53. Change in time points of operation of inverters for volt-VAR GSF use cases compared with PF=1 operation

9 Conclusions

The work detailed in this report describes the development of a holistic set of analysis tools for TANGEDCO for the future planning of the distribution network in Tamil Nadu and the day-to-day analysis of new interconnection requests for DERs. This report has focused on developing out analysis capabilities for TANGEDCO in addition to performing detailed analysis studies on the integration of solar rooftop PV on TANGEDCO's distribution network. The analysis capabilities developed in this report, released as an open-source analysis framework - *Emerging technologies Management and Risk evaluation on distribution Grids Evolution (EMeRGE)*, are as follows:

- **Load Class Profile Analysis:** A methodology to use SCADA, bimonthly billing data, and tariff data to help develop load profiles for separate load classes (e.g., residential, commercial, industrial, and agricultural).

- **Distribution Feeder Modeling Framework:** A tool to convert TANGEDCO GIS data into distribution network feeder models that can be used for network analysis in the power-flow analysis tool OpenDSS.

- **Distribution Risk Analysis Framework:** A holistic framework to examine the impact of DERs on the distribution network, analyzing the impact on distribution network voltage violations, asset overloading, transformer loss of life, and system over-generation.

NREL has established several findings and recommendations for TANGEDCO based on the analysis:

- The risk associated with voltage and thermal violations decreases in the TANGEDCO feeders with the deployment of distributed PV up to a certain penetration level and increases afterwards. For example, in GR PALAYAM feeder, aggregated SARDI decreases up to 70%–100% (70% of customers with PV production matching 100% of energy consumption) PV scenario.

- The risk associated with thermal violations occurs first when compared to voltage violations with increasing PV penetration in TANGEDCO feeders. For example, in the TOWN feeder, the risk associated with thermal violations (both line and transformer overloading) increases after the 60%–100% PV scenario; however, the risk associated with voltage violations continues to decrease up to the 100%-100% PV scenario.

- The efficiency of power delivery for conductors and transformers remains almost constant with increasing PV penetration levels in TANGEDCO feeders, although it decreases at the highest levels of PV penetration.

- The coincidence of solar irradiance with customer energy consumption has an inverse relationship with transformer loss of life, meaning that the higher the correlation between solar and load, the lower the impact on the transformer loss of life. This is due to transformer loading being reduced at a time when the outside temperature is higher, which is during the middle of the day.

- The percentage of PV generation exported at the substation level is lower than the percentage of PV export at distribution transformers due to the load diversity (i.e., export from one distribution transformer will be absorbed by another one, avoiding the back-feed at the substation transformer).

- Smart inverters providing Volt-VAR support did not use VAR support to reduce voltages but instead used it to increase under-voltages. Inverters operating in the continuous Volt-VAR support mode (i.e., during PV and non-PV production hours) were able to mitigate 85% of the annual nodal under-voltage violations and reduce the nodal violation severity by 90% compared with the base case scenario (i.e., with no PV present) for the GWC feeder.

- The reactive power support from the inverters did not cause any additional line or transformer overloads. The transformer overloading was reduced by 31% compared with the base case (i.e., with no PV present) scenario.

- Due to inverter capacity constraints, 0%–0.4% of the annual energy was curtailed to provide reactive power support. This curtailment is significantly smaller than the 2.4%–2.8% of the annual energy clipped if the customer chooses an undersized inverter (i.e., one that is sized at 80% of panel capacity, which is commonly done for cost savings) compared to the PV panel rating.

- The additional reactive power support marginally increased the inverter kVAh (apparent power output over the year) by about 8% compared with the unity power factor PV scenario for the daytime volt-VAR support mode. The kVAh increase was about 31% for the continuous VAR support scenario. The total inverter operation time increased by about 68% for the continuous VAR support mode. Further analysis is required to determine the economic impacts of the continuous VAR support mode before it may be adopted. The daytime VAR support mode can be implemented without significant customer impacts.

In this report, we also performed detailed analysis on the integration of solar rooftop PV onto TANGEDCO's distribution network. The analysis examined three distribution feeders and ran a scenario analysis of PV penetration from 0% to 100% of customers having rooftop PV. The overall analysis discussed the following high-level findings:

- **Impact of Rooftop Solar PV:** Increasing solar PV adoption levels for the modeled TANGEDCO feeders improves overall power quality by increasing low voltages originally found on the network. Only at very high PV penetration levels were there negative impacts, with a small number of distribution assets experiencing overloading.

- **Potential of PV Inverter Volt-VAR Support:** Volt-VAR support, which has traditionally been used to lower potential over-voltages that can be caused by large-scale PV integration, when used on TANGEDCO feeders, serves to bring low voltages up toward nominal. NREL also examined continuous Volt-VAR support (i.e., inverters providing constant support rather than just during PV production hours), this provided additional support in increasing nighttime low voltages.

Throughout the analysis, NREL found a number of actions that would assist TANGEDCO in distribution network analysis and modeling and in helping integrate solar PV:

- **Increased Data Collection:** To increase visibility of power quality on the distribution network, TANGEDCO could extend their SCADA system to monitor LT distribution transformers. This would help validate the modeled voltage drop from the primary substation to the LT network.

Rolling out advanced metering infrastructure could also be a long-term solution to monitor DER at a customer level, help with billing, and provide visibility of power quality on the low-tension network.

- **Interconnection Power Flow Analysis:** To help successfully integrate solar PV to the network, TANGEDCO could start to run power-flow analyses for new interconnection applications. This analysis could check the impact of new PV applications on system power quality and asset loading.

- **Inverter Volt-VAR Support:** Although PV systems were not seen to increase power quality violations on the distribution network, providing inverter Volt-VAR support improved power quality on the network. By requesting new interconnection application to provide Volt-VAR support, TANGEDCO could help improve power quality throughout remote end-of-line regions of the network.

This report has shown that the integration of solar PV to TANGEDCO's distribution network has the potential to improve network voltages and decrease loading on distribution assets. The tools NREL has generated should help TANGEDCO into the future in assessing interconnections and with the integration of distribution solar PV.

References

[1] B. Balachandar, "Tamil Nadu and Karnataka remain key pillars of India's clean energy growth," *The HINDU*, 04-Dec-2019.

[2] NITI (National Institution for Transforming India). 2015. *Report of the Expert Group on 175 GW RE by 2022.* New Delhi, India: NITI. https://niti.gov.in/writereaddata/files/writereaddata/files/document_publication/report-175-GW-RE.pdf.

[3] Press Trust of India, "PM Modi vows to more than double India's non-fossil fuel target to 450 GW," *India Today*, Sep-2019.

[4] CEA (Central Electric Authority). 2019. *Load Generation Balance Balance Report 2015-16*. Fulfilment CEA's Oblig. under Sect. 73(a) Electr. Act, 2003.

[5] Central Statistics Office of India. "Energy statistics 2019." *Minist. Stat. Progr. Implement. Gov. India* 26 (2019): 1–123. *www.mospi.gov.in.*

[6] Tamil Nadu Generation and Distribution Coporation Limited (TANGEDCO), "TANGEDCO Profile," *https://www.tangedco.gov.in/profile.html*, 2020. .

[7] MNRE (Minisitry of New & Renewable Energy). *Phase II of Grid Connected Rooftop Solar - MNRE*. https://mnre.gov.in/img/documents/uploads/7ccd3b4b3bb94a51af516e2ee4fdede3.pdf Accessed: January 2021

[8] Government of India, "PM KUSUM SCHEME 70 PERCENT GOVERNMENT SUBSIDY OFFERED FOR INSTALLING SOLAR PUMPS," *Press Information Bureau*, 2020. .

[9] Tamil Nadu Electricity Regulatory Commission. 2019. *Order on Rooftop Solar Generation TNERC Order No. 3 25.03.2019*. http://www.tnerc.gov.in/orders/Tariff%20Order%202009/2019/Solar-25-03-2019.pdf Accessed: January 2021

[10] Van Rossu, G., and F. L. Drake, Jr. *Python 3 Reference Manual*. Scotts Valley, CA: Createspace, 2009.

[11] Duwadi, K., and K. McKenna. "Emerging technologies Management and Risk evaluation of distribution Grids Evolution." https://github.com/NREL/EMeRGE. Accessed: January 2021

[12] EPRI (Electric Power Research Institute). "Open Distribution System Simulator (OpenDSS)." https://sourceforge.net/projects/electricdss/ Accessed: January 2021

[13] Ihaka, R., and R. Gentleman. "The R Project for Statistical Computing." Last modified October 10, 2020. https://www.r-project.org/. Accessed: January 2021

[14] Geospatial Foundation Project. "QGIS Geographic Information System QGIS.org." 2020. https://www.qgis.org/en/site/ Accessed: January 2021

[15] Elgindy, T., Nicolas Gensollen, Dheepak Krishnamurthy, Michael Rossol, Elaine Hale, and Bryan Palmintier. 2018. *DiTTo (Distribution Transformation Tool)*. Golden, CO: NREL. DOI: 10.11578/dc.20181129.8. https://www.osti.gov/doecode/biblio/20924.

[16] NOAA (National Oceanic and Atmospheric Administration.) "Chennai Airport METeorological Aerodrome Reports (METARs)," *NOAA FTP METAR Reports*, 2019. https://tgftp.nws.noaa.gov/data/observations/metar/stations/ Accessed: January 2021.

[17] Tamil Nadu Generation and Distribution Coporation Limited (TANGEDCO), "Tariff Rates As in the TNERC," 2020.

[18] Giraldez, J.I., Adarsh Nagarajan, Peter Gotseff, Venkat Krishnan, Andy Hoke, Reid Ueda, Jon Shindo, Marc Asano, and Earle Ifuku. 2017. *Simulation of Hawaiian Electric Companies Feeder Operations with Advanced Inverters and Analysis of Annual Photovoltaic Energy Curtailment*. Golden, CO: NREL. NREL/TP-5D00-68681. https://www.nrel.gov/docs/fy17osti/68681.pdf.

[19] Seguin, R., J. Woyak, D. Costyk, J. Hambrick, and B. Mather. 2016. *High-Penetration PV Integration Handbook for Distribution Engineers*. Golden, CO: NREL. NREL/TP-5D00-63114. https://www.nrel.gov/docs/fy16osti/63114.pdf.

[20] NREL. "National Solar Radiation Database." https://nsrdb.nrel.gov/ Accessed: January 2021

[21] IEEE Standards Coordinating Committee 21 on Fuel Cell, Photovoltaics, Dispersed Generation, and Energy Storage. "{IEEE} 1547-2018 -{IEEE} Standard for Interconnection and Interoperability of Distributed Energy Resources with Associated Electric Power Systems Interfaces." April 6, 2018. https://ieeexplore.ieee.org/document/8332112.

[22] Underwriters Laboratories, *UL 1741 inverters, Converters, Controllers and Interconnection System Equipment for use with Distributed Energy Resources*. 2010.

[23] American National Standards Institute, "C84. 1-1995," *Electr. Power Syst. Equip. Volt. Ratings*.

[24] Navarro, A., L. F. Ochoa, and D. Randles. "Monte Carlo-based assessment of PV impacts on real UK low voltage networks." *Power and Energy Society General Meeting (PES), 2013 IEEE*, July 21-25, 2013, pp. 1–5. https://ieeexplore.ieee.org/document/6672620.

[25] Tonkoski, R., D. Turcotte, and T. H. M. El-Fouly. "Impact of high PV penetration on voltage profiles in residential neighborhoods." *IEEE Trans. Sustain. Energy* 3, no. 3 (2012): pp. 518–527.

[26] Institute of Electrical and Electronic Engineers Standards Association, *1366-2012 - IEEE Guide for Electric Power Distribution Reliability Indices*. 2012.

[27] Institute of Electrical and Electronic Engineers Standards Association, *IEEE C57.115-1991 - IEEE Guide for Loading Mineral-Oil-Immersed Power Transformers Rated in Excess of 100 MVA (65C Winding Rise) (Folded into C57.91-1995) (65C Winding Rise)*. 1991.

[28] Ding, F., B. Mather, and P. Gotseff. "Technologies to increase PV hosting capacity in distribution feeders." *IEEE Power Energy Soc. Gen. Meet.*, vol. 2016.

[29] Thiagarajan, R., A. Nagarajan, P. Hacke, and I. Repins, "Effects of Reactive Power on Photovoltaic Inverter Reliability and Lifetime," Presented at the 46th IEEE Photovoltaic Specialists Conference (PVSC 46) Chicago, Illinois June 16–21, 2019, pp. 2970–2976, 2019. NREL/CP-5D00-73648. https://www.nrel.gov/docs/fy19osti/73648.pdf.